THE SYNTHESIS OF FLUORESCENT AND PHOSPHORESCENT DYES FOR BIOCHEMICAL APPLICATION

by

Elizabeth Ann Sanger

A thesis submitted in partial fulfillment
of the requirements for the degree

of

Master of Science
in

Chemistry

MONTANA STATE UNIVERSITY
Bozeman, Montana

March 2010

©COPYRIGHT

by

Elizabeth Ann Sanger

2010

All Rights Reserved

APPROVAL

of a thesis submitted by

Elizabeth Ann Sanger

This thesis has been read by each member of the thesis committee and has been found to be satisfactory regarding content, English usage, format, citation, bibliographic style, and consistency and is ready for submission to the Division of Graduate Education.

Dr. Paul A Grieco

Approved for the Department of Chemistry

Dr. David Singel

Approved for the Division of Graduate Education

Dr. Carl A. Fox

STATEMENT OF PERMISSION TO USE

In presenting this thesis in partial fulfillment of the requirements for a master's degree at Montana State University, I agree that the Library shall make it available to borrowers under rules of the Library.

If I have indicated my intention to copyright this thesis by including a copyright notice page, copying is allowable only for scholarly purposes, consistent with "fair use" as prescribed in the U.S. Copyright Law. Requests for permission for extended quotation from or reproduction of this thesis in whole or in parts may be granted only by the copyright holder.

Elizabeth Ann Sanger

March 2010

ACKNOWLEDGEMENTS

Thank you to Professor Paul Grieco for all of his support and mentorship and all the members of the Grieco lab, especially Dr. Jennifer Vance and Dr. Benjamin Reeves. Also, a big thank you to my professors and committee members here at Montana State University, including Dr. Mary Cloninger, Dr. Thomas Livinghouse, and Dr. Hien Nguyen.

Also, love and thanks to my family and friends. Thank you for all of your help and support. Especially my wonderful husband to be, Will Brown.

TABLE OF CONTENTS

1. RHODAMINE ZDYES 1

Introduction to Proteomics 1
Separation of Proteins 1
Electrophoresis 1
Sodium Dodecyl Sulfate (SDS) 2
Isoelectric Focusing 3
Two Dimensional Gel Electrophoresis (2-DGE) 3
Detection and Identification of Proteins 4
Nonfluorescent Methods of Protein Detection 4
Coomassie Brilliant Blue 4
Silver Staining 6
Isotopic Labeling and Negative Staining 6
Fluorescent Labeling 7
Noncovalent Fluorescent Labeling 7
Covalent Fluorescent Labeling of Cysteine Residues 8
Covalent Fluorescent Labeling of Lysine Residues: CyDyes and Difference Gel Electrophoresis (DIGE) 8
Rhodamine ZDyes 12
Background on Xanthene Derivatives 12
Rhodamine Derivatives of Xanthenes 13
Rhodamine for the Development of a Green ZDye 15
Proposed Synthetic Pathway 17
Results and Discussion 21
Summary 29

2. IRIDIUM DYES 30

Introduction 30
Background on Transition Metal Complexes 31
Phosphorescence of TM Complexes 32
Iridium(III) Complexes as Phosphorescent Emitters 35
Tuning of Ir(III) Complexes 37
Conjugation 38
Electronic Effects 39
Variation of Ligand Structure 39
Applications of Iridium(III) Complexes 40
Ir(III) Complexes for Biological Applications 41
Iridium Dye Synthesis 44
Synthetic Strategy 44
Photochemistry 49

TABLE OF CONTENTS CONTINUED

Results and Discussion 50
Functionalization of the Iridium Fluorophores 59
Synthetic Strategy 59
Results and Discussion 61
Summary 65

APPENDIX A: Experimentals 66

REFERENCES CITED 110

LIST OF TABLES

Table Page

1.1. Comparison of the most common protein detection methods 12

1.2. Absorption, Emission, Extinction Coefficient, Quantum Yield and Brightness of rhodamine fluorophores before coupling of the Zdye peptide side chain.....24

1.3. Absorption, Emission, Extinction Coefficient, Quantum Yield, and Brightness of Rhodamine Dyes BDR_II_013 and 1.....26

2.1. Common transition metals used in phosphorescent complexes.....31

2.2. Comparison of some metal centered phosphorescent complexes.....37

2.3. Absorption and Emission Data for Iridium Fluorophores 6-23 54

LIST OF FIGURES

Figure Page

1.1. Structure of Sodium dodecyl sulfate (SDS) 3
1.2. Structure of Coomassie Brilliant Blue 5
1.3. Structure of a) monobromobimane b) cysteine 8
1.4. Structure of lysine 9
1.5. Structure of CyDyes™ 11
1.6. a) Xanthene b) Fluorescein c) Oregon Green d) Tokyo Green
e) Pennsylvania Green 13
1.7. A) Rhodamine 123 B) Rhodamine 6G C) Rhodamine B 14
1.8. Texas Red® 14
1.9. Series of Rhodamine Alexa® Dyes 15
1.10. ZDye "peptide" side chain for rhodamines 16
1.11. a. Internal Positive Charge on Rhodamine, b. Cysteic Acid Functionality
c. Lysine reactive group, d. Titrateable Amine 17
1.12. Squaraine and BODIPY fluorophores 17
1.13. Tridentate chelation of bis[2-(N,N-dimethylamino]ethyl] ether
to Grignard reagent 19
1.14. Tetramethyl rhodamine ester fluorophores 20
1.15. Zwitterionic tetramethyl Rhodamine dye **1** for protein Labeling 21
1.16. Target for Future Rhodamine Synthesis 29
2.1. BODIPY, Rhodamine, and Squaraine cores 30
2.2. Singlet and Triplet States 33
2.3. Fluorescence vs. Phosphorescence and Intersystem Crossing 34
2.4. Cationic Iridium (III) Complex 35
2.5. Neutral vs. Cationic Iridium (III) Complexes 36
2.6. Intersystem Crossing and SOC 36

LIST OF FIGURES – CONTINUED

Figure Page

2.7. Example of a Tridentate Iridium Complex 38

2.8. Series of Cationic Ir(III) blue, green, and red phosphorescent OLEDs....40

2.9. NCS and Iodoacetamide Complexes 41

2.10. A) Terpyridine Complex with NCS linker B) Aldehyde linker....42

2.11. Avidin Binding Iridium Probe (Contains Biotin) 42

2.12. A) Estradiol conjugate B) Thiourea polypyridine complex C) Ir(III) complex containing alkyl chain for lipid interaction 43

2.13. Green and Red Iridium Dyes of Huang et al. 43

2.14. Yellow, Blue and Green Iridium Dimers....47

2.15. Iridium Fluorophore Series (6-23)....48

2.16. Iridium dye series under radiation 58

2.17. 4-amino-1,10-phenanthroline dyes 59

2.18. Iridium ZDyes 24, 25, and 26 59

2.19. Iridium ZDyes 27, 28, and 29 60

2.20. Phenanthroline ligand with valeric acid linker 64

2.21. Bipyridyl ligand with valeric acid linker 64

LIST OF SCHEMES

Scheme Page

1.1. Addition of Grignard Reagents to xanthenone 18

1.2. Retrosynthesis of Rhodamine ZDye 1 19

1.3. Preparation of Xanthenone 8 20

1.4. Synthesis of Water Soluble Side Chain 4....21

1.5. Synthesis of Intermediate 23....22

1.6. Synthesis of tetramethyl rhodamine dye esters....23

1.7. Coupling of the Zwitterionic Side Chain to Rhodamine Esters....25

1.8. Synthesis of BDR_I_227 (25): A Rhodamine Piperazine Derivative....27

1.9. Rhodamine Condensation Strategy....28

2.1. Nonoyama Reaction....45

2.2. Addition of Nitrogen-Nitrogen (N^N) Cyclometalating Ancillary Ligand 45

2.3. Oxidation of 4,4'-dimethyl bipyridine....46

2.4. Oxidation of 4-methyl-1,10-phenanthroline 46

2.5. Synthesis of Yellow Iridium Dimer 3 51

2.6. Synthesis of Blue Iridium Dimer 4 51

2.7. Synthesis of Green Iridium Dimer 5....52

2.8. Synthesis of Cationic Iridium Fluorophores A, B, C....52

2.9. Retrosynthetic Analysis 61

2.10. Synthesis of Iridium Dye 24 61

2.11. NHS/DCC Activation of Phenanthroline Acids....62

LIST OF SCHEMES – CONTINUED

Scheme Page

2.12. NHS/EDC Activation of Phenanthroline Acids 62

2.13. PyBOP coupling to 17 63

2.14. NHS/EDC/HOBt Activation of Phenanthroline Compounds 63

NOMENCLATURE

(C^N) = carbon nitrogen cyclometalating ligand
(N^N) = nitrogen nitrogen cyclometalating ligand
μg = microgram
2-DGE = two dimensional gel electrophoresis
BDMEE = bis[2-(N,N-dimethylamino]ethyl] ether
Boc = t-butyl carbonate
BODIPY = boron-dipyrromethene
bpy = bipyridine
C = Celsius
CBB = Coomassie Brilliant Blue
CH_3CN = acetonitrile
cm = centimeters
DCC = dicyclohexyl carbodiimide
DCM/ CH_2Cl_2 = dichloromethane/ methylene chloride
DIGE = difference gel electrophoresis
DMF = dimethylformamide
DMSO = dimethyl sulfoxide
EDC = 1-ethyl-3-(3-dimethylaminopropyl) carbodiimide
ESI = electrospray ionization
EtOAc = ethyl acetate
F_2ppy = 2-(2,4-difluorophenyl)pyridine
$FeCl_3$ = ferric chloride
h = hours
H_2O = water
HCl = hydrochloric acid
HOBt = 1-hydroxy-benzotriazole
HOMO = highest occupied molecular orbital
IEF = isoelectric focusing
ILCT = intraligand charge transfer
IR = infrared
Ir = Iridium
KCN = potassium cyanide
kD = kilodaltons
$KMnO_4$ = potassium permanganate
LUMO = lowest unoccupied molecular orbital

NOMENCLATURE – CONTINUED

mBBr = monobromobimane
MeOH = methanol
mg = milligram
MHz = megahertz
mL = milliliter
MLCT = metal to ligand charge transfer
mmol = millimole
MS = mass spectrometry
Na_2CO_3 = sodium carbonate
NaOH = sodium hydroxide
NCS = isothiocyanate
ng = nanogram
NH_4PF_6 = ammonium hexafluorophosphate
NHS = N-hydroxysuccinimide
NMM = N-methylmorpholine
NMR = nuclear magnetic resonance
OLED = organic light emitting diode
PAGE = polyacrylamide gel electrophoresis
phen = phenanthroline
pI = isoelectric point
$POCl_3$ = phosphoryl chloride
ppy = pheny pyridine
ppyz = pyrazole
PyBOP = Benzotriazol-1-yl-oxytripyrrolidinophosphonium hexafluorophosphate
R_f = Retention factor
RP = reverse phase
RP HPLC = reverse phase high performance liquid chromatography
RT = room temperature
SDS = sodium dodecyl sulfate
SOC = spin orbit coupling
Su = succinimide
TFA = trifluoroacetate
THF = tetrahydrofuran
THF = tetrahydrofuran
TMEDA = tetramethylethylenediamine

NOMENCLATURE – CONTINUED

TOF = time of flight
t_R = retention time
Trt = trityl
UV = ultraviolet

ABSTRACT

Current dyes for proteomics that are applicable to multiplexing experiments suffer from lack of sensitivity and poor water solubility. A series of tetramethyl rhodamine derivatives were developed to study the effects of substitution patterns on the photophysical properties of the fluorophores. After identifying the superior fluorophore a zwitterionic side chain with properties beneficial for two dimensional applications was coupled to the fluorophore and the photophysical properties were studied.

Iridium(III) cationic fluorophores are interesting synthetic targets due to their ultraviolet absorption wavelengths and visible emission properties. A series of Iridium(III) fluorophores, some of which contain a handle for further synthetic extension, has been made to study the ligand effects on the emission properties of the dyes. Finally, some of these dyes have been synthetically modified for proteomic labeling applications.

RHODAMINE ZDYES

Introduction to Proteomics

The term "proteomics" was first coined in 1994 by Marc Wilkins, a graduate student at Macquarie University in Sydney Australia.[1] Used to define the study of proteins, particularly their structure and function, the word parallels the term genomics, the study of genes. The proteome of an organism is the sum of its proteins and their post-translational modifications. Unlike the genome of an organism, the proteome is ever changing due to external influences on cells.[2] Among the reasons for studying proteins are the identification of potential drug targets and the observation of protein biomarkers for disease diagnosis. The detection and identification of individual proteins, as well as measurement of their abundance, location, post-translational modifications, and interactions with other proteins are all important aspects of proteomic research.[3]

Currently, the best method for separation and identification of proteins is two-dimensional gel electrophoresis (2-DGE) followed by detection using stains and identification with mass spectrometry (MS).[4]

Separation of Proteins

Electrophoresis

Electrophoresis is the migration of ions in an electric field; and proteins can be thought of as ions when subjected to such a field. In the separation of proteins, the sample is applied to the end of a stationary phase through which a current is applied. The proteins migrate to the electrode of the opposite charge (at the opposite end of the

stationary phase) at different rates dependent on their mass, consequently separating into different bands. The different bands are characteristic of dissimilar types of proteins. The use of electrophoresis for the separation of proteins has become one of the most powerful methods available to biochemists.[2]

Two types of polymers are used as the stationary phase for electrophoresis, polyacrylamide and agarose. These materials impede the movement of large molecules relative to small molecules and therefore separate molecules on the basis of not only their electrophoretic mobilities but also their size. Both polyacrylamide gel electrophoresis (PAGE) and agarose gel electrophoresis are run in a buffer at pH 9, so that the proteins have net negative charges and migrate toward an anode in the opposite end of the gel reservoir. Whereas PAGE gels separate proteins of small molecular mass (<200kD), agarose gels, which contain larger pores, separate proteins from 200 to 50,000 kD.[2]

Sodium Dodecyl Sulfate (SDS)

Sodium dodecyl sulfate (SDS) is a detergent used in electrophoretic gels to bind to proteins and force them into negatively charged, rod-like structures. The large negative charge imparted by the SDS (**Figure 1.1**) overshadows any charge the individual proteins might have thereby giving all of the proteins in the sample approximately equal charge to mass ratios. Due to the similar shape of the bound proteins, electrophoresis performed in gels containing SDS (SDS-PAGE gels) separate proteins according to their molecular masses, independent of their original charges because the pores in the gel prevent larger proteins from migrating as far as smaller proteins. Protein masses may be determined from the gel using a standard composed of proteins of known mass, which is run alongside the sample.[2]

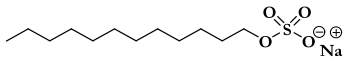


Figure 1.1. Structure of Sodium dodecyl sulfate (SDS)

Although SDS-PAGE simplifies the separation of proteins it disrupts noncovalent interactions between subunits of proteins, leading to separation of the subunits. Thus, the disadvantage of SDS-PAGE is that the mass of the individual subunits and not the protein as a whole is measured.[2]

Isoelectric Focusing

Isoelectric Focusing (IEF) is also used as a method of protein separation. This technique uses the isoelectric point (pI) of a protein, the pH at which a molecule carries no net electric charge.[5] When the pH is equal to the pI of a protein, the protein becomes immobile in an electric field. Thus, if an electric field is applied to a gel with a pH gradient from the anode to the cathode, proteins introduced into the gel will migrate to positions on the gel where their isoelectric point is reached and form bands. This separates them for isolation and identification.[2]

Two Dimensional Gel Electrophoresis (2-DGE)

By combining gel electrophoresis and isoelectric focusing a two-dimensional "map" of a proteome can be studied. This technique is aptly called two-dimensional gel electrophoresis (2-DGE). Due to the increased resolution offered by 2-DGE individual protein bands can be recovered, characterized, and identified via mass spectrometry. Also, by comparing the positions and intensities of bands in separate gels, proteins can be differentially resolved.[2]

Detection and Identification of Proteins

Hindering the use of gel electrophoresis in proteomics research is the actual detection of the proteins from the background medium, the gel.[6] Methods of labeling proteins for detection include the covalent binding of radioactive tags, affinity tags, and organic fluorophores to the proteins before or after running the gel or the use of dyes that associate noncovalently to the proteins after separation by electrophoresis. In two-dimensional gels, factors such as sensitivity, reproducibility, and the variation in the extent a dye labels different proteins must be considered when choosing the method for protein detection.[6] It is important to determine whether or not a labeling technique is applicable to 2-DGE and if so, at what step it can be applied to the gel. Labels can theoretically be attached before IEF, between IEF and SDS PAGE, or after completion of both dimensions. Dyes have limitations and benefits associated with which stage they can be applied to the proteins. For example, labeling prior to IEF is convenient due to lower sample loading and high concentrations of proteins, however only covalent binding can be used at this stage due to the highly denaturing conditions of the IEF process. Also, the labels must be acid and base stable. Using labels that are applied after IEF or 2-DGE is beneficial because the maintenance of pI is no longer an issue. However because all proteins labeled at this stage are subject to the same labeling conditions there is no possibility for multiplexing experiments, the importance of which will be discussed later.[6]

Nonfluorescent Methods of Protein Detection

Coomassie Brilliant Blue

Staining gels with Coomassie Brilliant Blue (CBB) is the most common method

of protein detection (**Figure 1.2**). The finished gel is soaked in an acidic alcohol solution containing CBB, which denatures the proteins and complexes the dye to the proteins. This complex is thought to be a combination of hydrophobic effects and a noncovalent electrostatic interaction between the anionic dye and the cationic lysine residues of the proteins.[7] Excess dye is removed by washing with acidic solution, a procedure referred to as "destaining".[2] Staining with CBB can detect protein bands containing as little as 0.1µg of protein. However, stoichiometric binding of dye is difficult using CBB because the destaining procedure is nonlinear in pulling color away from different proteins.[2,8]

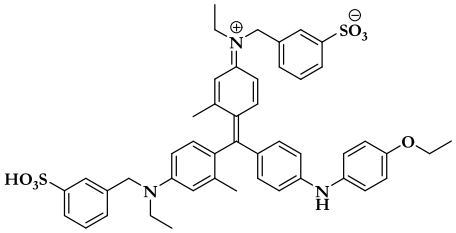


Figure 1.2. Structure of Coomassie Brilliant Blue

The development of colloidal CBB for detection without destaining gives an improvement in the nonlinearity of traditional CBB methods. This technique will detect 8-10 ng of protein and involves the formation of micelles of Coomassie. However, acid present in colloidal CBB stains catalyzes the irreversible esterification of glutamic and aspartic acid carboxylic acid residues with alcohols also present in the staining solution.[8,9]

Nonlinear effects in traditional CBB methods and esterification side reactions in colloidal CBB dyes, combined with the low sensitivity of CBB dyes overall, are deterrents from this method of protein detection; yet, it remains the most common

method of protein detection in 2-DGE.[8,10]

Silver Staining

Silver staining methods are the leading methods for detection of low levels of protein following 2-DGE.[3] Silver staining is ten to one hundred times more sensitive than Coomassie staining methods and allows for the detection of nanogram quantities of proteins.[11] However, problems with reproducibility and the complexity of the process limit the utility of quantitative silver staining.[8] Silver staining procedures consist of acidic silver nitrate or alkaline silver diamine methods, both of which use glutaraldehyde and formaldehyde and are known to alkylate the amino groups of proteins, making further analysis by Edman sequencing unsuccessful. Eliminating glutaraldehyde from the staining procedure reduces the sensitivity of the stain, thereby reducing any advantage over CBB staining procedures.[10] Another drawback of silver stains is that they are much more sensitive to parameters such as temperature, solvents and developing times than CBB stain, making gel to gel reproducibility poor.[11]

Isotopic Labeling and Negative Staining

The use of radioisotopes is an additional method of protein detection. This technique involves labeling the amino acids of the proteins themselves and is advantageous over other methods of staining because it has a larger linear response with respect to the amount of protein present in the sample in comparison to stains such as CBB and silver.[6,8] Radioactive labeling is simple, as it can be done without noticeable modifications of the pIs or the molecular weights of the proteins.[6] However, the inherent dangers of radioactivity, poor shelf life, and difficult disposal of radioactive waste have

led many to seek alternative methods for protein detection.[8] Also, some of the most versatile and convenient labels, such as Tritium emit, only low-levels of radiation, which are hard to detect.[4]

Finally, reverse stain methods or negative staining involves staining the gel matrix itself while leaving areas of protein accumulation clear as a result of the formation of insoluble metal salts. This allows for detection of the proteins while keeping their biological integrity intact.[11] Zinc-imidazole reverse staining, for example, has excellent linear response. However, the linear dynamic range of such stains is generally very low. This means that reverse stains are not useful for quantitative studies of proteins because the intensity of the reverse stain in relation to the amount of protein is only linear when using µg to ng amounts of protein. Also, prolonged exposure to reverse stains begins to be problematic because protein spots become obscured by the stain.[6,8]

Fluorescent Labeling

Noncovalent Fluorescent Labeling

Few noncovalent fluorescent labels are currently used for protein detection due to their poor performance. SYPRO dyes present the anomaly in that they provide protein detection with sensitivities rivaling, even superseding CBB and silver stain. SYPRO Ruby, a ruthenium based dye that binds proteins similarly to CBB, provides a broad linear dynamic response while allowing for characterization of the excised proteins.[8]

Developed to overcome limitations of silver stain procedures, SYPRO Ruby is far superior to silver staining.[3] Detecting 0.25-1 ng of protein with a simple staining procedure SYPRO Ruby is not confounded by destaining or overdevelopment of gels

because it is an end point stain.[3,8] SYPRO Ruby provides comparable, if not superior, sensitivity to CBB and silver staining techniques. The option of multiple excitation sources, including lasers, lamps, and LEDs, and the ability to profile proteins with mass spectrometry make SYPRO Ruby a more convenient stain to use.[8] A major limitation of SYPRO Ruby is that it can only be used after 2-DGE so gel-to-gel reproducibility is still an issue with this protein label. Also, SYPRO Ruby is commercially available but costly at $74.00 for a 200mL solution, ready for application to the gel.[12]

Covalent Fluorescent Labeling of Cysteine Residues

Monobromobimane (mBBr) is a fluorescent dye that binds cysteine residues in proteins by nucleophilic substitution (**Figure 1.3**). mBBr can be problematic because it targets only reduced cysteine residues, while many proteins maintain the majority of their cysteine sulfhydryl residues in the oxidized, disulfide form. Although mBBr is similar to silver stain in effectiveness, cysteine labeling is generally regarded as a poor choice for fluorophore targeting. Due to the overly high abundance of cysteine residues in some proteins, such as vascular endothelial cell growth factor, and the absence of cysteine residues in others, such as Concanavalin A, uniform protein labeling cannot be achieved by targeting cysteine residues.[8]

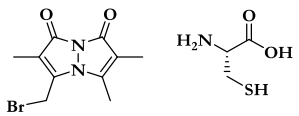


Figure 1.3. Structure of a) monobromobimane b) cysteine

Covalent Fluorescent Labeling of Lysine Residues:
CyDyes and Difference Gel Electrophoresis (DIGE)

One of the major problems in detecting differences between protein samples using

multiple 2-DGE is inconsistent gel-to-gel reproducibility. Differences in the gel structure itself, electric fields, pH fields, and temperature fluctuations cause identical gels to be almost impossible to obtain and therefore require special software for comparison. These obstacles can be circumvented using a technique called difference gel electrophoresis (DIGE). The labeling of equivalent protein samples prior to separation with fluorescent, lysine reactive, cyanine dyes of different excitation and emission wavelengths can be used to distinguish differences in different protein samples. The separate protein samples are labeled with different dyes and applied to the same gel which allows for separation of the different protein samples in equivalent environments. Fluorescence imaging can be used to detect proteins following DIGE separation and differences in protein composition can be identified by exciting at different wavelengths and measuring the emissions of the different dyes independently. These images can then be compared to identify differences in the samples.[13] This technique is called multiplexing.

In designing covalent labels, lysine residues are a more representative target for fluorescent labels than cysteine residues when comparing the number of residues to the molecular weight of the protein. Cysteine is a nonessential amino acid and is not necessarily prevalent in all proteins whereas lysine (**Figure 1.4**) is an essential amino acid that is required for protein formation and is widespread in all proteins. This makes lysine residues superior targets for quantitative fluorescent labeling.[8]

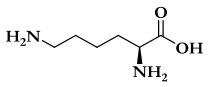


Figure 1.4. Structure of lysine

CyDyes™ (based on polymethines) contain N-hydroxysuccinimide (NHS) groups

which react with the amino group on the lysine side chains of protein residues to form amide linkages between the fluorescent dyes and the proteins. To preserve the charge of the protein after the attachment of the CyDyes™ a non-ionizable quaternary amino group is incorporated into the dye structure (**Figure 1.5**). Although CyDyes do shift the protein in the molecular weight dimension, they are designed with similar molecular weights to provide uniform molecular weight shifts in proteins, thereby preserving the capability of comparison between spots.[8]

Although DIGE evades problems with reproducibility by providing the same gel environment for different protein samples, the labeling of proteins with CyDyes™ is difficult due to the hydrophobicity of the dyes themselves, which may cause issues with protein solubility and is directly related to the extent of protein labeling. This problem can be avoided by labeling only 1-2% of the lysine residues in the protein sample consequently lowering the detection limit of the dyes.[13] In some cases however, detection limits of 0.025ng are possible.[14] Also, because the ionizable positively charged primary amino groups are replaced by a nonionizable quaternary amine, the pK_a of each residue shifts from approximately 9 to 14. This changes the pI of the protein and can alter the first dimension separation.[13] Along with the high cost of the CyDyes™, which are sold in nanomole (nmol) quantities for approximately $1600 per 10nmol sample, these shifts in the pI and solubility issues are all problems associated with the use of CyDyes™.[15]

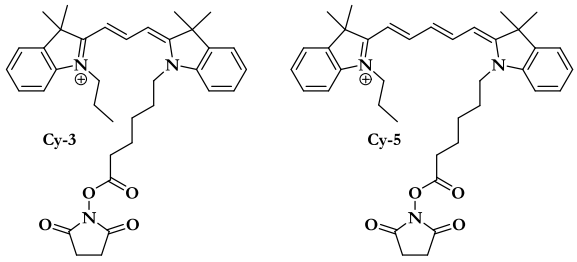


Figure 1.5. Structure of CyDyes™

Along with the development of DIGE comes the need for excitation of multiple fluorescent labels and processing of emission spectra at different wavelengths. This level of complexity has spurred development of new imagers such as the Typhoon™ 8600, which combines lasers of different wavelengths with sensitive detection techniques.[16] Not only is detection and visualization difficult but due to the special equipment needed to measure the emission of the fluorescent labels excision of the proteins from the gel for analysis by mass spectrometry is complicated.[8] Further complicating matters is the fact that because some of the protein is invariably left unlabeled due to solubility issues there is always a small amount of unlabeled protein (shifted to a lesser extent in the molecular weight dimension of the gel) that cannot be recovered.[8]

In summary, multiple methods for protein detection are available. However, most methods suffer from poor detection limits and limited capabilities exist for multiplexing. (**Table 1.1**). Although significant improvements have been made in the development of covalent fluorescent labels, such as CyDyes™, the detection of lower levels of protein while maintaining protein water solubility for use in DIGE applications are still needed.

Table 1.1. Comparison of the most common protein detection methods

Stain	Detection Limits (ng of protein)	End Point Stain?	MS Compatible?	Labeling Step	Multiplexing Compatible?
SYPRO Ruby	1-2 ng	Yes	Yes	After 2DGE	No
Silver Stain	1-4 ng	No	No	After 2DGE	No
CBB	8-16 ng	No	Yes	After 2DGE	No
Colloidal CBB	8-16 ng	Yes	Sometimes	After 2DGE	No
Monobromobimane	4-32 ng	NA	No	Before 2DGE	No
Zinc-Imidazole Reverse Stain	1-2 ng	No	Yes	After 2DGE	No
CyDyes™	0.025ng	NA	Yes	Before 2DGE	Yes

Covalently binding dyes with better detection limits while maintaining multiplexing capabilities are needed. Organic dyes keeping the concepts of CyDyes™ in mind, pI preservation and lysine binding capabilities, while implementing zwitterionic character for improved water solubility have been proposed as alternatives to CyDyes™ for two dimensional protein labeling reagents. These dyes would be available in three colors, similar to the CyDyes™, but would have increased detection limits for protein labeling studies.

Rhodamine ZDyes

Background on Xanthene Derivatives

Multiple dyes have been synthesized based on the Xanthene fluorophore (**Figure 1.6, A**). These dyes have characteristically high quantum yields and extinction coefficients.[17] A series of dyes based on the Xanthene analogue Fluorescein (**Figure 1.6,**

B) have been developed for use as molecular and cellular probes (**Figure 1.6**).

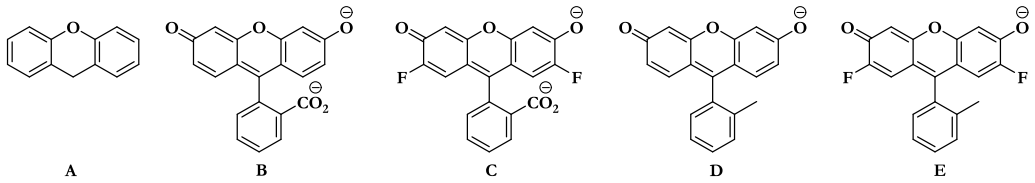


Figure 1.6. a) Xanthene b) Fluorescein c) Oregon Green d) Tokyo Green e) Pennsylvania Green.

Fluorescein has been used as a valuable fluorescent probe because of its high molar absorptivity and quantum yield. However, problems with acid sensitivity and photobleaching have led to the investigation of alternate options derived from the fluorescein backbone.[18]

Oregon Green, developed as a less pH sensitive alternative to Fluorescein, is much more photostable than Fluorescein and is highly polar. Tokyo Green was subsequently developed as a more hydrophobic alternative to Oregon Green by the incorporation of a methyl group. Finally, the incorporation of both functionalities, fluorine and methyl, in Pennsylvania Green, proves both more hydrophobic and less pH sensitive.[18]

Rhodamine Derivatives of Xanthene

Rhodamine, another Xanthene analogue, has also been extensively employed as a fluorescent probe and has been used in a variety of applications including enzyme assays, DNA sequencing, pharmacological studies, and studies of complex biochemical processes.[19] Rhodamine is known to be a very robust fluorophore due to its resistance to photodegradation and pH fluctuations (at low to neutral pH), as well as its high extinction

coefficient and high quantum yield (**Figure 1.7**).[20,21]

Although derivatives of Rhodamine typically have limited wavelength tuneability, their absorption (~500nm) and emission wavelengths (~600nm) fall within the range that is excited with the green argon laser.[22]

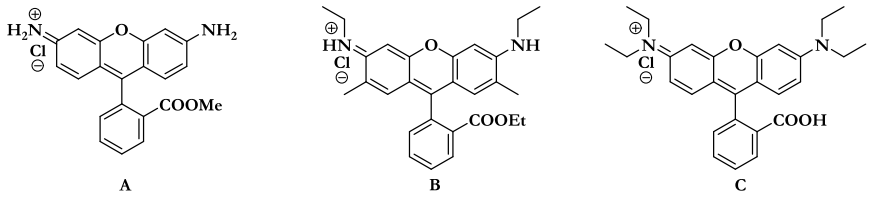


Figure 1.7. A) Rhodamine 123 B) Rhodamine 6G C) Rhodamine B

Texas Red®, a sulfonated rhodamine derivative, is commercially available through Molecular Probes® as a protein dye (**Figure 1.8**). Texas Red® uses sulfonyl chloride and sulfonate moieties to covalently bind the free amino groups on proteins and confer water solubility respectively.[23] Sulfonation has been shown to decrease the aggregation of dye molecules, possibly by imparting more polar character to the dye. It has also been shown to increase the brightness of certain dyes.[20]

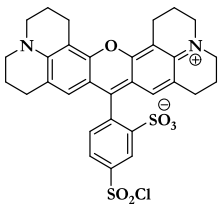


Figure 1.8. Texas Red®

Alexa® Fluors, which contain sulfonate moieties as well, are also commercially available (**Figure 1.9**). The Alexa® dyes were developed in an attempt to compensate for

the quenching phenomenon observed in flourescein and rhodamine derivatives upon binding to proteins as well as their photolability and pH sensitivity. Alexa® dyes are superior to many of the xanthene dyes discussed above in brightness, resistance to photobleaching, and water solubility. However, they carry a net negative charge, which disrupts the overall pI of the protein after binding, making them inapplicable for 2-DGE.[23] Finally, the high cost of Alexa® dyes is a large deterrent in their use compared to more conventional choices. One milligram of Alexa® dye can cost anywhere from $50 to $190.[21]

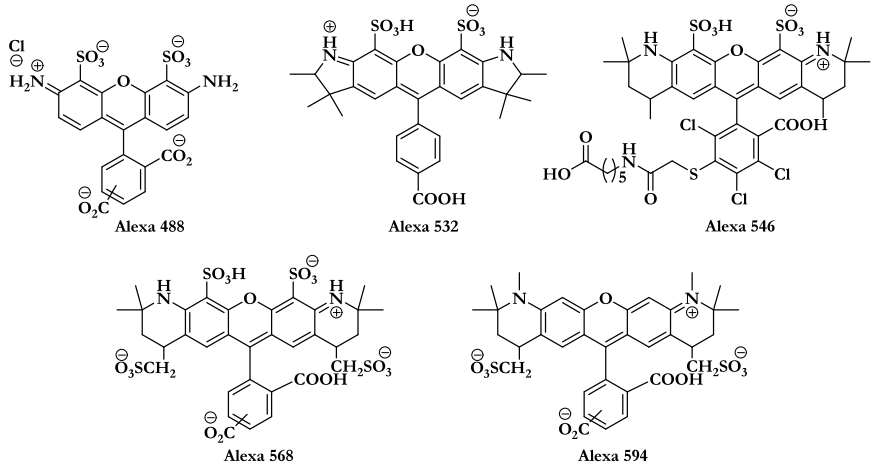


Figure 1.9. Series of Rhodamine Alexa® Dyes

Rhodamine for the Development of a Green ZDye

Rhodamine dyes have received less attention than one might expect because they emit at the same wavelength as other biological molecules in serum and they are therefore indistinguishable from background fluorescence in *in vivo* studies.[24] However, experimentation with variation of the amine substituents, so as to prevent rotation of the aromatic core, variation of the oxygen in the xanthene core with tellurium, and the coupling of different linkers to the Rhodamine acid have been performed to study the

influence on absorption and emission wavelengths as well as pH sensitivity.[19,24,25] To date, only the sulfonated rhodamine Texas Red, and rhodamine Alexa Fuors®, have been used significantly in protein labeling experiments, both of which are not useful in two dimensional protein experiments. The synthesis of a cost-effective green dye with a large fluorescence quantum yield and high extinction coefficient began on a series of Rhodamine dyes amenable to the introduction of a side chain, characteristic of other dyes previously developed in the Grieco/Dratz laboratory.[26]

The following side chain was developed by the Grieco/Dratz lab for incorporation into the cationic Rhodamine fluorophores to improve the water solubility and the detection limits of protein labeling while maintaining the pI and allowing for application in multiplexing technologies (**Figure 1.10**).

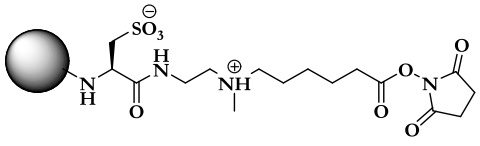


Figure 1.10. ZDye "peptide" side chain for rhodamines

This "peptide side chain" incorporates both an N-hydroxysuccinimide activated carboxylic acid group to react with the lysine amine residues of proteins and a titrateable amine to preserve the pI of the protein after binding of the dye. A cysteic acid residue is included to charge balance the quaternary non-titratable amine present in the Rhodamine fluorophore itself, making the dye zwitterionic, hence the name "ZDye" (**Figure 1.11**).

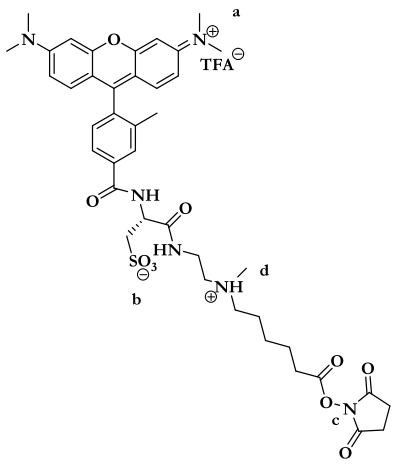


Figure 1.11. ***a.*** *Internal Positive Charge on Rhodamine,* ***b.*** *Cysteic Acid Functionality,* ***c.*** *Lysine reactive group,* ***d****. Titrateable Amine*

These charged groups have been added to confer water solubility to the bound protein and increase the binding capacity of the dye, which is subsequently expected to increase the detection limit. Similar peptide linkers have been incorporated into many different fluorophores by the Grieco/Dratz lab, including the squaraine and boron-dipyrromethene (BODIPY) families of fluorescent dyes (**Figure 1.12**).[26]

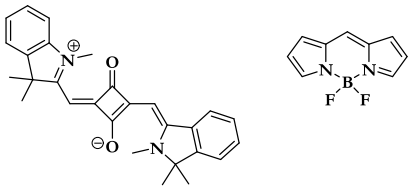
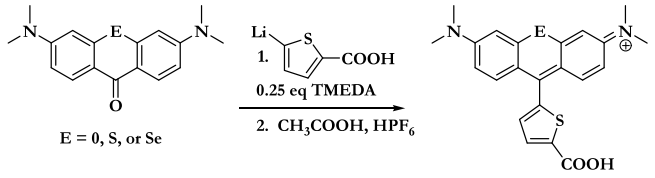


Figure 1.12. Squaraine and BODIPY fluorophores

Proposed Synthetic Pathway

Previous syntheses of Rhodamine derivatives have utilized condensation reactions

or organo-halide exchange reactions to form the Rhodamine core as shown in **Scheme 1.1**.[27]



Scheme 1.1. Addition of Grignard Reagents to xanthenone

Detty and coworkers identified this exchange route to a wide variety of Rhodamine dyes with various substitution patterns containing an ester substituent on the aryl ring through which a zwitterionic side chain could be appended.[27]

The protocol for Rhodamine synthesis developed by Detty involves the addition of tetramethylethylenediamine (TMEDA) to mediate Grignard formation from an aryl halide containing a carboxylic acid group using isopropyl magnesium chloride, followed by addition to a carbonyl and treatment with acid to eliminate water and complete the aromatic framework of the dye.[28]

The use of bis[2-(N,N-dimethylamino]ethyl] ether (BDMEE) for mediation of Grignard reactions has also been previously reported in the literature and assists in the same manner as TMEDA, but with superior selectivity. BDMEE is known to moderate the nucleophilicity of Grignard reagents by complexing the organomagnesium reagent, allowing for chemoselective exchange of the halogen with isopropylmagnesium chloride (**Figure 1.13**). This chelating reagent is especially useful in the formation of Grignard reagents on aryl iodides containing sensitive functional groups, such as esters, because it allows for higher reaction temperatures (greater than -20^{o}C) while still minimizing side

reactions with the sensitive functional groups.[28]

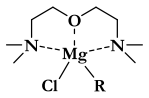
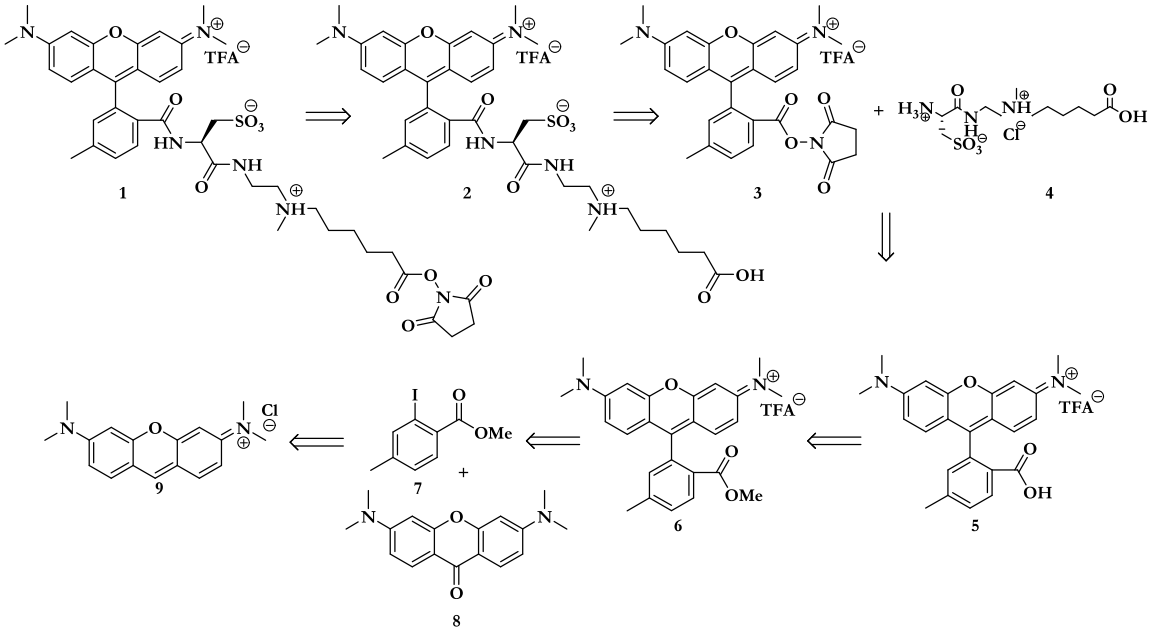


Figure 1.13. Tridentate chelation of bis[2-(N,N-dimethylamino]ethyl] ether to Grignard reagent.

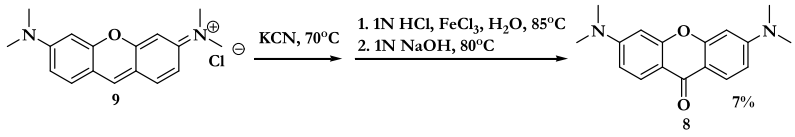
After identifying the organo-halide exchange protocol as the best method for introducing a series of various aryl substituents into the Rhodamine core, the following retrosynthetic analysis for tetramethyl rhodamine ZDye **1** was proposed (**Scheme 1.2**)



*Scheme 1.2. Retrosynthesis of Rhodamine ZDye **1***

The synthesis of Rhodamine ZDye **1** (**Scheme 1.2**) was envisioned to proceed by the activation of the corresponding carboxylic acid **2** made from coupling of the zwitterionic side chain **4** to the NHS activated rhodamine acid **3**. This acid would be

formed from the hydrolysis of the respective ester **6** to the acid **5**. Rhodamine ester **6** and others of varying substitution patterns, were envisioned to come from the direct coupling of xanthenone **8** to the appropriate iodo aryl ester **7** by Grignard addition mediated by BDMEE to avoid Grignard reaction with sensitive functionalities in other parts of the molecule. The synthesis of xanthenone **8** from the oxidation of pyronin Y **9** was previously reported and is still widely used in the preparation of Rhodamine derivatives (**Scheme 1.3**).[29]



*Scheme 1.3. Preparation of Xanthenone **8***

With this synthesis in mind the following tetramethyl rhodamine fluorophores (**6, 10-13**) were proposed and made. Each was characterized to determine their photophysical data and study the effects of various substitution patterns on the characteristics of the dye (**Figure 1.14**).

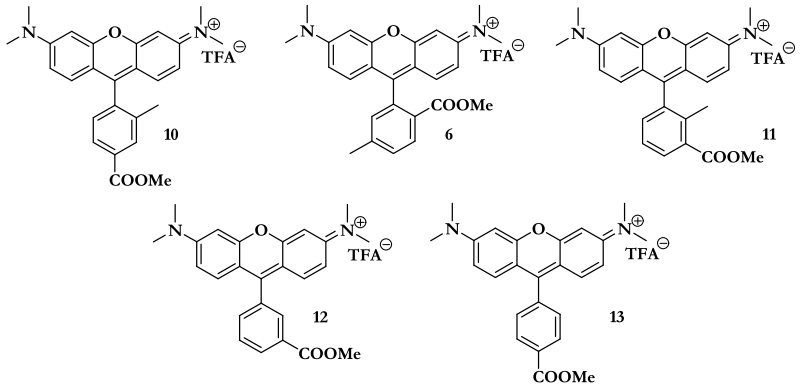


Figure 1.14. Tetramethyl rhodamine ester fluorophores

The following Rhodamine dye **1,** which contains the zwitterionic side chain for protein labeling (**Figure 1.15**), was also synthesized.

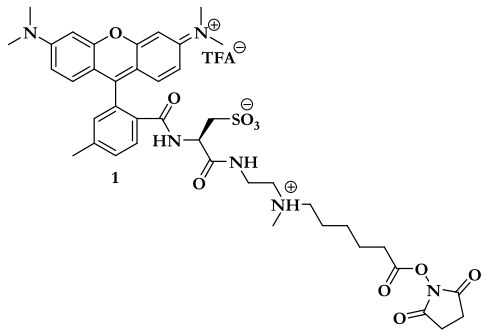
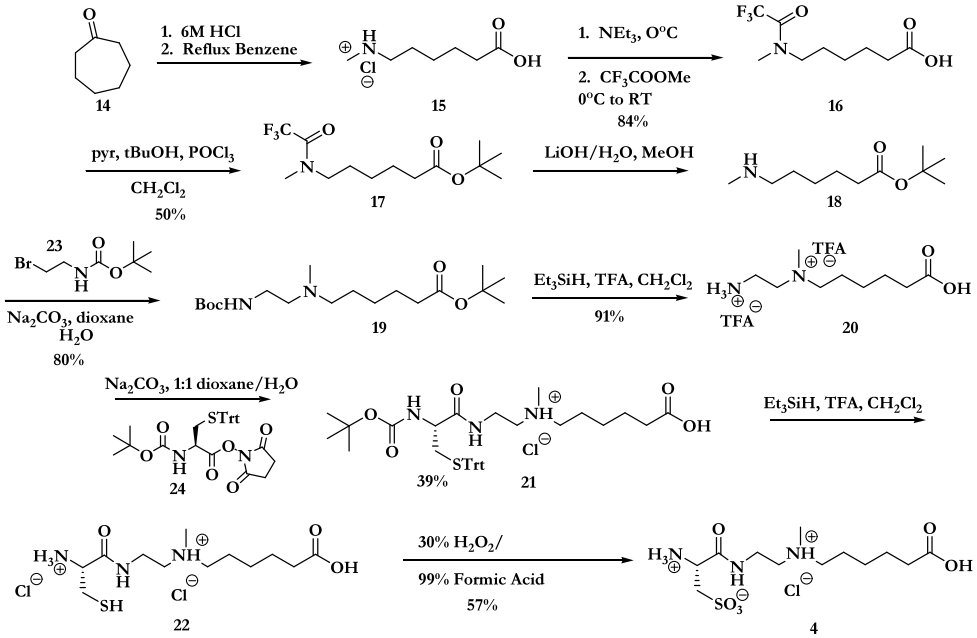


*Figure 1.15. Zwitterionic tetramethyl Rhodamine dye **1** for protein labeling*

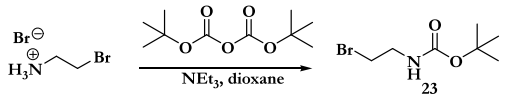
Results and Discussion

*Synthesis of Water Soluble Peptide Side Chain **4***



*Scheme 1.4. Synthesis of Water Soluble Side Chain **4***

The synthesis of the water-soluble side chain **4** was previously reported in our laboratory for attachment to various organic fluorophores. Its synthesis begins with the cleavage of the amide bond in N-methylcaprolactam **14** by heating in acid to give 5-(methylamino)pentanoic acid hydrochloride **15**. The amine group was protected as its trifluoroacetamide (**16**) followed by subsequent protection of the carboxylic acid by esterification with t-butanol (**17)**. Deprotection of the trifluoroacetamide using lithium hydroxide in methanol yielded **18**. Coupling of **18** with 2-bromoethylcarbamate **23** using sodium carbonate gave compound **19**. Triethylsilane and trifluoroacetic acid were added to cleave the Boc and t-butyl protecting groups to yield **20**, which was coupled with (R)-Boc-Cys (Trt)-OSu (**24)** using sodium carbonate in aqueous dioxane to yield the amidation product **21**. The trityl protected thiol was subsequently deprotected using trifluoroacetic acid to yield **22** and oxidized to the cysteic acid **4** using performic acid (**Scheme 1.4**).



*Scheme 1.5. Synthesis of Intermediate **23***

The synthesis of **23** was realized by coupling of 2-bromoethylamine with di-t-butyl dicarbonate in dioxane containing triethylamine (**Scheme 1.5**).

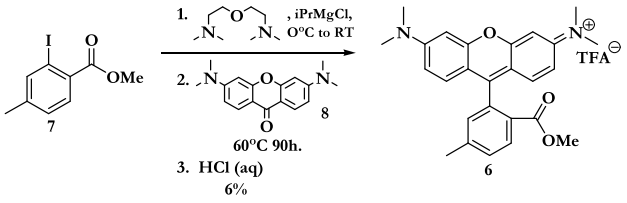
Rhodamine Dyes

All of the tetramethyl rhodamine dye esters (**6, 10-13**) were synthesized using an identical strategy. Each varied only in the aromatic substituents of the ring coupled to the

xanthenone core. Methyl groups were placed on the ring coupled to the xanthenone at various positions to study the electronic effects. These methyl groups were also left out in esters **12** and **13** to compare the effects of the methyl substitution on the hydrophobicity of the rhodamine dyes. However, no noticeable change in hydrophobicity was observed when comparing dyes containing the methyl group to those without the methyl substituent. Also, the position of the ester group on the ring was varied to study steric effects on the synthesis of the fluorophore as well as inductive effects, which could lead to different photophysical properties.

*Synthesis of Xanthenone **8***

The xanthenone starting material **7** was synthesized from pyronin Y **9** by oxidation with potassium cyanide followed by treatment with acid and iron (III) chloride (**Refer to Scheme 1.3**). The resulting intermediate was treated with base and purified using column chromatography. Xanthenone **8** served as the starting material for all of the tetramethylrhodamine dyes.

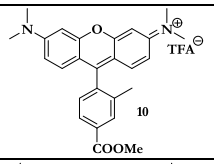
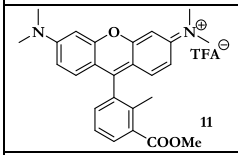
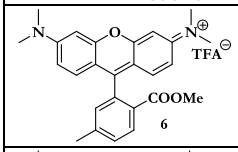
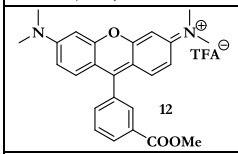
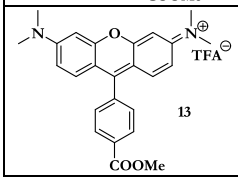


Scheme 1.6. Synthesis of tetramethyl rhodamine dye esters

The synthetic strategy for making the series of rhodamine esters is shown for compound **6** in **Scheme 1.6**. The addition of the non-fused iodoester aromatic ring **7** utilizing the Grignard reaction proceeded by the dropwise addition of isopropylmagnesium chloride in THF to a mixture of aromatic iodide and freshly distilled BDMEE in anhydrous THF at

0ºC under argon. This solution was warmed to room temperature and stirred for 5 hours. Xanthenone **8** was added and refluxed at 60ºC under argon for 90 hours. Evaporation of THF followed by treatment with trifluoroacetic acid yielded a purple solid, which was purified by reverse phase HPLC (RP HPLC) to yield the Rhodamine ester **6 (Scheme 1.6**). Each Rhodamine ester was submitted for photochemical analysis, including absorption and fluorescence emission. These results are shown in **Table 1.2.** It can be seen that compounds **10** and **11** show the largest extinction coefficients but that compound **6** has the greatest quantum yield and brightness.

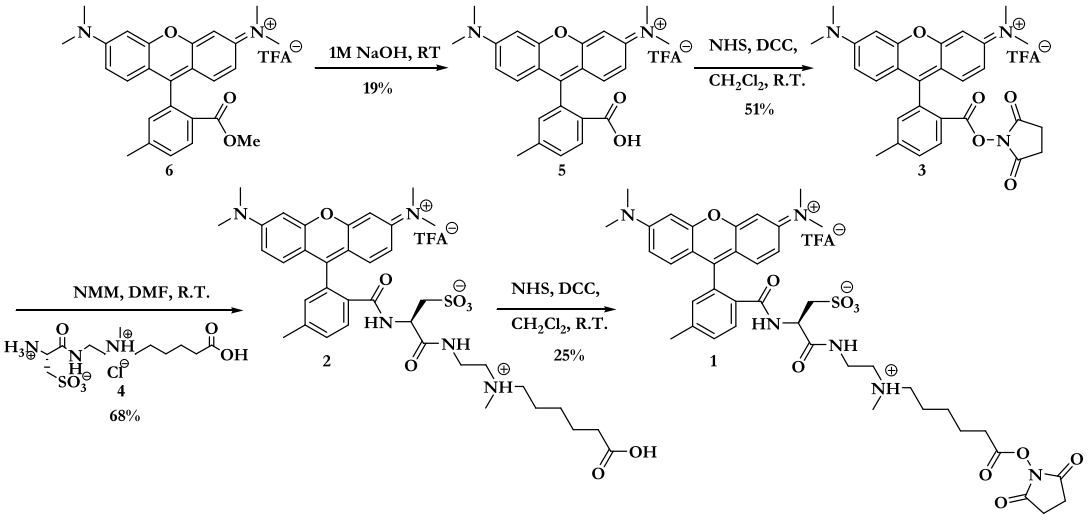
Table 1.2. Absorption, Emission, Extinction Coefficient, Quantum Yield, and Brightness of rhodamine fluorophores before coupling of the ZDye peptide side chain.

Structure	λ_{max} (nm)	λ_{em} (nm)	ε (l/(cm*mol)	QY (%)	B $_{(532nm)}$
 10	557	583	73185	40	29347
 11	552	577	74016	73	23887
 6	554	577	49403	90	44314
 12	554	582	39225	76	13040
 13	555	586	56229	57	13653

* Brightness = QY x Extinction Coefficient at 532nm

Coupling of the Zwitterionic Side Chain

Rhodamine ester **6** was then carried forward to rhodamine dye **1** by the coupling of the zwitterionic side chain to the rhodamine ester core using standard peptide coupling methods (**Scheme 1.7**).



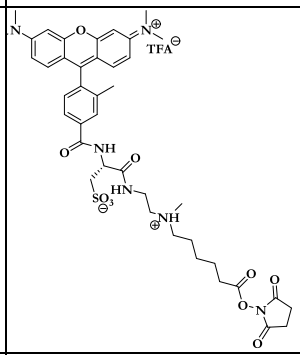
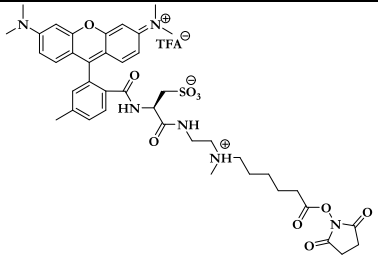
Scheme 1.7: Coupling of the Zwitterionic Side Chain to Rhodamine Esters

Hydrolysis of the rhodamine ester **6** with 1 M NaOH and purification by reverse phase high performance liquid chromatography (RP HPLC) provided the corresponding acid **5**. Activation of the carboxylic acid with N-hydroxysuccinimide (NHS) and purification by RP HPLC gave **3,** and subsequent coupling to the ZDye side chain **4** yielded rhodamine acid **2**. The final dye was NHS activated to complete the tetramethyl rhodamine dye **1**.

The absorption and emission spectra of the completed dye **1** and previously made dye **BDR_II_013** were found to vary slightly from their synthetic precursors lacking the side chain (**Table 1.3**). The attachment of the zwitterionic side chain appears not change

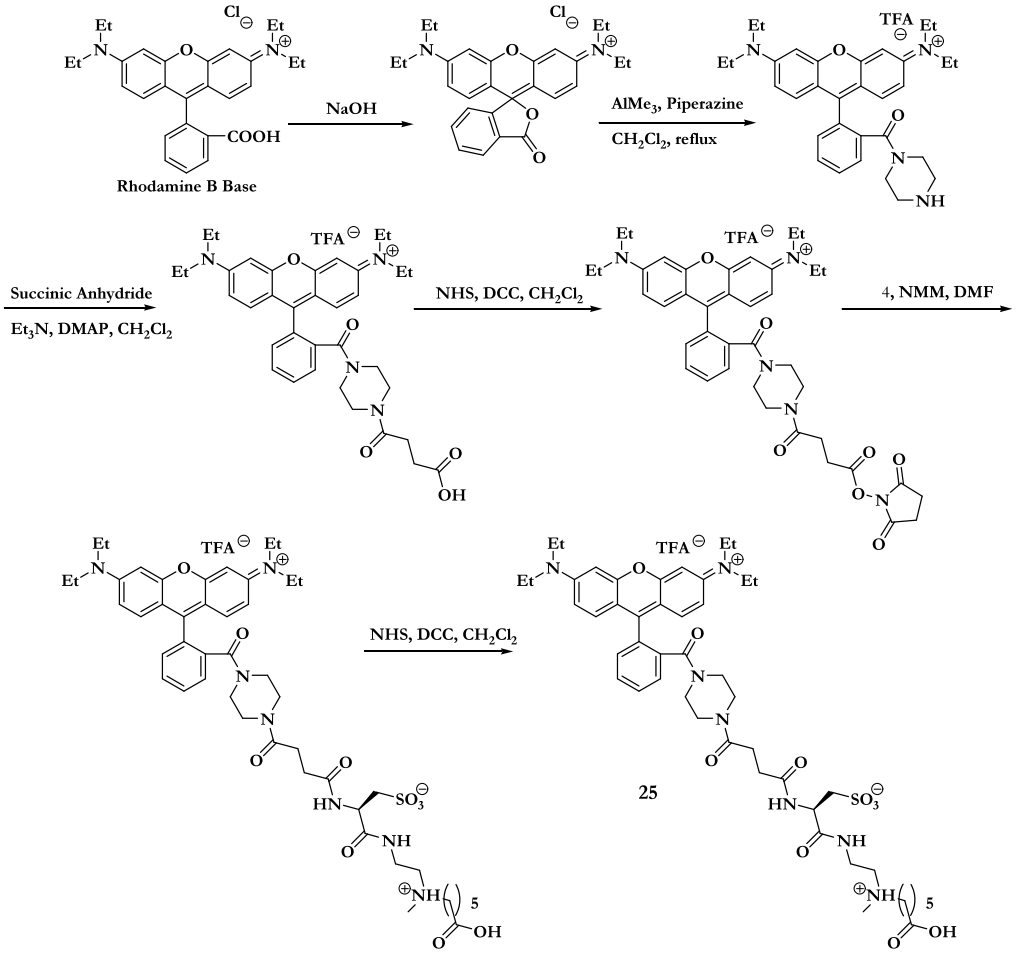
the absorption or emission properties of the fluorophore to any great extent although the extinction coefficient of compound **1** did increase. However, when looking at the extinction coefficients of the starting ester **6** is slightly lower than that of its derivatives. The spectrophotometric data of these compounds also indicate that there was a drop in the quantum yield and brightness of both dyes upon attachment of the side chain, which was rather significant when comparing the brightness of compound **10** to that of compound **14**. Although there were slight variations in the properties of the completed dye when compared to those of the starting esters it appears as though the spectral data of the esters is a good way to gauge the usefulness of the completed dye before the side chain is attached.

*Table 1.3. Absorption, Emission, Extinction Coefficient, Quantum Yield, and Brightness of Rhodamine Dyes **BDR_II_013** and **1**.*

Name	Structure	λ_{max} (nm)	λ_{em} (nm)	ε/(l(cm*mol)	QY (%)	B_{532nm}
BDR_II_013		556	579	80751	33	9699
1 EAS II 61		555	578	82713	67	55418

Although the tetramethyl rhodamine derivatives have been made and exhibit good

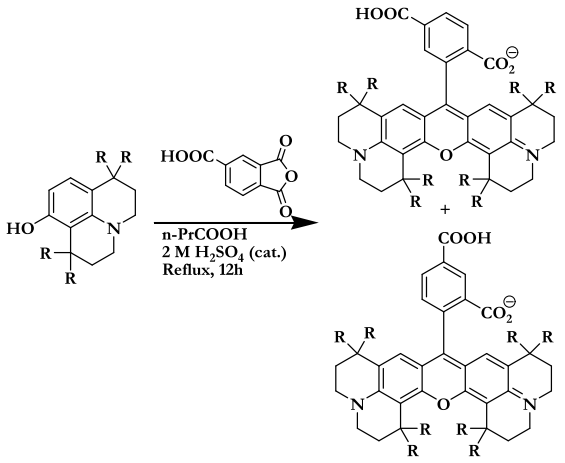
fluorescence properties, they require many steps for synthesis. Thus, the Grieco/Dratz lab has replaced these tetramethyl rhodamine dyes with BDR_I_227 (**25**) for use in proteomics due to its ease of synthesis starting from commercially available Rhodamine B base (**Scheme 1.8**). This prevents the need for the exhaustive Grignard addition of the aryl iodide to the xanthenone core which has proved troublesome and low yielding (6-43% yields).



*Scheme 1.8: Synthesis of BDR_I_227 (**25**): A Rhodamine Piperazine Derivative*

The Grignard reaction for the coupling of aromatic iodides to xanthenone has not been a high yielding reaction in our laboratory (<50% yield). Recent literature presents

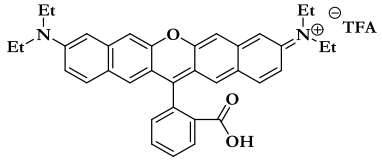
several new variations to synthesize functionalized rhodamines. Among these approaches is the formation of carboxyrhodamines by a symmetrical condensation reaction between the desired components of the rhodamine core and a carboxyphthalic anhydride of choice to form the entire xanthene core with the amended aromatic moiety in one step (**Scheme 1.9**).[30] This would not only improve the tetramethyl rhodamine synthesis by leaving out the troublesome, time consuming (90h) Grignard addition, but it would also circumvent the hydrolysis step required for side chain attachment and provide a way to access a variety of rhodamine derivatives with various functionality and ring systems.



Scheme 1.9. Rhodamine Condensation Strategy

This chemistry would be an interesting and useful addition to the rhodamine dyes already synthesized in the Grieco/Dratz laboratory. It is thought that extending the conjugated pi system of the rhodamine core might shift the emission characteristics of the dye to the red, which would be extremely useful as the current squaraine based red dyes in the Grieco/Dratz laboratory are acid sensitive and have lower quantum yields when applied to two dimensional gels. Thus, target **26** (**Figure 1.16**) is proposed as an interesting synthetic goal using condensation reactions to extend the conjugation using

naphthalene starting material while providing a handle for side chain attachment.



26

Figure 1.16. Target for Future Rhodamine Synthesis

Summary

Tetramethyl rhodamine dyes containing a variety of substitution patterns and an ester linkage for attachment of the ZDye side chain have been shown to have good extinction coefficients and quantum yields. Although the formation of the rhodamine ester core from xanthenone require long reaction times, side chains have been shown to be easily amended using standard peptide coupling reagents. A series of these dyes has been developed to study the effects of various substitution patterns in these dyes. Of this series, dye **6** was shown to have the best quantum yield and brightness. This dye was then carried on to ZDye **1** for use in proteomic labeling studies.

IRIDIUM DYES

Introduction

Most commercially available dyes require complex laser systems and analytical computer programs to respectively excite the fluorophores and detect, analyze, and view the emission. The process is complex as well as costly. For example, the use of three different lasers to excite blue, green, and red dyes has been traditionally used for multiplexing experiments. The three organic fluorophores selected by the Grieco/Dratz laboratory for blue, green, and red emission contain the BODIPY, rhodamine, and squaraine dye cores (**Figure 2.1**).

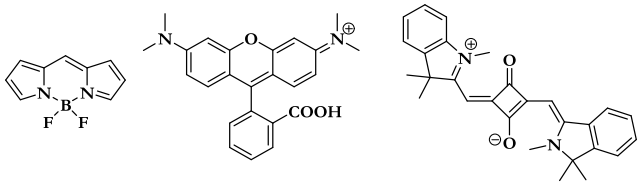


Figure 2.1. BODIPY, Rhodamine, and Squaraine cores

Iridium(III) cationic fluorophores are dyes which are highly stable, emit at room temperature, absorb ultraviolet light and emit in the visible region of the electromagnetic spectrum. It is thought that these dyes could be the solution to some of the problems encountered with traditional dyes because they can be excited with a simple hand held UV light. Furthermore the large Stoke's shifts of these compounds give emission wavelengths in the visible region which would circumvent the need for specialized emission equipment for detection.

Background on Transition Metal Complexes

Transition metal complexes exhibiting luminescence have been used in a wide range of applications including organic light emitting diodes (OLEDs), photovoltaic cells and solar energy conversion, photosynthesis imitation, sensors, photoinduced hydrogen production, and biological labeling. These complexes include Osmium(II), Rhenium(I), Ruthenium(II), and Platinum(II) metal centers (**Table 2.1**) among others; all well known phosphorescent emitters with high quantum yields.[31]

Table 2.1. Common transition metals used in phosphorescent complexes

Ox. State	Ru	Os	Rh	Ir	Pd	Pt
II	$\boldsymbol{d^6}$	$\boldsymbol{d^6}$	d^7	d^7	d^8	d^8
III	d^5	d^5	$\boldsymbol{d^6}$	$\boldsymbol{d^6}$	d^7	d^7
IV	d^4	d^4	d^5	d^5	$\boldsymbol{d^6}$	$\boldsymbol{d^6}$
V	d^3	d^3	d^4	d^4	d^5	d^5
VI	d^2	d^2	d^3	d^3	d^4	d^4

Most coordination compounds containing transition metals are highly colored. For example, Prussian Blue dye, found in blueprints, contains Fe(II) and Fe(III) coordination compounds with cyanide ligands and emeralds exhibit their green coloring due to Cr(III) found in their crystal lattice. Absorption of energy by coordination compounds involves electronic transitions between the *d* orbitals of the metals and the contribution of electrons from the ligands coordinated to the metals. These ligand effects can be altered by changing the ligands or by altering the electronic effects of the ligands by substitution with functional groups. Although coordination compounds portray the complementary color to which they absorb, for example if they absorb orange light they

appear blue, they often contain many absorption bands of different energies and intensities as well as numerous emission bands resulting from multiple types of electronic transitions.[32]

Phosphorescence of TM Complexes

There has been considerable synthetic interest in transition metal complexes because of their phosphorescence properties.[33] Their unique properties are due to complex electron transfer processes upon irradiation. The high emission quantum yields of coordination compounds are based on a combination of effects:

- Metal to ligand charge transfer (MLCT)
- Intraligand charge transfer (ILCT)
- Intersystem crossing between singlet and triplet excited states
- Strong spin orbit coupling found in heavy transition metals.

Metal to ligand charge transfer (MLCT) is found in complexes containing ligands with π electron acceptor capabilities, such as bipyridine ligands. Empty π* orbitals on these ligands can accept electrons from the metal *d* orbitals upon absorption of light, resulting in the oxidation of the metal and an excited state (*d*-π*). These MLCT transitions (d-π*) yield absorptions that are much more intense than *d*-*d* transitions, which are referred to as metal-centered (MC) excitations (*d*-*d**).[32,33]

Whereas MLCT involves transition of electrons between ligands and the metal center, intraligand charge transfer (ILCT) involves the absorption of energy and transfer of electrons within the ligands themselves (π-π*). This occurs when the ligands bound to the metal center are chromophoric. Organic chromophores are commonly composed of

carbon-carbon double bonds and carbonyl groups, which absorb radiation at characteristic wavelengths in all compounds.[33]

Spin orbit coupling (SOC) is most important in organometallic complexes containing heavier metal centers (those heavier than Zr) and can significantly alter the electronic spectra of these complexes. This phenomenon is used to describe the coupling of both the spin angular momentum and the orbital angular momentum of atoms.[34]

All electronic transitions must conserve energy and momentum upon irradiation. The ground state for most organometallic complexes is usually the singlet state, meaning that all electrons are spin paired. Upon absorption of energy, electrons are excited to higher energy levels. If the excited state is still spin paired it is a singlet excited state. Triplet states exist when one pair of electron spins is unpaired (**Figure 2.2**).[33]

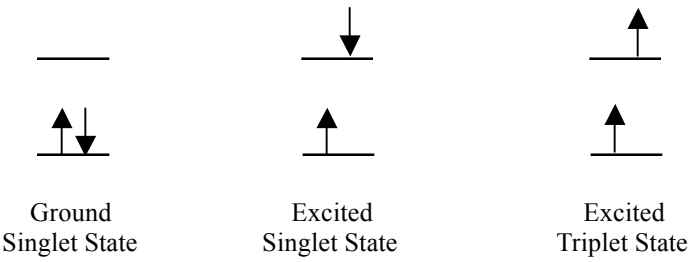


Figure 2.2. Singlet and Triplet States

After absorption of energy the molecule must return to its stable ground state configuration through radiation. There are two types of radiation by which energy can be transferred between a molecule and its surroundings. Radiative transitions are from the emission or absorption of a photon, whereas nonradiative transitions occur when energy is transferred to the surroundings or through internal transition of electrons by rotational, vibrational, or electronic states.[33]

Fluorescence is observed when electrons are excited from the singlet ground state to the excited singlet state and return to the ground state through emission of a photon. If the molecule has high spin orbit coupling the spin of an excited electron can be flipped so that one pair of electron spins is unpaired, the triplet excited state, which is lower in energy than the singlet state. This process is termed intersystem crossing. The triplet excited state can then lose energy by photon emission giving phosphorescence (**Figure 2.3**). Phosphorescence emission can occur for longer periods after irradiation because the excited triplet state can exist for as long as 10^{-3} seconds in comparison to the very short lifetimes of the singlet excited state (10^{-7} sec), leading to longer emission lifetimes.[32] However, because radiationless decay and internal relaxations compete with phosphorescence it is often only seen at low temperatures, although second and third row transition metal complexes are more likely to phosphoresce at room temperature due to enhanced intersystem crossing.[35]

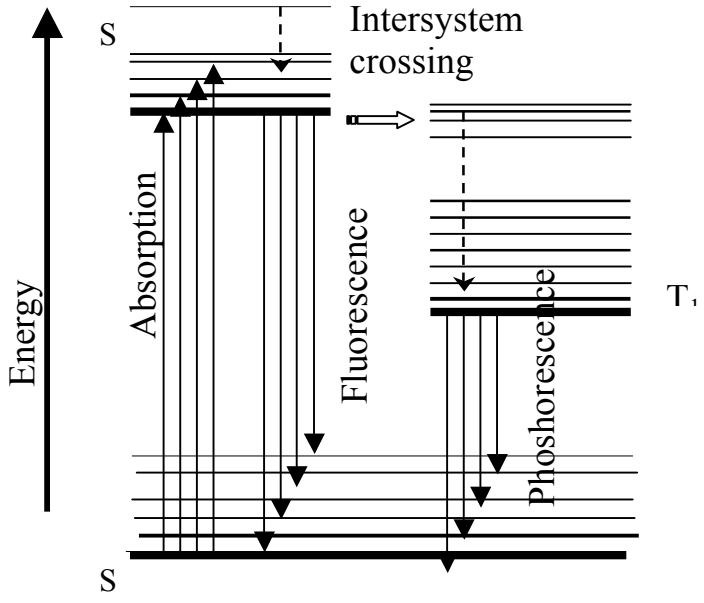


Figure 2.3. Fluorescence vs. Phosphorescence and Intersystem Crossing

Iridium(III) Complexes as Phosphorescent Emitters

Iridium(III), with six *d* electrons, exists as an octahedral complex and forms both neutral and cationic complexes with cyclometalating ligands; both of which have been reported for numerous applications. Neutral Iridium(III) compounds consist of an Iridium core bound to three cyclometalating ligands (C^N). However, the focus of much Iridium chemistry for photoluminescent compounds has turned to cationic Iridium(III) complexes containing bidentate ligands. These compounds are composed of two equivalent cyclometalating ligands bound through an aromatic carbon ring and heterocyclic ring (C^N) and a third ancillary ligand bound to the metal center through two nitrogen centers (N^N) (**Figure 2.4**).[36]

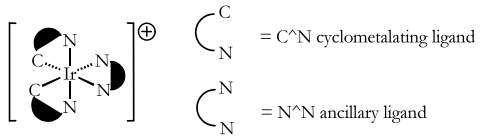


Figure 2.4. Cationic Iridium (III) Complex

This shift towards cationic Iridium is due to the ease of synthesis and mild reaction conditions for cationic Iridium complexes compared to their neutral counterparts (**Figure 2.5**). The synthesis of neutral Iridium complexes often leads to mixtures of *mer*- and *fac*- isomeric products, complicating analysis because of their different photophysical properties.[36] Ir(III) cationic complexes have good solubility in polar solvents, are stable to air, and have rich photophysical properties and ionic character as well as efficient phosphorescence at room temperature.[35]

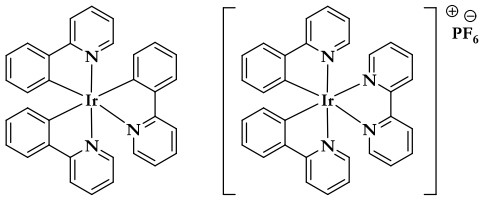


Figure 2.5. Neutral vs. Cationic Iridium (III) Complexes

Iridium(III) complexes ($5d^6$) have shown promise as room temperature phosphorescent materials for their synthetic versatility and color tunability, in addition to recent advances in thermal and photo-stability, high phosphorescence quantum efficiency, and short excited state lifetimes.[37,38] Ir(III) complexes are triplet emitters: the lowest energy excited state is the triplet state and is localized on one ligand. The enhanced emission efficiency of Iridium(III) complexes comes from the mixing of a ligand centered triplet excited state with singlet and triplet MLCT made possible by the large amount of SOC present in heavy Iridium atoms facilitating intersystem crossing (**Figure 2.6**).[33]

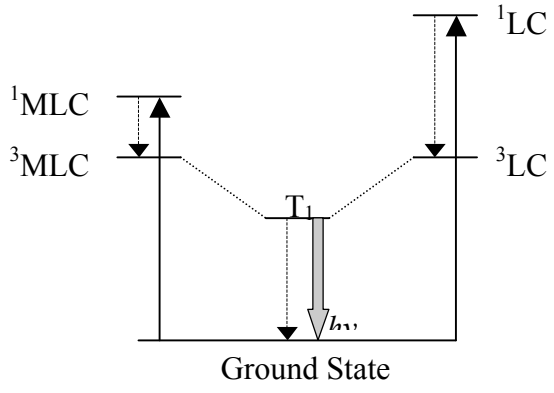


Figure 2.6. Intersystem Crossing and SOC

The extent to which SOC can affect emission can be seen by comparing isoelectronic Ir(III) and Rh(III) complexes. While the complexes with the heavier

Iridium metal, and thus greater SOC, give intense photoluminescence at room temperature the lighter rhodium analogues emit only at low temperatures.[39] This mixing of MLCT character into the ligand centered triplet state gives complexes with large quantum yields and in some cases 100% luminescent efficiency, which differs from counterparts such as Ru(II), Os(II), and Re(I) complexes where nonradiative relaxation causes low emission efficiency (**Table 2.2**).[33, 40]

Table 2.2. Comparison of some metal centered phosphorescent complexes

	TM Row	QY	Emission	Phosphorescence	Implementations
Mn(I) d^6 Mn(II) d^5 Ni(0) d^{10} Cr(III) d^3 Cu(I) d^{10}	1	Poor	Weak red	Only weakly in Cr(III) and Cu(I) complexes	Few
Re(I) $5d^6$	3	10^{-3} to (0.39-0.77)	orange-yellow emission	Strong RT	Use in OLEDs hindered by expense
Ru(II) $4d^6$	2	10^{-1} to 10^{-3}	orange-red emission, poor tenability	Strong RT	OLEDs
Os(II) $5d^6$	3	0.63-0.75	Green, yellow, and red/IR emission	Strong RT	OLEDs
Rh(III) $4d^6$	2			Low temperature only	
Ir(III) $5d^6$	3	0.1-0.9	White/Blue-Red	Strong RT	OLEDs
Pd(II) $4d^8$	2	Up to 0.43	Red	Low temperature, rare	Rare
Pt(II) $5d^8$	3	up to 0.68	White/blue- red	Strong RT	Recent OLED

Tuning of Ir(III) Complexes

In addition to their efficiency as phosphorescent emitters, Ir(III) complexes display a large Stokes shift. While absorbing in the ultraviolet (UV) region of the electromagnetic spectrum these complexes emit visible light. This emission can be tuned to different wavelengths in a variety of ways, resulting in the synthesis of Ir(III) complexes emitting blue, green, yellow, orange, and red light. There are multiple ways to tune the emission of Ir(III) complexes, however they are classified under two categories.

The first strategy involves variation of ligand substituents while the second involves ligand replacement. Both approaches change the energy of the metal and ligand orbitals, which alters the extent of MLCT and LC mixing.[40] These strategies are based on the stabilization of the metal HOMO or destabilization of the ancillary ligand (N^N) LUMO. Cationic Ir(III) complexes have further tunability because the cyclometalating ligands can be altered independently of the ancillary ligand.[41]

Conjugation

By changing the degree of conjugation in the cyclometalating or ancillary ligands, tuning of the complex can be achieved. Alteration of the size or aromaticity of the ligands changes the excited state transitions. While extending the conjugated aromatic systems used as ligands stabilizes the complex, by diffusing electron density, and leads to longer phosphorescence lifetimes, bulky aromatic ligands can be used to distort ligands from planarity. This distortion breaks aromaticity, destabilizing π orbitals and increasing the MLCT to LC transition. However, this approach can lead to greater nonradiative decay resulting in lower quantum yields.[40]

One way to increase the size and conjugation of the π system without sacrificing planarity is to implement tridentate ligands. This preserves the phosphorescent properties of the Ir (III) complex while also providing tunability (**Figure 2.7**).[40, 42]

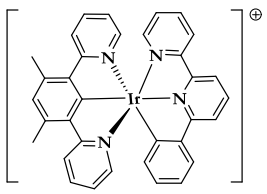


Figure 2.7. Example of a Tridentate Iridium Complex

Electronic Effects

Electronic effects are easily incorporated into ligand structures and the use of electron withdrawing or electron donating groups for HOMO alteration by giving and accepting electrons from the metal respectively has been extensively applied. However, integration of withdrawing or donating groups into ligand structure can also alter the energy of the LUMO. This problem can be mitigated because the third ancillary ligand can be independently substituted from the cyclometalating ligands due to the combinatorial approach to the synthesis of these compounds.[40] Thus, application of an electron-withdrawing substituent on the cyclometalating (C^N) ligands decreases the donation of electrons to the metal, stabilizing the metal HOMO. Conversely, the addition of electron donating substituents to the ancillary ligand (N^N) destabilizes the LUMO of the ligand. Both the stabilization of the HOMO and the destabilization of the LUMO provide for increased HOMO-LUMO gaps and higher emission energies.[40]

The position of substituents on the coordinating ligands also has a large effect on the emission characteristics. Electron withdrawing groups *meta* to coordination sites on the ligand increase both the field strength of the ligand and *d* orbital splitting. Fluoro substition is the exception to this rule. The same effects to field strength and *d* orbital splitting can be observed by the placement of electron donating groups ortho and para to the coordination site.[40]

Variation of Ligand Structure

Although substitution of ligands for tuning of emission properties is unpredictable and not well understood, libraries of Ir(III) complexes consisting of different ligands and their color tuning capabilities have been composed.[43] Referencing these libraries for

insight into ligand character is key in developing cationic Iridium(III) complexes of the desired color.

Applications of Iridium (III) Complexes

Iridium(III) complexes have been applied to a wide variety of applications. The primary focus of this work has been based on applications for organic light emitting diodes (OLEDs) and flat panel display applications. Ir(III), along with other heavy metal centers such as Ru(II) and Os(II), has been a target for these applications because the theoretical emission efficiencies are near 100% for triplet emitters. While neutral Ir(III) complexes have been extensively applied to this technology the introduction of cationic Ir(III) complexes has been beneficial for the simplification of the OLED device. The presence of the counterions in cationic Iridium complexes has proven useful for charge injection purposes in OLED applications and has reduced the required voltage for device operation and led to alternating current (AC) power sources (**Figure 2.8**).[44]

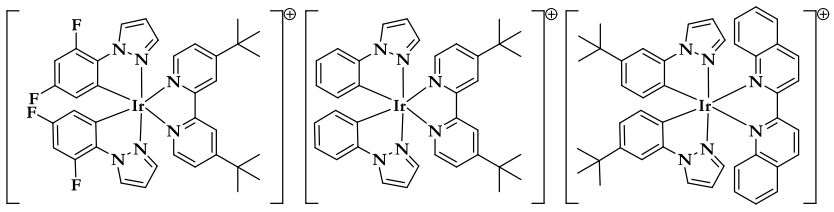


Figure 2.8. Series of Cationic Ir(III) blue, green, and red phosphorescent OLEDs

Iridium complexes have also been utilized as oxygen sensors in a variety of different contexts because the transfer of energy from the excited triplet states of Iridium complexes to the triplet ground state of molecular oxygen quenches the iridium luminescence and forms singlet oxygen. However, the use of Ir(III) oxygen sensors has

been problematic due to self-quenching.[40]

Applications ranging from photosensitizers, hydrogen production by water splitting, photosynthesis mimicking, and ion sensors have utilized Ir(III) complexes, however their use in biological applications by Kenneth Lo could be a useful precedent for future Iridium ZDye applications.[40,45,46] The large Stokes shift and visible emission wavelength of Ir(III) complexes make them a promising target for biological applications. Cheap and easy excitation of these complexes using UV lamps and visible emission of the dyes are beneficial in a setting where most covalent fluorescent dyes require expensive and complex lasers for excitation and detection equipment for proper analysis.

Ir(III) Complexes for Biological Applications

Lo *et al.* first reported the use of Ir(III) complexes as biological labeling reagents in 2001. These were cylcometalated Iridium(III) polypyridine complexes containing a third phenanothroline ligand to which isothiocyanate (NCS) and iodacetamide groups were added for reaction with primary amine and sulfhydryl groups of biological molecules respectively (**Figure 2.9**).[47]

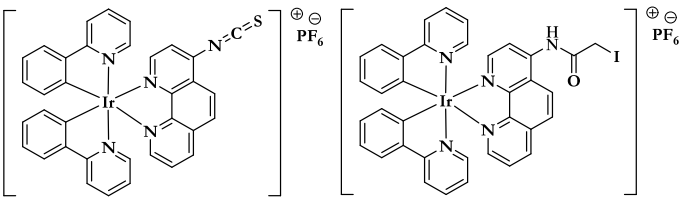


Figure 2.9. NCS and Iodoacetamide complexes

Extension of this work by Lo involved terpyridine ligands with NCS groups, various diimine complexes with both NCS and iodoacetamide groups, and bipyridine-aldehyde complexes for reaction with primary amines (**Figure 2.10**).[48,49,50]

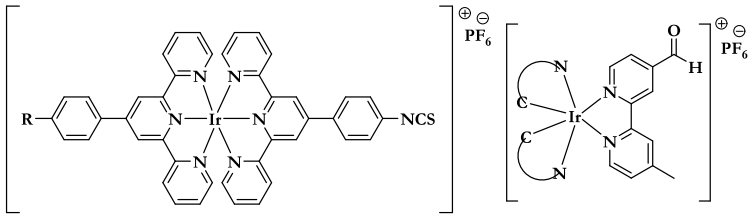


Figure 2.10. A) Terpyridine Complex with NCS linker B) Aldehyde linker

As an extension of Ir(III) biological labeling reagents, Lo and coworkers have reported the synthesis of biotin containing Iridium complexes as crosslinking probes for avidin. The biotin-avidin interaction has been used in a variety of analytical applications wherein biomolecules are modified with biotin and then recognized by avidin molecules labeled with fluorophores or vice versa (**Figure 2.11**).[51]

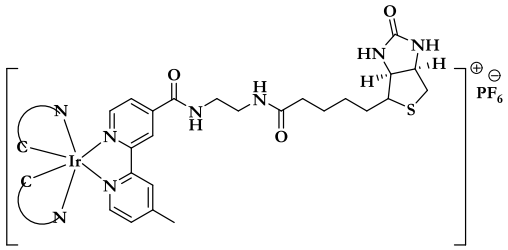


Figure 2.11. Avidin Binding Iridium Probe (Contains Biotin)

Finally, Lo and coworkers have synthesized examples of estradiol conjugates as biological probes for estradiol binding proteins, thiourea polypyridine complexes for anion binding, and complexes containing alkyl chains for interaction with lipids, surfactants and cells (**Figure 2.12)**.[52]

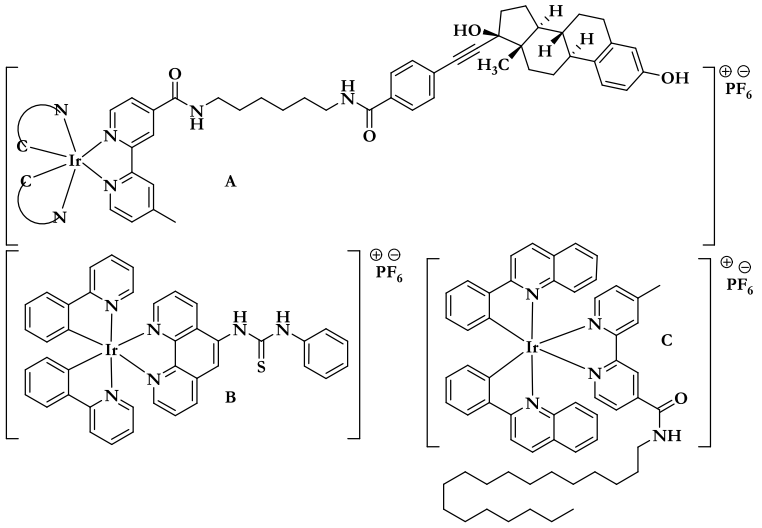


Figure 2.12. A) Estradiol conjugate B) Thiourea polypyridine complex C) Ir(III) complex containing alkyl chain for lipid interaction

Although Lo has been the primary driving force for Iridium applications to biological labeling, work using cationic Ir(III) complexes for internal cytoplasm staining with low cytotoxicity and decreased levels of photobleaching in living cells has been reported by Huang and coworkers (**Figure 2.13**). Intracellular staining using Iridium dyes avoids autofluorescence from the absorbance and emission of cellular components due to the large Stokes shift of the dyes and the easy resolution of absorption and emission. Autofluorescence has been a long-term problem when using fluorescent organic molecules.[53]

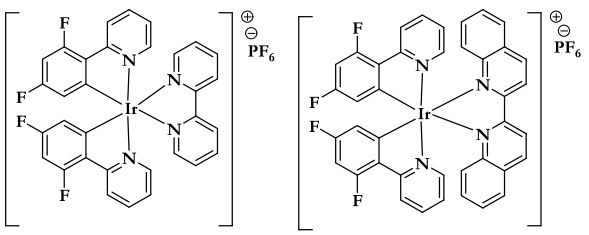


Figure 2.13. Green and Red Iridium Dyes of Huang et al.

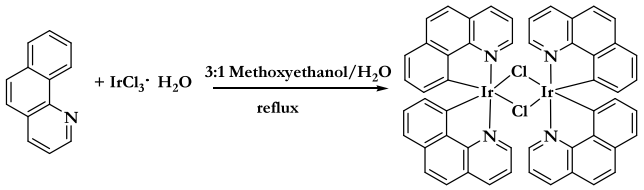
Iridium Dye Synthesis

Synthetic Strategy

In summary cationic Ir(III) phosphors are robust, tunable, highly efficient complexes with high quantum yields and large Stokes shifts. The ease of application of these dyes in a laboratory setting due to UV excitation and visible emission has made them interesting targets not only for traditional ZDye chemistry but for other possible applications.

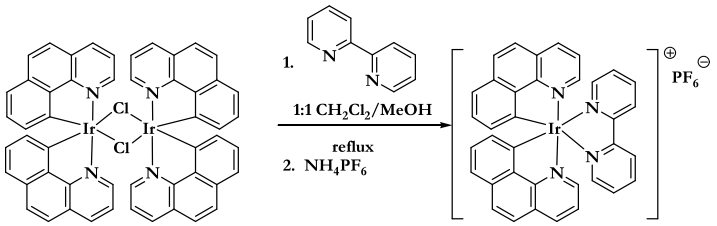
With this in mind a series of Iridium cationic fluorophores, some of which contain a carboxylic acid handle for further synthetic extension of the fluorophore core, were proposed to study their absorption and emission characteristics. This handle would serve a variety of purposes, from extension with the standard Grieco/Dratz side chain for possible use in protein labeling, to addition of other bio recognition sequences for other applications and molecular recognition technologies.

The synthesis of these cationic Iridium fluorophores is well established in the literature and proceeds with the formation of a dichloro bridged Iridium "dimer" complex from Iridium trichloride and the carbon-nitrogen cyclometalating ligand of choice. This Nonoyama Reaction was first reported in 1974 and has become the standard method for preparation of Ir(III) intermediate complexes ever since. The inertness of Ir(III) requires refluxing in methoxyethanol in order to form the dichloro bridged complex and to proceed in good yields (**Scheme 2.1**).[54]



Scheme 2.1. Nonoyama Reaction

After formation of the Iridium dimer it is relatively simple to install a nitrogen-nitrogen (N^N) cyclometalating heterocyclic ligand by refluxing the ligand of choice with the dimer in an equal ratio of methanol and dichloromethane using anhydrous conditions (**Scheme 2.2**).[44] Addition of ammonium hexafluorophosphate provides the Iridium(III) complex as a hexafluorophosphate salt.

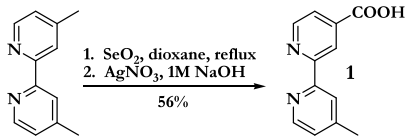


Scheme 2.2. Addition of Nitrogen-Nitrogen (N^N) Cyclometalating Ancillary Ligand

The addition of a carboxylic acid functionalized (N^N) cyclometalating ligand might shift the emission characteristics of an Iridium fluorophore to great extent based upon the electron withdrawing nature of the group. It was therefore deemed useful to develop a series of Iridium (III) cationic fluorophores to determine the extent to which the carboxylic acid linker shifts the emission characteristics of the dye. The goal of creating this series of Iridium dyes was to create a series of Iridium dyes with multiple emission wavelengths so as to achieve a "rainbow" of colors while also studying the effects of the carboxylic acid group on the spectral properties.

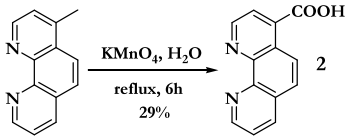
With these goals in mind two carboxylic acid containing N^N cyclometalating

ligands were proposed. The first, ligand **1**, was made from the selective oxidation of one methyl group of 4,4'-dimethyl bipyridine by allylic oxidation using one equivalent of selenium dioxide followed by further oxidation to the carboxylic acid with silver nitrate (**Scheme 2.3**).[55]



Scheme 2.3. Oxidation of 4,4'-dimethyl bipyridine

The second ligand, compound **2**, was suggested as the alternative ancillary ligand possessing a carboxylic acid handle in the hopes of preventing unwanted interactions at the metal center. Large, sterically crowded ligands have previously been reported to enhance lifetimes and quantum yields. By increasing the hydrophobicity of the complex it is thought that the sensitivity of the metal center to water based reactions is reduced and the steric bulk is thought to hinder overlapping aromatic rings of cyclometalating ligands, reducing nonradiative transformations.[56] Ligand **2** was made by oxidation of 4-methyl-1,10-phenanthroline using potassium permanganate in water (**Scheme 2.4**).



Scheme 2.4. Oxidation of 4-methyl-1,10-phenanthroline

With these ligands in hand, Iridium dimers containing 2-phenyl pyridine **3**, 2-phenyl pyrazole **4**, and 2-(2,4-difluorophenyl)pyridine **5** were made through the standard Nonoyama procedure (**Figure** 2.**14**). Previous examples of blue-emitting Iridium

complexes have been reported using 1,2,4-triazole ancillary ligands.[57] Thus, the pyrazole ligand was proposed for tuning of the blue Iridium dye precursor **4**. Compound **5** was chosen as a precursor because literature has also shown that the addition of fluorine substituents on the phenyl pyridine ring of cyclometalating ligands provides compounds of green color.[58]

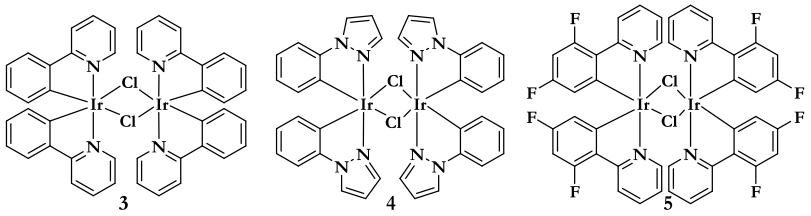


Figure 2.14. Yellow, Blue and Green Iridium Dimers

To complete a series of Iridium dyes these Iridium dimers were then combined with various C^N cyclometalating ancillary ligands in refluxing methanol and dichloromethane to form a series of Iridium(III) cationic dyes. These ancillary ligands included bipyridine, 4,4'-dimethyl bipyridine, 4-methyl-1,10-phenanthroline, and 5-methyl-1,10-phenanthroline, in addition to the carboxylic acid ligands **1** and **2,** to give compounds **6** through **23** (**Figure 2.15**).

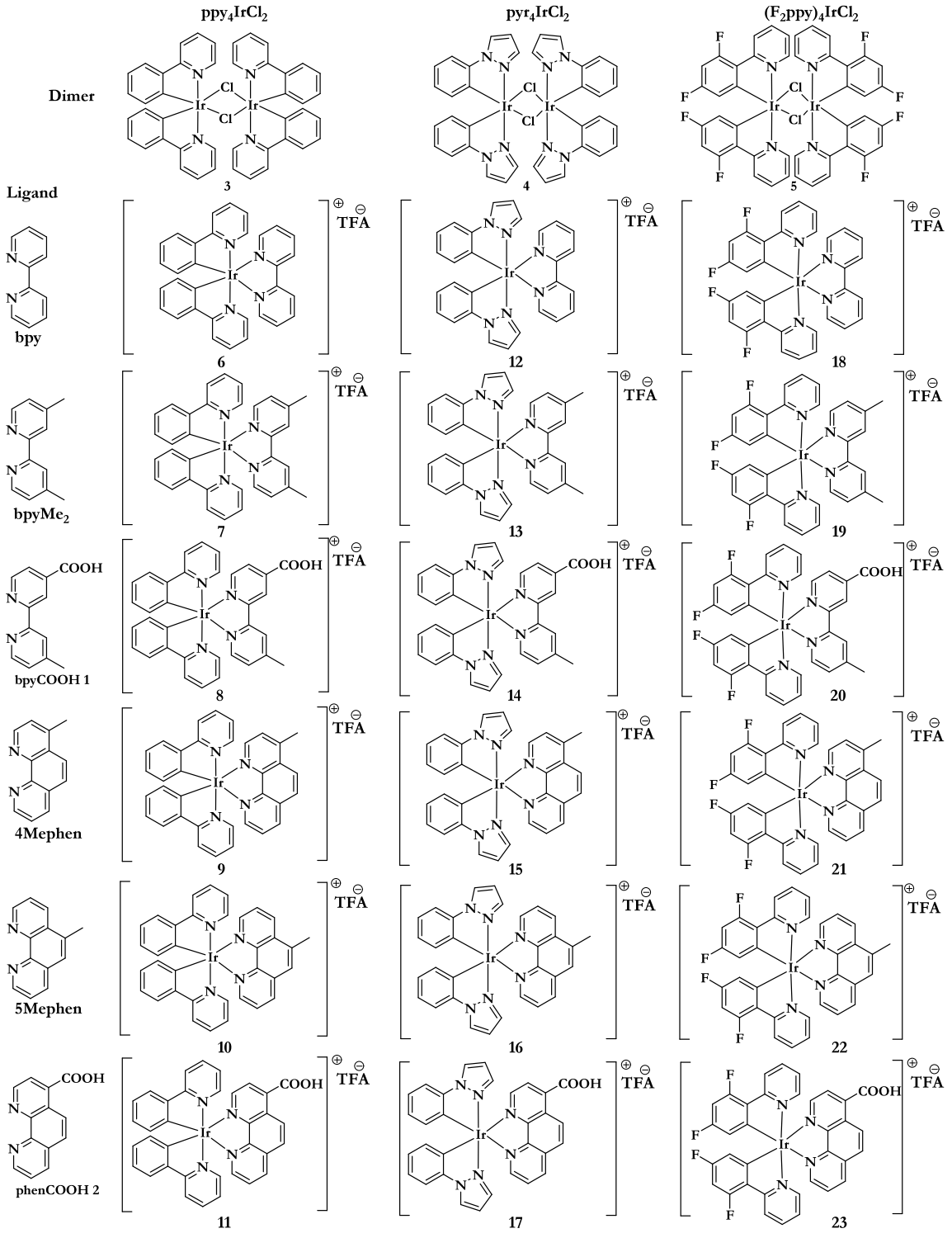


Figure 2.15. Iridium Fluorophore Series ***(6-23)***

Photochemistry

The absorption and emission characteristics of these complexes were studied to better determine which dyes would be good targets for further development and to compare the effects of various substitution on both the ancillary ligand and the dimer ligands. The absorption maximum, extinction coefficient, emission maximum, quantum yield, and brightness were determined for each fluorophore.

The extinction coefficient of each dye was calculated using the Beer-Lambert Law where A is equal to the absorbance of the molecule, ε is equal to the extinction coefficient of the molecule, b is equal to the pathlength of the cuvet, and c is equal to the concentration of the solution (**Equation 2.1**).

$$\mathbf{A = \varepsilon bc}$$

Equation 2.1. Beer-Lambert Law

The quantum yield of each dye was calculated using the optically dilute method, a commonly accepted and widely used technique for quantum yield determination.[59,60] Each dye was diluted to the same volume with acetonitrile to five different concentrations corresponding to 0.02, 0.04, 0.06, 0.08, and 0.1 absorbance units at 400nm. The samples were all degassed by bubbling with argon gas in 25mL vials for 5 minutes each and the emission spectrum of each dilution sample was measured from 400 to 900nm using a Cary fluorimeter, exciting at 400nm. The emission spectra of each dye were then plotted, after applying the lamp correction for the fluorimeter to each measurement and the area under each emission curve was taken. A linear plot of integrated emission intensity vs. absorbance intensity of each solution was then made and the slope of that line was used

to calculate the quantum yield by comparison with a ruthenium standard using **Equation 2.2**.

$$\mathbf{QY_{cpd} = QY_{std}\ (slope_{cpd}/slope_{std})}$$

Equation 2.2. Calculation for Quantum Yield

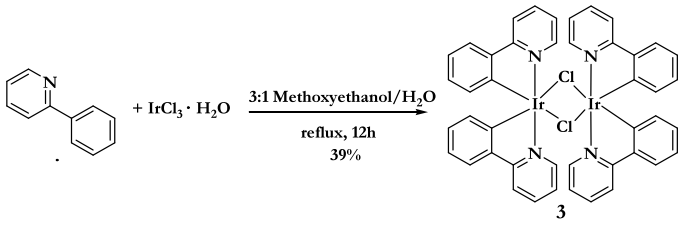
Normally the ratio of the refractive indices of the solvents for both the compound of interest and the standard are also included in the formula, however both the standard and the compounds were measured in acetonitrile and thus, these terms are omitted from the equation. The Ruthenium standard used was Tris(2,2'-bipyridyl)dichlororuthenium(II)hexahydrate [$Ru(ppy)_2Cl_2$] purchased from Sigma Aldrich, CAS No. 50525-27-4. This standard has a reported quantum yield of 0.062 in acetonitrile.[43]

Results and Discussion

Synthesis of Iridium Compounds

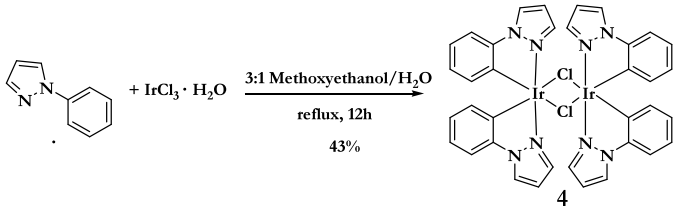
Carboxylic acid ligand **1** was made by allylic oxidation of 4,4'-dimethyl-2,2'-bipyridine with one equivalent of selenium dioxide followed by silver nitrate to further oxidize any aldehyde products to the carboxylic acid, isolated as a white powder (**Refer to Scheme 2.3**).

The carboxylic acid containing 1,10-phenanthroline ligand **2** was synthesized from the commercially available 4-methyl-1,10-phenanthroline by refluxing in water with potassium permanganate. The solution was then acidified and the solid white/grey compound **2** was isolated by recrystallization from water (**Refer to Scheme 2.4**).



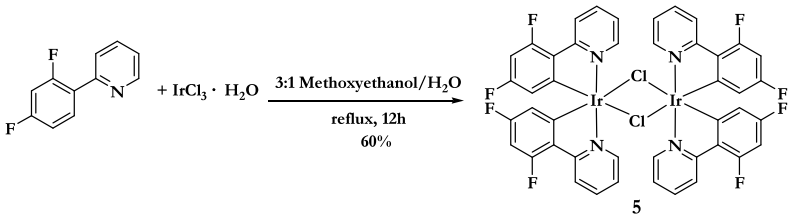
*Scheme 2.5. Synthesis of Yellow Iridium Dimer **3***

The yellow Iridium dimer, compound **3**, was made using standard Iridium chemistry. A solution of Iridium trichloride monohydrate was refluxed with excess phenyl pyridine in a 3:1 mixture of 2-methoxyethanol and water under argon for 12h. The resulting yellow solid was purified using column chromatography to yield a yellow powder, compound **3 (Scheme 2.5**).



*Scheme 2.6. Synthesis of Blue Iridium Dimer **4***

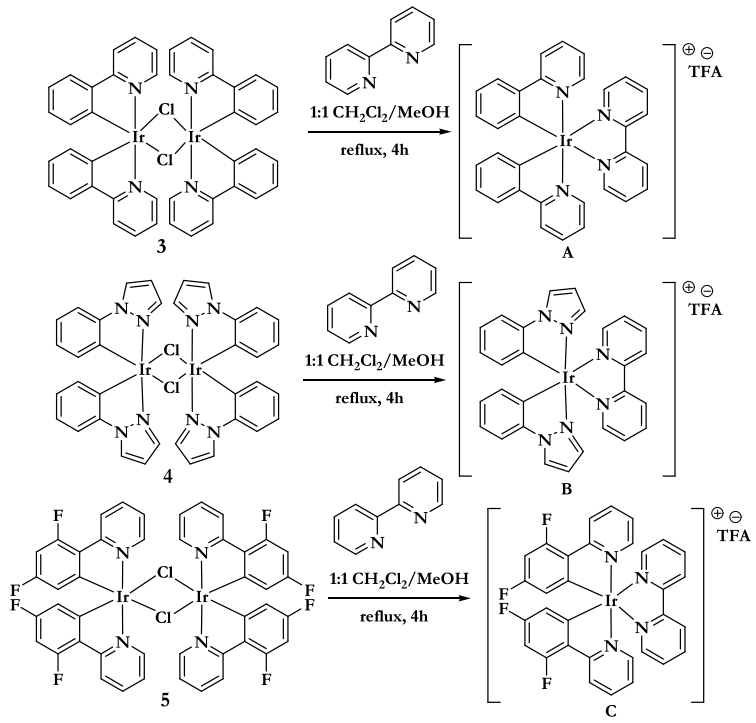
The blue dimer **4** containing cyclometalating 2-phenylpyrazole ligands was obtained in the same way as compound **3**. A solution of Iridium trichloride monohydrate and 2-phenylpyrazole was refluxed in 3:1 2-methoxyethanol and water for 12h. The compound was then purified by column chromatography and washed with acetone to yield a white/grey solid, compound **4** (**Scheme 2.6**).



*Scheme 2.7. Synthesis of Green Iridium Dimer **5***

The green Iridium dimer containing fluorinated phenylpyridine ligands, was made in the same way as both the phenylpyridine and phenylpyrazole dimer. The addition of the cyclometalating ligand, 2-(2,4-difluorophenyl)pyridine, to a solution of Iridium trichloride monohydrate in refluxing 2-methoxyethanol and water yielded compound **5** as a yellow powder (**Scheme 2.7**).

*Synthesis of Cationic Iridium Complexes **6-23***



*Scheme 2.8. Synthesis of Cationic Iridium Fluorophores **A, B, C***

Compounds **6-23** were all made by the same method. They are represented by compounds **A-C** in **Scheme 2.8**. The standard Nonoyama procedure for Iridium (III) cationic fluorophore formation (**A,B,C**) was followed for each dye. Combining Iridium dimer **3**, **4,** or **5** with the ancillary ligand of choice in a refluxing solution of 1:1 CH_2Cl_2 and MeOH for approximately four hours yields the corresponding cationic Iridium(III) complex shown generically as **A**, **B,** or **C**. Purification of each dye was done using RPHPLC methods. It was confirmed that the hexafluorophosphate ion used in the workup procedure for the Iridium dyes does exchange with the trifluoroacetate anion used in the HPLC solvent by the absence of peaks in phosphorous NMR spectra and the presence of peaks in fluorine NMR data. All of the Iridium fluorophores exhibit easily observable room temperature phosphorescence when submitted to long wave UV light on the bench top, in solid phase, liquid acetonitrile solution, and dichloromethane solution. The emission can be amplified with lower temperatures or degassed solvents.

Spectrophometry

Table 2.3 shows the absorption wavelength, emission wavelength, quantum yield, extinction coefficient, and brightness of each Iridium fluorophore with respect to the Ruthenium standard in acetonitrile solution at room temperature. All solutions were degassed by bubbling with acetonitrile for 5 minutes. The brightness calculation is determined by the multiplication of the quantum yield by the extinction coefficient at a given wavelength and has been determined at both the absorption maxima and the excitation wavelength, 400nm.

Table 2.3. Absorption and Emission Data for Iridium Fluorophores ***6-23***

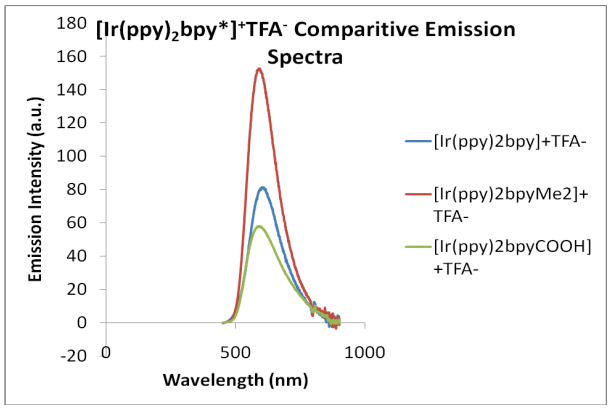
	Abs λ_{max} *(nm)*	*ε* λ_{max} *(1/cm* M)*	*ε 400nm (1/cm* M)*	*Em* λ_{max} *(nm)*	*QY (%)*	*B* λ_{max}	*B 400nm*
6 $[Ir(ppy)_2bpy]^+TFA^-$	**253**	42971	3663	**602**	20	8508	725
7 $[Ir(ppy)_2bpyMe_2]^+TFA^-$	**256**	49359	3424	**589**	27	13326	924
8 $[Ir(ppy_2)_2bpyCOOH]^+TFA^-$	**253**	50443	4824	**598**	14	7162	685
9 $[Ir(ppy)_2\ ^4Mephen]^+TFA^-$	**267**	59748	4172	**586**	24	14339	1001
10 $[Ir(ppy)_2\ ^5Mephen]^+TFA^-$	**268**	70508	5641	**588**	24	17203	1376
11 $[Ir(ppy)_2phenCOOH]^+TFA^-$	**267**	42344	3954	**581**	13	5589	522
12 $[Ir(ppyz)_2\ bpy]^+TFA^-$	**252**	55215	768	**595**	19	10215	142
13 $[Ir(ppyz)_2\ bpyMe_2]^+TFA^-$	**247**	54214	653	**567**	31	16589	200
14 $[Ir(ppyz)_2bpyCOOH]^+TFA^-$	**248**	49848	1477	**650**	6.8	3389	100
15 $[Ir(\ ppyz)_2{}^4Mephen]^+TFA^-$	**268**	46925	1513	**570**	23	10652	343
16 $[Ir(\ ppyz)_2{}^5Mephen]^+TFA^-$	**274**	56730	1404	**576**	21	11913	295
$ppyz)_2phenCOOH\ ]^+TFA^-$	**277**	32017	1915	**560**	6.8	2177	130
18 $[Ir(F_2ppy)_2bpy]^+TFA^-$	**250**	52647	2070	**533**	54	28429	1118
19 $[Ir(F_2ppy)_2bpyMe_2]^+TFA^-$	**248**	49479	1839	**521**	42	20781	772
20 $[Ir(F_2ppy)_2\ bpyCOOH]^+TFA^-$	**252**	52926	2382	**587**	37	19583	881
21 $[Ir(F_2ppy)_2\ ^4Mephen\ ]^+TFA^-$	**229**	49942	2554	**513**	18	8940	457
22 $[Ir(F_2ppy)_2\ ^5Mephen]^+TFA^-$	**270**	47471	2169	**524**	25	11773	538
23$[Ir(F_2ppy)_2phenCOOH]^+TFA^-$	**233**	55929	2599	**636**	11	6376	296
Standard $[Ru(ppy)_2bpy]Cl_2$	**287**				6.2		

*ppy_2 = phenyl pyridine, ppyz = 2-phenyl pyrazole, F_2ppy = 2-(2,4-difluorophenyl)pyridine, bpy = bipyridyl ligand, $bpyMe_2$ = 4,4'-dimethyl bipyridyl, bpyCOOH = ligand **1**, ^{4}Mephen = 4-methyl 1,10-phenanthroline ligand, ^{5}Mephen = 5-methyl 1,10-phenanthroline, phenCOOH = ligand **2**.

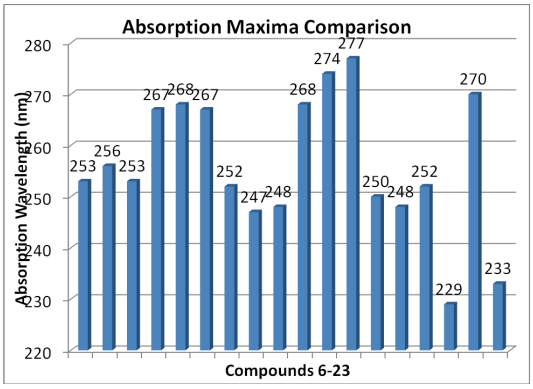
It can be seen that the dye with the greatest extinction coefficient is $[Ir(ppy)_2{}^5Mephen]^+TFA^-$, compound **10**. Since the extinction coefficient is a measure of how well a substance absorbs light at a given wavelength it can be seen that at its maximum absorbance of 268nm compound **10** is the most efficient at absorbing light. It is also the most efficient at absorbing light at the excitation wavelength of 400nm. However, the compound with the greatest quantum yield, that is photons emitted per photons absorbed, is compound **18,** $[Ir(F_2ppy)_2bpy]^+TFA^-$. As the quantum yield is a measure of the efficiency of a compound as a fluorophore at 54% percent this compound is the best fluorophore of the series.

When comparing those compounds functionalized with carboxylic acid groups there are not extremely noticeable trends. For example, **Graph 2.1** shows the emission spectra of the three Iridium dye compounds **6**, **7**, and **8**. Both compounds **6** and **7** lack a carboxylic acid on their bipyridyl ancillary ligand, but compound **8** contains the acid ligand **1.** They all have similar emission wavelengths and extinction coefficients although the electron withdrawing nature of ligand **1** would lead to the hypothesis that the emission should be red shifted.

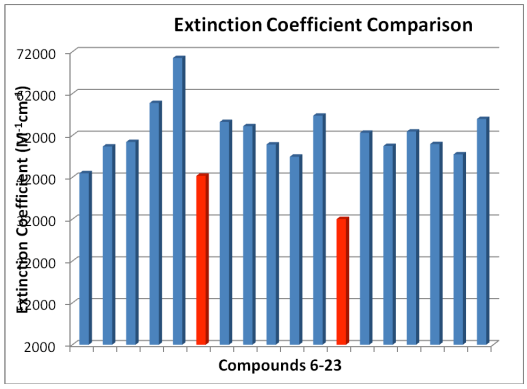
*Graph 2.1. Comparison of the Emission Spectra of Compounds **6, 7, 8***



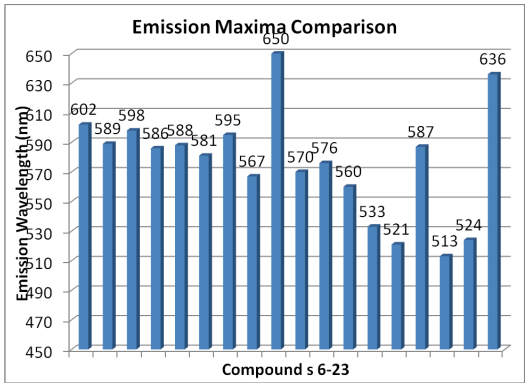
These similarities are present throughout the dye series in that all of the absorption maxima show similar wavelengths (**Graph 2.2**), all of the extinction coefficients are similar (**Graph 2.3**), and finally, and dissapointingly, the emission wavelengths are also similar (**Graph 2.4**). It is interesting to note however, that both compound **11** and compound **17**, containing the phenanthroline carboxylic acid ligand **2** show significant decreases in their extinction coefficients in comparison to their phenanthroline counterparts that do not contain the acid group as shown in red in **Graph 2.3**.



Graph 2.2. Comparison of Absorbance Coefficients



Graph 2.3. Comparison of Extinction Maxima



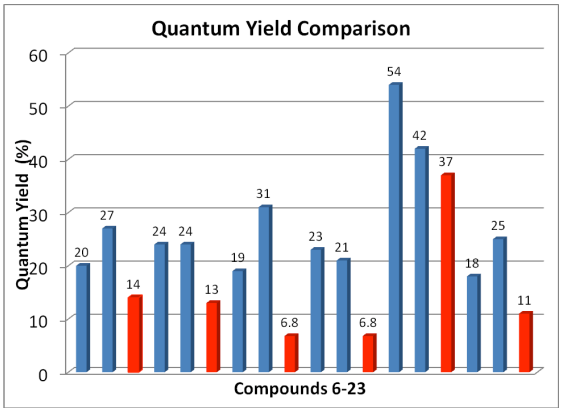
Graph 2.4. Comparison of Emission Maxima

Although the addition of the carboxylic acid functional group was expected to

give more red character to the emission wavelength of the dyes, this trend was less pronounced than expected except in the 2-(2,4-difluorophenyl)pyridine containing dyes (**Graph 2.4**). It can be seen that the addition of electron donating methyl groups onto the ancillary ligand of dye **18** to create dye **19** decreases the emission wavelength from 533nm to 521nm and the addition of the carboxylic acid functionality increases the emission wavelength in compound **20** to 587nm. Also, in the phenanthroline series, dyes **21** and **22** containing the methylated phenanthroline ligands have only a 9nm difference in emission wavelength (513nm and 524nm) while the addition of the carboxylic acid onto the phenanthroline ligand to form complex **23** shifts the wavelength of emission to 636nm.

There is also a surprising decrease in the quantum yield when comparing those compounds with the acid functionality to the fluorophores without this group as shown in **Graph 2.5**. Those fluorophores containing ligands **1** and **2** are shown in red.

Graph 2.5. Quantum Yield Comparisons



Although a variety of Iridium dyes have been synthesized it can be seen that the series excludes any true blue fluorophore (**Figure 2.16**).

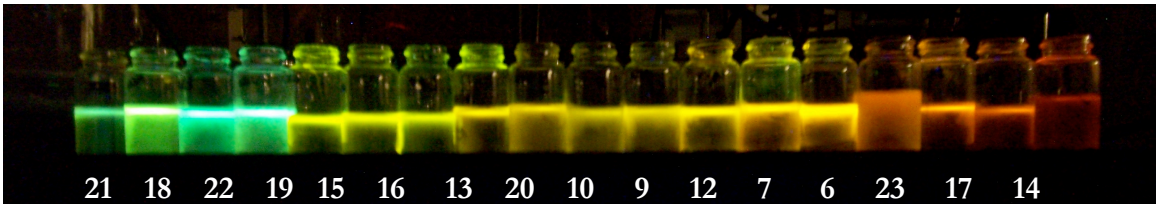


*Figure 2.16. Picture of the dye series **6-23** under radiation*

When considering the effects of ligand structure on the HOMO and LUMO of the metal and ancillary ligand respectively, the following list of strategies for blue shifting the emission of Iridium(III) complexes can be compiled:

- Addition of electron withdrawing groups to the phenyl rings of the carbon nitrogen (C^N) cyclometalating ligands to stabilize the HOMO
- Addition of ancillary groups that are nonaromatic (cyano and isocyanide)
- Destabilization of the LUMO by addition of electron donating groups to the ancillary (N^N) ligand
- Chelation of strong, sigma-donating carbine ligands

It was thought that the presence of an electron donating substituent on the phenanthroline ring would provide a handle for side chain attachment that would also shift the spectrum towards more of a true blue color. It is believed that incorporation of the 4-amino-1,10-phenanthroline ligand into each of the iridium dimers would provide dyes that would have a blue shift in their emission spectrum (**Figure 2.17**). This work is ongoing.

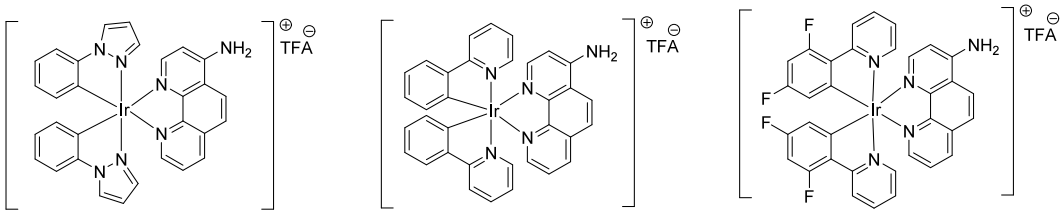


Figure 2.17. 4-amino-1,10-phenanthroline dyes

Functionalization of the Iridium Fluorophores

Synthetic Strategy

Following the successful synthesis of several fluorophores containing a carboxylic acid functionalized ancillary ligand the functionalization of each dye was attempted with the following ZDye targets in mind. Peptide coupling of the zwitterionic "peptide side chain" to bipyridyl complexes **8**, **14**, and **20** would give compounds **24**, **25,** and **26** respectively (**Figure 2.18**) which could be further activated to the N-hydroxysuccinimide esters for labeling of protein amine residues.

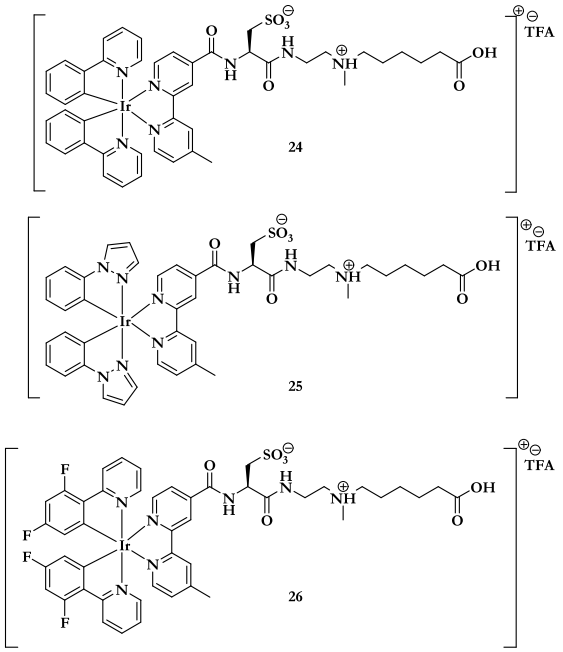


*Figure 2.18. Iridium ZDyes **24, 25,** and **26***

Similarly, the Iridium compounds containing ligand **2** were envisioned to be coupled to the "peptide side chain" to yield Iridium ZDyes **27, 28,** and **29** (**Figure 2.19**) which could also be activated for protein labeling purposes.

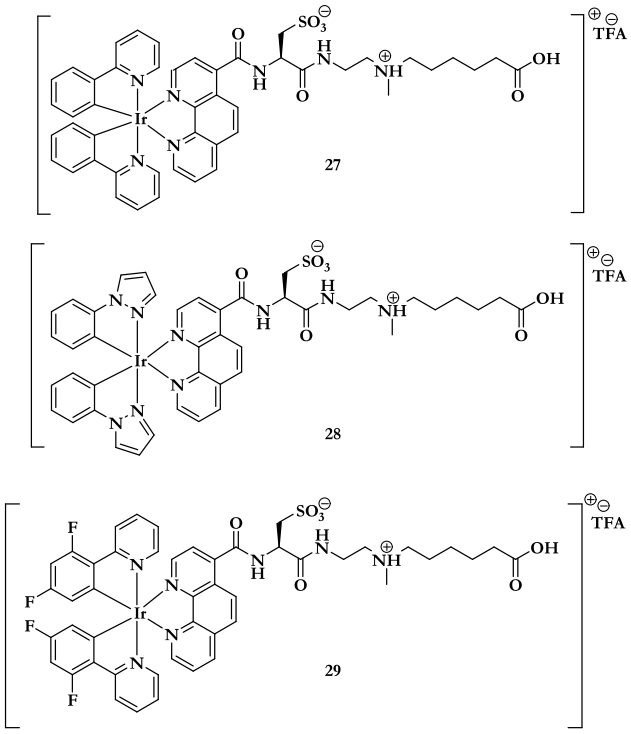
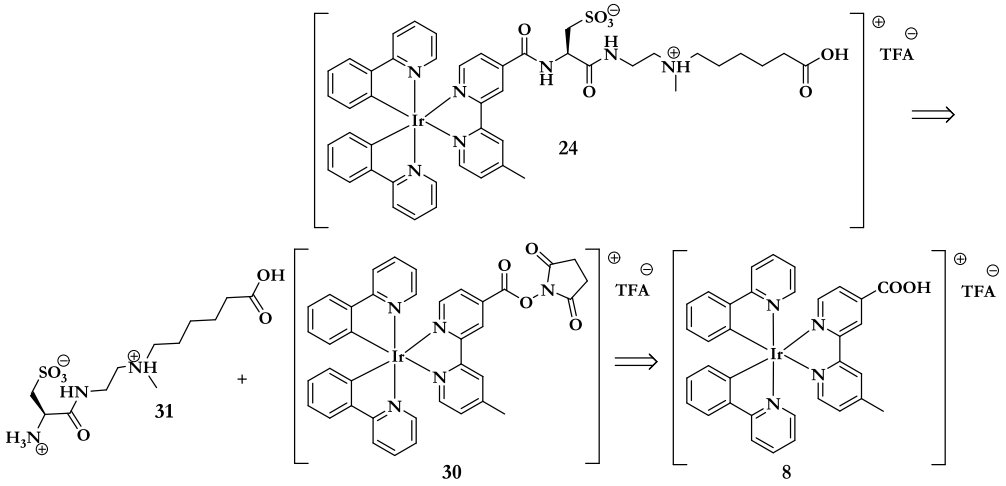


*Figure 2.19. Iridium ZDyes **27, 28,** and **29***

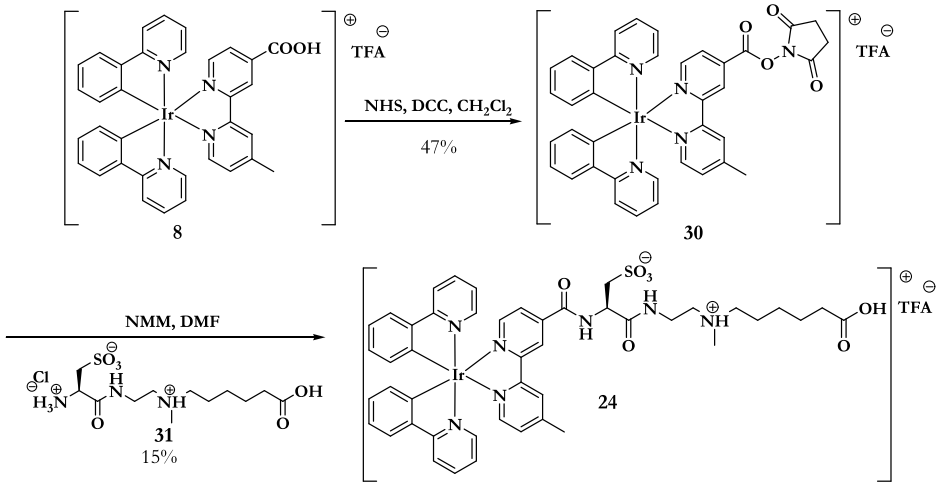
This syntheses of dyes **24-29** were attempted using standard peptide coupling chemistry. Iridium ZDyes were envisioned to come from N-hydroxysuccinimide activation of the corresponding acid, shown for compound **8** in **Scheme 2.9**, using N-hydroxysuccinimide and dicyclohexylcarbodiimide. The succinimide ester **30** could be coupled to the "peptide side chain" **31** to yield the completed dye **24**.



Scheme 2.9. Retrosynthetic Analysis

Results and Discussion

Synthesis of Bipyridyl Compounds

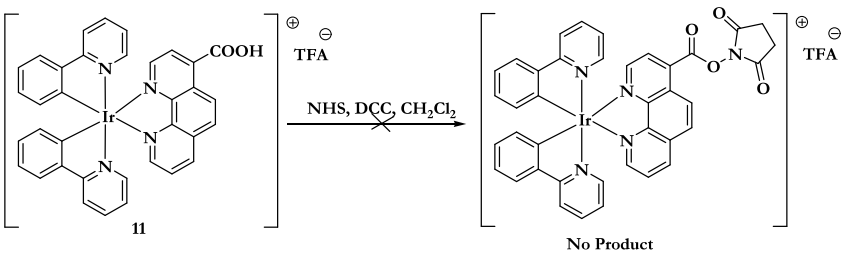


*Scheme 2.10. Synthesis of Iridium Dye **24***

The Iridium ZDye **24** was synthesized by NHS activation of carboxylic acid **8** using dicyclohexylcarbodiimide (DCC) in dichloromethane under argon at room temperature. The activated compound **30** was purified using RP HPLC. Compound **30** was then coupled to the "peptide side chain" **31** using N-methylmorpholine in DMF at

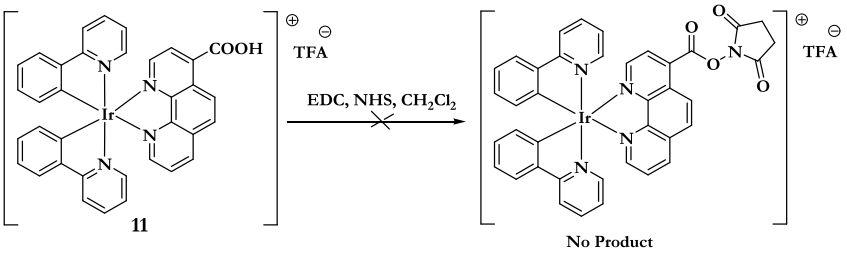
room temperature to yield **24**. All of the Iridium dyes containing the carboxylated bipyridyl ligand, **24, 25,** and **26** were made in this way (**Scheme 2.10**).

Synthesis of Phenanthroline compounds



Scheme 2.11. NHS/DCC Activation of Phenanthroline Acids

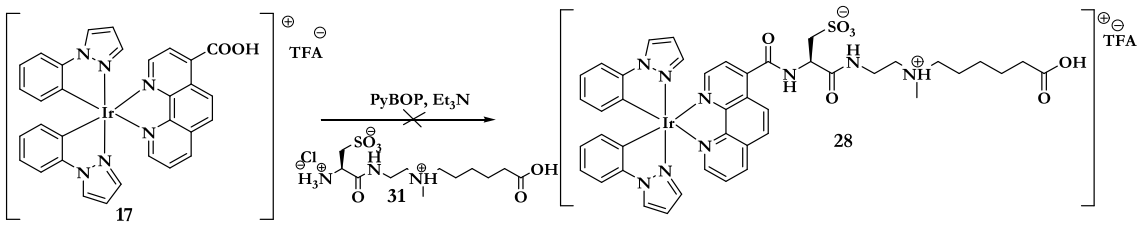
Iridium ZDyes **27, 28,** and **29** were much more difficult to make. Starting from compounds **11**, **17**, and **23** these dyes proved unreactive to the DCC/NHS activating conditions. Reaction of **11**, **17**, and **23** produced no activated product (**Scheme 2.11**). However, NMR analysis showed coupling of the dicyclohexylurea byproduct to the acid.



Scheme 2.12. NHS/EDC Activation of Phenanthroline Acids

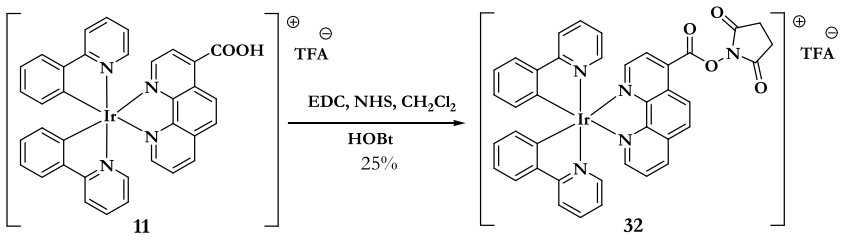
NHS activation of Iridium dyes **11** and **17** was also attempted using NHS and 1-ethyl-3-(3-dimethylaminopropyl) carbodiimide (EDC), an alternative peptide coupling reagent, in dichloromethane at room temperature (**Scheme 2.12**). Both reactions produced no product. NMR and MS analysis show coupling of the EDC urea byproduct

to the carboxylic acid.



*Scheme 2.13. PyBOP coupling to **17***

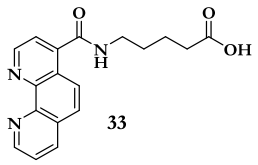
Further efforts to extend the phenanthroline ligand **2** system using a more direct approach were also unsuccessful. Benzotriazol-1-yl-oxytripyrrolidinophosphonium hexafluorophosphate (PyBOP), which is a peptide coupling reagent that allows for coupling of an amine directly to the carboxylic acid using triethylamine did not give the expected product (**Scheme 2.13**).



Scheme 2.14. NHS/EDC/HOBt Activation of Phenanthroline Compounds

Ultimately it was found that EDC/NHS conditions combined with a catalytic amount of Hydroxybenzotriazole (HOBt) to react with the EDC adduct before it rearranged to the urea byproduct did produce small amounts of activated acid **32** as well as the activated acid of compound **17**. However, the presence of starting material and urea byproduct coupling products as well as HOBt byproducts amounted to very poor yields for this activation (**Scheme 2.14**). Further extension of this work would be to

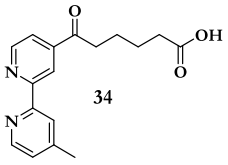
include the synthesis of a phenanthroline ligand similar to compound **33,** wherein an amino valeric acid linker is used to extend the carboxylic acid handle prior to installation of the ancillary ligand into the Iridium core (**Figure 2.20**). It is thought that this extension would help to electronically favor typical NHS/DCC activation and side chain installment while remaining stable enough to survive the high temperatures needed for the cationic complex formation.



33

Figure 2.20. Phenanthroline ligand with valeric acid linker

This valeric acid linker might also prove useful if applied to the iridium dye syntheses containing the bipyridyl carboxylic acid ligands as yields of these reactions are also low. Addition of the linker to ligand **1** to give compound **34** and installation into the iridium dyes in place of ligand **1** might prove to increase yields by improving the steric constraints of the carboxylic acid group (**Figure 2.21**). This linker might also decrease the electronegative effects of the Iridium center which may be causing low yields due to deactivation of the carboxylic acid group or even electrostatic interaction between the acid and positively charged iridium core.



34

Figure 2.21. Bipyridyl ligand with valeric acid linker

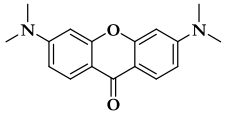
Summary

A series of cationic Iridium(III) complexes **6-23** have been developed to study ligand effects on the absorption and emission characteristics of these dyes. Novel iridium complexes containing carboxylated ligands for further synthetic extension have been made for future applications of these complexes. The extinction coefficients, quantum yields, brightnesses and full characterization of these iridium dyes have been reported. Compound **18** has been shown to be the best fluorophore in that it has the highest quantum yield and is therefore most efficient at emitting photons. Not only are these dyes easily exciteable by UV light, but the emissions of these compounds are easily seen by the naked eye due to their large Stoke's shifts. This feature makes them particularly valuable targets for detection applications.

APPENDIX A

EXPERIMENTALS

All NMR experiments were performed on Bruker AC-500MHz or AC-300MHz spectrometer. IR spectra were collected on a JASCO FT/IR 4100 Fourier Transform Infrared Spectrometer. Melting point temperatures were measured using a Mel-Temp® electrothermal apparatus. Photophysical data were obtained using a Varian Cary 50 Bio UV Vis Spectrometer and Varian Cary Eclipse Fluorescence fluorimeter. All RP HPLC performed using Synergie polar RP (250x21.21mm, 4 micron, 80A) column or Synergie polar RP (250 x 10.00mm, 4micron, 80A) column. The solvents employed were A: water with 0.1% TFA and B: 94.9% acetonitrile with 5% water and 0.1% TFA. Starting materials and solvents were purchased commercially and used as provided unless noted.



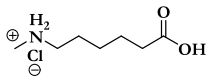
*Synthesis of Xanthenone (**7**)*[29]

Commericially available Pyronin Y **9** (10g, 1eq, 33.0mmol) was dissolved in 125 mL H_2O and heated to 70°C. KCN (7.44g, 114.3mmol, 3.5eq) in 100 mL H_2O was added and the solution was heated at 70°C for 15m. The solution was cooled to RT and filtered overnight. The precipitate was dissolved in 120 mL of 1N HCl. $FeCl_3$ (13.5g, 83.2mmol, 2.5eq) in 17 mL of H_2O was added and the solution was heated to 85 °C for 5m. The solution was cooled to RT and filtered overnight. The resulting precipitate was dissolved in 200mL H_2O. 1N NaOH (120mL) was added and the solution was heated to 80 °C for 15m. The solution was cooled to RT and filtered overnight. The solid was dissolved in DCM and purified by column chromatography using 10% EtOAc/DCM, followed by 20% EtOAc/DCM, and finally 50% EtOAc/DCM to elute 629.2 mg of the product **7** as a grey/purple powder (7%). R_f = 0.4 (9:1 DCM/EtOAc). ^{1}H NMR ($CDCl_3$, 500MHz) δ

3.099 (s, 12H), 6.474-6.479 (d, 2H, J= 2.5Hz), 6.68 (dd, 2H, J= 2.5Hz, 9Hz), 8.127 (d, 2H, J= 8Hz).

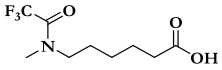
*Synthesis of Water Soluble Side Chain (**4**)*

Side Chain **4** was made using the procedures established by Dr. Kevin Spicka, a former graduate student in the Grieco laboratory.[61]



*5-(methylamino)pentanoic acid hydrochloride(**18**)*

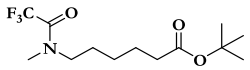
6 M HCl (100mL) was added to N-methylcaprolactam **17** (13mL, 101mmol) while stirring. The solution was heated under argon overnight and the solvent was removed *in vacuo* to yield an orange liquid. This liquid was then refluxed in benzene (250mL) at 100 ^{o}C for 5h using a Dean Stark trap. The resulting solvent was removed *in vacuo* to give 32.66g product **18** (>100%). ^{1}H NMR (D_2O, 300MHz) δ 1.39 (m, 2H), 1.625 (m, 4H), 2.37-2.41 (m, 2H), 2.65 (s, 3H), 3.00 (t, 2H, J = 15Hz). This data agrees with previously observed spectra.[61]



*6-(2,2,2 – Trifluoro-N-methylacetamido) hexanoic acid (**19**)*

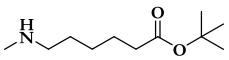
Compound **18** (18.40g, 101.3mmol, 1eq) was stirred in anhydrous methanol (20mL) at 0^{o}C under argon. Distilled triethylamine (43.3mL, 310mmol, 3.06eq) was added while stirring. A white cloudy precipitate was observed. Trifluoromethyl acetate (12.5mL, 125mmol, 1.23eq) was added dropwise at 0^{o}C. The solution was allowed to stir for 5m and then warmed to RT. The solution was stirred overnight under argon at RT. The solvent was removed *in vacuo* and 35mL H_2O was added. The solution was acidified to

pH=1 with 1M HCl (80mL) and extracted with 4 x 50mL EtOAc. The organic layer was washed with 2 x 50 mL H_2O, and 1 x 50 mL brine. The solvent was dried with sodium sulfate and removed *in vacuo* to give 20.51g of brown oil **19** (84%). ^{1}H NMR ($CDCl_3$, 300MHz) δ 1.29-1.39 (m, 2H), 1.55-1.71 (m, 4H), 2.33-2.38 (m, 2H), 3.00 and 3.09 (2s, 3H), 3.34-3.43 (2t, 2H, J=9.9Hz). This data agrees with previously observed spectra.[61]



*tert-Butyl 6-(2,2,2-trifluoro-N-methylacetamido) hexnoate (**20**)*

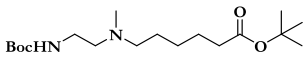
Distilled pyridine (13.7 mL, 170mmol, 2eq) was added to a solution of **19** (20.5g, 85.0mmol, 1eq) in anhydrous DCM (235mL) under argon at RT. t-Butanol (39.9mL, 420mmol, 5eq) and $POCl_3$ (15.6mL, 167mmol, 2eq) were added dropwise and the mixture was stirred at RT for 18h. A small amount of DCM was added and the organic layer was washed with 3 x 80 mL of H_2O and 2 x 80 mL of brine. The solvent was dried with sodium sulfate and removed *in vacuo*. The product was purified using DAVISIL and DCM to provide 13.25g of clear oil **20** (50%). ^{1}H NMR ($CDCl_3$, 300MHz) δ 1.21-1.31 (m, 2H), 1.37 (d, 9H), 1.49-1.63 (m, 4H), 2.13-2.18 (m, 2H), 2.95 and 3.05 (2s, 3H), 3.29-3.39 (2t, 2H, J = 9.9Hz). This data agrees with previously observed spectra.[61]



*tert-Butyl-6-(methylamino) hexanoate (**21**)*

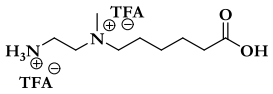
A solution of LiOH (1.12g) in H_2O (52mL) was added dropwise to a solution of compound **20** (13.25g, 42.3mmol) in MeOH (105mL) at 0 ^oC while stirring. The mixture was stirred at 0 ^oC for 10m and then warmed to RT under argon for 5h. The solvent was removed *in vacuo* and 250 mL of diethyl ether was added. The solution was washed with

3 x 30 mL H_2O and 1 x 30 mL brine. The solvent was dried with sodium sulfate and removed *in vacuo* to yield 9.03g of product **21** (>100%). ^{1}H NMR ($CDCl_3$, 300MHz) δ 1.28-1.36 (m, 2H), 1.41 (d, 9H), 1.50-1.62 (m, 4H), 2.16-2.21 (t, 2H, J= 7.2Hz), 2.40 (s, 3H), 2.52-2.56 (t,2H, J = 6Hz). This data agrees with previously observed spectra.[61]



*tert-Butyl-2-(N-methyl-N-(6-(tert-butoxycarbonyl)hexylamino))ethylcarbamate (**22**)*

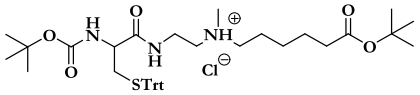
The deprotected compound **21** (8.51g, 42.3mmol, 1.15eq), tert-butyl 2–bromoethylcarbamate **26** (8.27g, 36.8mmol, 1eq), and Na_2CO_3 (11.7g, 110.4mmol, 3eq) were dissolved in H_2O (100mL) and dioxane (100mL) and stirred at 80 ^oC for 3h. The solution was cooled to RT and solvent was removed *in vacuo*. 125mL of H_2O was added and the solution was extracted with 3 x 20mL DCM. The solvent was dried with magnesium sulfate and removed *in vacuo* to give 13.54 g of clear yellow oil (80%) **22**, which was used without purification.



*6-(N-(2-aminoethyl)-N-methylamino)hexanoic acid, bishydrofluoroacetate (**23**)*

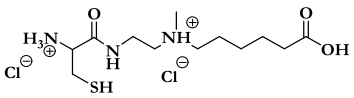
Compound **22** (13.54g, 29.5mmol, 1eq) was deprotected by the addition of triethylsilane (9.42g, 59mmol, 2eq) and TFA (80mL) in anhydrous DCM (80mL) while stirring under argon at RT for 1h. The solvent was then removed *in vacuo*. Ethyl ether (80mL) and H_2O (80mL) were added and the aqueous layer was evaporated to yield 11.19 g of product **23** (91%) which was used without purification. ^{1}H NMR (300MHz, D_2O) δ 1.21-1.28 (p, 2H, J= 7.8Hz), 1.45-1.64 (m, 4H), 2.21-2.26 (t, 2H, J = 4.8Hz), 2.77 (s, 3H), 2.829-2.880 (t, 1H, J= 7.5Hz), 3.02-3.12 (m, 2H), 3.29 (m, 2H), 3.45-3.51 (m, 1H). This

data agrees with previously observed spectra.[61]



*t-butyl-6-(N-methyl-N-(2-(2-tert-butoxycarbonylamino-3-tritylsulfanylpropionamido)ethyl)amino)hexanoate (**24**)*

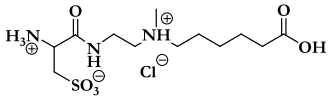
Compound **23** (11.19g, 26.9mmol, 1eq) and Na_2CO_3 (11.4g, 107.6mmol, 4eq) were dissolved in 1:1 H_2O/dioxane (240mL) to which Boc-Cys(Trt)-Osu **27** (30.14g, 53.8mmol, 2eq) was added. Stirred under argon for 2d. The organic solvent was removed *in vacuo* and the aqueous layer extracted with EtOAc. The organic layer was then dried with sodium sulfate and the solvent was removed *in vacuo*. The resulting compound was purified by flash chromatography on DAVISIL (DCM to 50:50 DCM/MeOH) to yield 7.74g white solid (39% yield). ^{1}H NMR (MeOD, 300MHz) δ 1.33-1.36 (m, 2H), 1.42 (d, 9H), 1.56-1.62 (m, 2H), 2.18-1.21 (t, 2H, J= 3Hz), 2.45-2.55 (m, 2H), 2.68 (s, 3H), 2.91-2.93 (t, 2H, J= 6Hz), 3.01 (br, 2H), 3.39-3.50 (m, 2H), 2.86-2.88 (t, 1H, J= 3Hz), 7.19-7.22 (t, 3H, J= 3Hz), 7.26-7.29 (t, 6H, J= 3Hz), 7.35-7.37 (d, 6H, J= 5Hz). This data agrees with previously observed spectra.[61]



*6-(N-methyl-N-(2-(2-amino-3-mercaptopropionamido)ethyl)amino)hexanoic acid, bishydrotrifluoroacetate (**25**)*

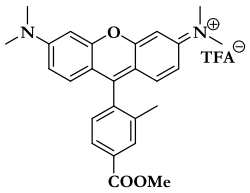
Triethylsilane (3.31mL, 20.7mmol, 2eq) was added to a solution of compound **24** (7.74g, 10.4mmol, 1eq) in TFA (30mL) and DCM (30mL) and the mixture was stirred at RT under argon for 4h. Solvents were removed *in vacuo* and the resulting residue partitioned between H_2O (100mL) and diethyl ether (100mL). The aqueous layer was separated and

the solvent removed *in vacuo* to yield 8g of white solid (>100%).



*6-(N-methyl-N-(2-(2-amino-3-sulfonato-propionamido)ethyl)amino)hexanoic acid, trifluoroacetate (**4**)*

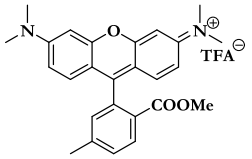
A solution of 50% hydrogen peroxide (15 mL), H_2O (10 mL) and 99% formic acid (250 mL) was allowed to stand at RT for 1 h. The solution was added to thiol **25** (8g, 15.4 mmol, 1 eq) at 0 ^oC and stirred at that temperature for 1h. The solvent was removed *in vacuo* and the resulting residue dissolved in H_2O (50 mL). The aqueous solvent was removed *in vacuo* and dried under vacuum to yield a white solid (57%). ^1H NMR (D_2O, 300MHz) δ 1.37-1.47 (p, 2H, J= 6Hz), 1.59-1.67 (p, 2H, J= 6Hz), 1.67-1.76 (m, 2H), 2.35-2.40 (t, 2H, J= 6Hz), 2.90 (s, 3H), 3.72-3.87 (m, 2H), 4.40-4.44 (t, 2H, J= 6Hz). This data agrees with previously observed spectra.[61]



*Rhodamine Ester (**10**)*

Rhodamine ester **10** was prepared following established procedures developed by Dr. Benjamin Reeves in the Grieco Laboratory. 2 M Isopropylmagnesium chloride (0.9mL, 1.8mmol, 5eq) was added dropwise to a solution of 3-iodobenzoic acid methyl ester (0.78g, 2.8mmol, 8eq) and freshly distilled Bis[2-(N,N-dimethylamino) ether]ether (0.35mL, 1.8mmol, 5eq) in 20mL anhydrous THF at 0°C under argon. The ice bath was removed after addition and the solution was stirred for 5 hours. Then 2,7-Bis-(N,N-

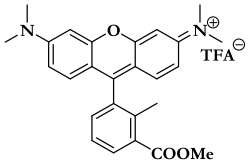
dimethylamino)xanthen-9-one **7** (100mg, 0.35mmol, 1eq) was added quickly and the solution was heated to 60 °C for 3d. The solution was cooled and 1 mL MeOH was added dropwise. The solvent was removed *in vacuo*. 8mL of DCM and 0.2 mL TFA was added and stirred under argon for 2 h. The solvent was removed *in vacuo* and the purple solid was purified by column chromatography using 2:1 DCM/Hexanes to remove benzoate impurities followed by 1:1 DCM/EtOAc to remove the 2,7- Bis-(N,N-dimethylamino)xanthen-9-one starting material. Then the crude product was recovered by eluting with 10:1 DCM/MeOH. R_f = 0.63 (1:1 DCM/EtOAc) Further purification was performed by reversed phase HPLC (30 to 70%CH_3CN, 30m, 20mL/min, 530nm, t_R = 22m) to obtain 80.8 mg purple/red solid (43% yield). ^{1}H NMR (300MHz, CD_3CN) δ 2.097 (s, 3H), 3.264 (s, 12H), 6.861 (d, 2H), 6.966 (dd, 2H), 7.101 (d, 2H), 8.046 (d, 1H), 8.109 (s, 1H). This data agrees with previously observed spectra.



*Rhodamine Ester (**11**)*

2 M Isopropylmagnesium chloride in THF (0.65 mL, 1.29 mmol, 5 eq) was added dropwise to a solution of 2-iodo 4-methylbenzoic acid methyl ester (570mg, 2.1mmol, 8eq) and freshly distilled Bis[2-(N,N-dimethylamino) ether]ether (0.25mL, 1.29mmol, 5eq) in anhydrous THF (20 mL) at 0 °C under argon. The ice bath was removed after addition and the solution was stirred for 5 hours. 2,7-Bis-(N,N-dimethylamino)xanthen-9-one **7** (73mg, 0.259mmol, 1eq) was added quickly and the solution was heated to 60 °C for 90 hrs. After the solution was cooled, 1 mL MeOH was added dropwise and the solvent was removed *in vacuo*. 8 mL of DCM and 0.2 mL TFA were added and the

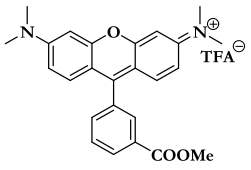
reaction was stirred under argon for 2 hrs. The solvent was removed *in vacuo* and the purple/red solid was purified by column chromatography using 2:1 DCM/Hexanes to remove benzoate impurities followed by 1:1 DCM/EtOAc to remove the 2,7- Bis-(N,N-dimethylamino)xanthen-9-one starting material. Then the crude product was recovered by eluting with 10:1 DCM/MeOH. R_f = 0.62 (6:1 DCM/MeOH). Further purification was performed by reversed phase HPLC (30 to 70% B, 35 min, 20mL/min, 525 nm, t_R = 29min) to obtain 7.8mg purple/red solid (6% yield). IR (thin film) 3195.47, 3058.55, 2924.52, 2846.42, 1721.16, 1661.37, 1595.81, 1494.56, 1407.78, 1365.35, 1348, 1184.08, 1137.8 cm^{-1} ^1H NMR (500MHz, CD_3CN) δ 2.00 (s, 3H), 3.30 (s, 12H), 3.90 (s, 3H), 6.85 (d, 2H, J=2.5 Hz), 6.97 (dd, 2H, J= 2.5 Hz, 9.5 Hz), 7.12 (d, 2H, J= 9.5 Hz), 7.62 (d, 1H, J= 8.5 Hz), 7.82 (s, 1H), 8.14 (dd, 1H, J=1.5 Hz, 8 Hz). ^{13}C NMR (125 MHz, CD_3CN) δ 24.98, 40.39, 51.99, 91.25, 96.36, 113.54, 114.70, 128.50, 129.75, 130.57, 130.98, 131.19, 132.51, 157.24, 157.63, 157.90, 171.78. HRMS *m/z* (ESI-TOF) for $C_{26}H_{27}N_2O_3^+$ Calculated 415.2016 Found 415.2008.



*Rhodamine Ester (**12**)*

2 M Isopropylmagnesium chloride in THF (0.6 mL, 1.2 mmol, 5 eq) was added dropwise to a solution of 3-iodo 2-methyl benzoic acid methyl ester (550mg, 2.0mmol, 8eq) and freshly distilled Bis[2-(N,N-dimethylamino) ether]ether (0.23 mL, 1.2 mmol, 5 eq) in anhydrous THF (20 mL) at 0 °C under argon. The ice bath was removed after addition and the solution was stirred for 5 hours. Then 2,7-Bis-(N,N-dimethylamino)xanthen-9-one **7** (70mg, 0.25mmol, 1eq) was added quickly and the solution was heated to 60 °C for

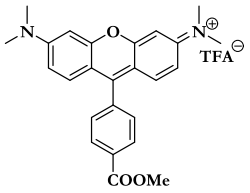
110 hrs. After the solution was cooled, 1 mL MeOH was added dropwise and the solvent was removed *in vacuo*. 8 mL of DCM and 0.2 mL TFA were added and the reaction was stirred under argon for 3 hrs. The solvent was removed *in vacuo* and the purple solid was purified by column chromatography using 2:1 DCM/Hexanes to remove benzoate impurities followed by 1:1 DCM/EtOAc to remove the 2,7- Bis-(N,N-dimethylamino)xanthen-9-one starting material. The crude product was recovered by eluting with 10:1 DCM/MeOH. Further purification was performed by RP HPLC (40 to 70% B, 35 min, 20 mL/min, 525 nm, t_R = 20 min) to obtain 28.5mg of red/purple solid **12** (22% yield). R_f = 0.48 (6:1 DCM/MeOH). mp = 180.8-181.7 ^oC. IR (thin film) 2922.59, 1682.59, 1597.73, 1495.53, 1409.71, 1367.28, 1348.96, 1186.97, 1132.97 cm^{-1} ^1H NMR (300MHz, CD_3CN) δ 2.195 (s, 3H), 3.380 (s, 12H), 3.88 (s, 3H), 6.84 (d, 2H, J= 2.4Hz), 6.97 (dd, 2H, J= 2.4Hz, 9.6Hz), 7.09 (d, 2H, J= 9.6Hz), 7.34 (d, 1H, J= 7.5Hz), 7.51 (t, 1H, J= 7.8Hz), 8.05 (d, 1H, J= 7.5Hz). ^{13}C NMR δ (125MHz, CD_3CN) δ 18.31, 41.4, 53.0, 97.4, 114.7, 115.4, 121.3, 127.2, 132.1, 132.5, 133.3, 158.5, 158.9, 185.9. HRMS *m/z* (ESI-TOF) for $C_{26}H_{27}N_2O_3^+$ Calculated 415.20162 Found 415.20437.



*Rhodamine Ester (**13**)*

2 M Isopropylmagnesium chloride in THF (0.9 mL, 1.8 mmol, 5 eq) was added dropwise to a solution of 3-iodobenzoic acid methyl ester (730mg, 2.98mmol, 8eq) and freshly distilled Bis[2-(N,N-dimethylamino)ether]ether (0.35 mL, 1.8 mmol, 5 eq) in 30 mL anhydrous THF at 0 °C under argon. The ice bath was removed after addition and the solution was stirred for 5 hours. Then 2,7-Bis-(N,N-dimethylamino)xanthen-9-one **7**

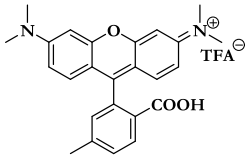
(100mg, 0.35mmol, 1eq) was added quickly and the solution was heated to 60 °C for 111 hrs. After the solution was cooled, 1 mL MeOH was added dropwise and the solvent was removed *in vacuo*. 8 mL of DCM and 0.2 mL TFA were added and the reaction was stirred under argon for 3 hrs. The solvent was removed *in vacuo* and the purple solid was purified by column chromatography using 2:1 DCM/Hexanes to remove benzoate impurities followed by 1:1 DCM/EtOAc to remove the 2,7- Bis-(N,N-dimethylamino)xanthen-9-one starting material. The crude product was recovered by eluting with 10:1 DCM/MeOH. R_f = 0.47 (6:1 DCM/MeOH). Further purification was performed by reversed phase HPLC (40 to 75 % B, 40 min, 20 mL/min, 525 nm, t_R = 19 min) to obtain 47.9mg of red/purple solid **13** (27 % yield). mp = 179.1-180.6 ^oC. IR (thin film) 2924.52, 2854.13, 1727.91, 1686.44, 1648.84, 1598.7, 1495.53, 1407.78, 1368.25, 1349.93, 1189.86, 1135.87 cm^{-1} ^1H NMR (500MHz, CD_3CN) δ 3.20 (s, 12H), 3.86 (s, 3H), 6.83 (d, 2H, J= 2Hz), 6.98 (dd, 2H, J= 2Hz, 9.5Hz), 7.25 (d, 2H, J= 9.5Hz), 7.65 (d, 1H, J= 7.5Hz), 7.77 (t, 1H, J= 7.5Hz), 8.01 (s, 1H), 8.27 (d, 1H, J= 7.5Hz). ^{13}C NMR (125MHz, CD_3CN) δ 41.4, 53.2, 97.3, 114.4, 115.4, 130.5, 131.1, 131.8, 132.3, 133.6, 134.8, 157.5, 158.4, 158.8, 167.1. HRMS *m/z* (ESI-TOF) for $C_{25}H_{25}N_2O_3^+$ Calculated 401.18597 Found 401.18453.



*Rhodamine Ester (**14**)*

2 M Isopropylmagnesium chloride in THF (0.9 mL, 1.8 mmol, 5 eq) was added dropwise to a solution of 4-iodobenzoic acid methyl ester (730mg, 2.8mmol, 8eq) and freshly

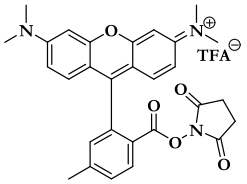
distilled Bis[2-(N,N-dimethylamino) ether]ether (0.35mL, 1.8mmol, 5eq) in anhydrous THF (30mL) at 0 °C under argon. The ice bath was removed after addition and the solution was stirred for 5 hours. 2,7-Bis-(N,N-dimethylamino)xanthen-9-one **7** (100mg, 0.35mmol, 1eq) was added quickly and the solution was heated to 60 °C for 90 hrs. After the solution was cooled, 1 mL MeOH was added dropwise and the solvent was removed *in vacuo*. 8 mL of DCM and 0.2 mL TFA were added and the reaction was stirred under argon for 110 hrs. The solvent was removed *in vacuo* and the purple solid was purified by column chromatography using 2:1 DCM/Hexanes to remove benzoate impurities followed by 1:1 DCM/EtOAc to remove the 2,7- Bis-(N,N-dimethylamino)xanthen-9-one starting material. Then the crude product was recovered by eluting with 10:1 DCM/MeOH. R_f =0.57 (6:1 DCM/MeOH). Further purification was performed by RP HPLC (40 to 75% B, 20mL/min, 40 min., 525 nm, t_R = 17 min) to obtain 36.8 mg of purple/red solid **14** (20%). mp = 143.5-144.1 ^{o}C. IR (thin film) 2923.56, 2852.2, 1721.16, 1684.52, 1647.88, 1600.63, 1494.56, 1417.42, 1369.21, 1348.96, 1191.79, 1136.83 cm^{-1}. ^{1}H NMR (500MHz, CD_3CN) δ 3.25 (s, 12H), 3.96 (s, 3H), 6.82 (s, 2H), 6.98 (d, 2H, J= 9.5Hz), 7.27 (dd, 2H, J= 1.5Hz, 9.5Hz), 7.55 (d, 2H, J= 7Hz), 8.25 (d, 2H, J= 7Hz). ^{13}C NMR (125MHz, CD_3CN) δ 41.4, 53.2, 97.4, 114.3, 115.9, 130.7, 131.0, 132.5, 132.6, 137.9, 157.7, 158.9, 160.5. HRMS *m/z* (ESI-TOF) for $C_{25}H_{25}N_2O_3^+$ Calculated 401.18597 Found 401.18736.



*Rhodamine Acid (**5**)*

Rhodamine ester **11** (4.4mg, 0.0083mmol, 1eq) was dissolved in DMF (2mL) and 1 M

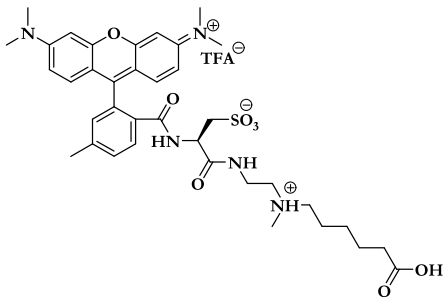
NaOH (2mL) and let stir under argon overnight. 1 M HCl was added until pH = 2 and the solvent was removed *in vacuo*. The resulting purple solid was purified by RP HPLC (30 to 60% B, 30 min, 20 mL/min, 525 nm, t_R = 24min) affording 0.8mg of Compound **5** as a purple/red solid. (19%) R_f = 0.51 (6:1 DCM/MeOH). mp= 130.1-133.0 ^oC. IR (thin film) 2921.63, 2345.02, 1653.66, 1421.28, 1275.68, 1261.22, 1071.26, 750.174 cm^{-1}. ^1H NMR (500MHz, CD_3CN) δ 1.94 (s, 3H), 3.26 (s, 12H), 6.85 (d, 2H, J= 2.5Hz), 6.98 (dd, 2H, J= 2.5Hz, 9.5Hz), 7.14 (d, 2H, J= 9.5Hz), 7.59 (d, 1H, J= 8Hz), 7.83 (s, 1H), 8.15 (d, 1H, J= 8Hz). HRMS *m/z* (ESI-TOF) for $C_{25}H_{25}N_2O_3^+$ Calculated 401.18597 Found 401.18597.



*Rhodamine Acid NHS (**3**)*

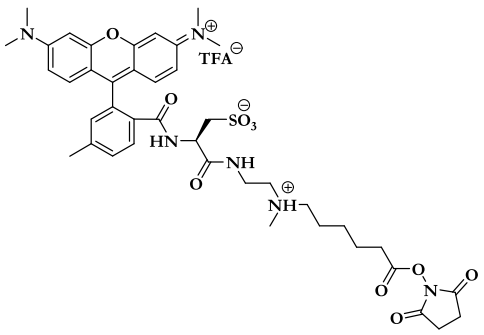
N-hydroxysuccinimide (17.98mg, 0.156mmol, 8eq), 1,3-dicyclohexylcarbodiimide (24.2mg, 0.117mmol, 6eq), and RhodamineCOOH **5** (11.1mg, 0.0195mmol, 1eq) were dissolved in dry DCM (3-5mL) and the resulting solution was stirred under argon overnight. The solvent was removed *in vacuo* and the resulting solid was purified by RP HPLC (30 to 70% B, 4 mL/min, 525 nm, t_R= 35 min) to obtain 6.1mg of compound **3** as a purple/red solid (51%). R_f = 0.38 (6:1 DCM/MeOH). mp = 106.9-108.9 ^oC. IR (thin film) 2925.48, 2855.1, 1740.44, 1688.37, 1649.8, 1596.77, 1497.45, 1409.71, 1366.32, 1348, 1186.01, 1132.97, 1071.26 cm^{-1} ^1HNMR (500MHz, CD_3CN) δ 2.14 (s, 3H), 2.86 (s, 4H), 3.31 (s, 12H), 6.92 (d, 2H, J= 2.5Hz), 7.09 (dd, 2H, J= 2.5Hz, 9.5Hz), 7.18 (d, 2H, J= 9Hz), 7.72 (d, 1H, J= 8.5Hz), 7.96 (d, 1H, J= 1.5Hz), 8.20 (dd, 1H, J= 2.5Hz,

8Hz). ^{13}C NMR (125MHz, CD_3CN) δ 20.56, 26.00, 41.53, 114.86, 116.72, 131.94, 132.31, 132.75, 133.39, 134.67, 145.75, 157.03, 159.17, 159.28, 162.75, 121.01. HRMS *m/z* (ESI-TOF) for $C_{29}H_{28}N_3O_5^+$ Calculated 498.2024 Found 498.2023.



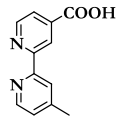
*Rhodamine S.C. **(2)***

Freshly distilled N-methylmorpholine (0.22mL, 0.199mmol, 20eq) was added dropwise to a solution of peptide **4** (27.1mg, 0.0598mmol, 6eq), and RhodamineCOONHS **3** (6.1mg, 0.00997mmol, 1eq) in anhydrous DMF (3mL). After 14h the solvent was removed *in vacuo* and the resulting solid was purified by reversed phase HPLC (30 to 70%B, 30 min, 4mL/min, t_R = 17min) to afford 5.6mg of Compound **2** as a purple/red solid (68%). R_f = 0 (6:1 DCM/MeOH). ^{1}H NMR (500 MHz, D_2O) δ 1.23 (p, 2H, J = 7.5Hz), 1.45 (p, 2H, J = 7Hz), 1.63 (m, 2H), 2.03 (s, 3H), 2.21 (t, 2H, J= 7Hz), 2.85 (d, 3H, J= 6Hz), 3.07 (s, 12H), 3.12 (s, 1H), 3.24 (m, 2H), 3.40 (m, 2H), 3.65 (2H), 4.89 (s, 1H), 6.41 (s, 2H), 6.76 (d, 2H, J= 7.5Hz), 7.03 (d, 2H, J= 9Hz), 7.60 (t, 2H, J= 9Hz), 7.94 (d, 1H, J= 8.5Hz). ^{13}C NMR (125 MHz, D_2O) δ 18.63, 23.13, 23.20, 24.72, 33.27, 34.57, 40.08, 50.79, 51.13, 55.31, 56.12, 56.32, 96.04, 112.63, 114.12, 128.10, 128.44, 130.14, 130.92, 130.93, 131.34, 132.07, 141.71, 155.54, 156.87, 172.25, 175.35. HRMS *m/z* (ESI-TOF) for $C_{37}H_{48}N_5O_8S^+$ Calculated 722.3218 Found 722.3214.



*Rhodamine Dye (**1**)*

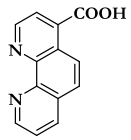
N-hydroxysuccinimide (6.2mg, 0.0536mmol, 8eq), 1,3-dicyclohexylcarbodiimide (8.3mg, 0.0402mmol, 6 eq), and RhodamineS.C. **2** (5.6mg, 0.0067mmol, 1 eq) were dissolved in dry DCM (3mL) and the resulting solution was stirred under argon for 17h. The solvent was removed *in vacuo* and the resulting solid was purified by reversed phase HPLC (30 to 70%B, 35m, 4mL/min, 525nm, t_R = 15min) to obtain 1.6mg of Compound **1** as a purple/red solid (25%). R_f = 0.68 (6:1 DCM/MeOH). mp= 187.9 ^oC. IR (thin film) 3293.82, 2923.56, 1781.9, 1736.58, 1650.77, 1596.77, 1495.53, 1409.71, 1366.32, 1348.96, 1187.94, 1133.94, 1069.33, 1038.48, 929.521, 826.348 cm^{-1}. ^{1}HNMR (500MHz, CD_3CN) δ 1.23 (p, 2H, J= 8Hz), 1.49 (m, 2H, J= 7.5Hz), 1.59 (m, 2H), 2.01 (s, 3H), 2.47 (t, 2H, J=6Hz), 2.79 (s, 4H), 2.82 (d, 3H, J= 4.5Hz), 3.11 (s, 12H), 3.22 (m, 2H), 3.46 (m, 2H), 3.64 (m, 2H), 6.58 (d, 2H, J= 10.5Hz), 6.82 (t, 2H, J= 10.5Hz), 7.08 (t, 2H, J= 9Hz), 7.61 (d, 2H, J= 8.5Hz), 7.94 (d, 1H, J= 8Hz). ^{13}C NMR (100 MHz, CD_3CN) δ 18.81, 22.84, 23.70, 25.12, 25.43, 30.12, 30.31, 35.58, 40.41, 51.10, 96.35, 113.56, 114.70, 128.38, 131.11, 157.68, 157.97, 162.33. HRMS *m/z* (ESI-TOF) for $C_{41}H_{51}N_6O_{10}S^+$ Calculated 819.3382 Found 819.3382.



*4-carboxy-4'-methyl 2,2'- bipyridine Ancillary Ligand (**1**)*

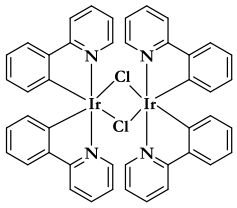
Established literature procedures were followed for the synthesis of ligand **1**.[55] 4,4'-dimethyl 2,2'-bipyridine (5.0g, 27.1mmol, 1.0eq) was suspended in 1,4 dioxane (295mL) with selenium dioxide (3.61g, 32.6mmol, 1.2eq). The solution was heated at reflux for 25h with stirring. The solution turned yellow and then black. The solution was then filtered hot through celite and the solvent was removed *in vacuo*. Ethanol (150mL) was added and silver nitrate (4.31g, 25.3mmol, 1.1eq in 40mL H_2O). 1M NaOH (100mL) was added dropwise over 30m while stirring under argon vigorously. The solution was allowed to stir for 24h. The ethanol was removed *in vacuo* and the aqueous residue filtered. The solid was washed with 1.3M NaOH (2 x 30mL) and extracted with DCM (4 x 100mL). 1:1 (v/v) 4.0 N HCl/acetic acid was added to pH= 3.5. A white solid precipitate formed which was filtered and dried. The solid was continuously extracted with acetone in a Soxhlet for 140h. The solution was then cooled and the solvent removed *in vacuo* to afford 3.24g of off-white solid (56%). R_f = 0 (6:1 DCM/MeOH). mp = 240.0-243.0 ^oC. IR (thin film) 3394.1, 3142.44, 3067.23, 2916.81, 2849.31, 1683.55, 1597.73, 1551.45, 1365.35, 1287.25, 1248.68, 1203.36, 1178.29, 1125.26, 1071.26, 1038.48, 1013.41, 835.026, 769.458, 743.424, 721.247 cm^{-1} ^1H NMR (500MHz, $CDCl_3$) δ 9.16 (s, 1H), 8.99 (d, 1H, J= 5.5Hz), 8.93-8.94 (d, 1H, J=5Hz), 8.48 (s, 1H), 8.04-8.05 (d, 1H, J=5Hz), 7.61 (s, 1H), 2.69 (s, 3H). ^{13}C NMR (125MHz, DMSO) δ 20.70, 119.69, 121.29, 123.06, 125.30, 148.21, 149.18, 150.05, 154.44, 156.27, 157.53, 166.57. HRMS *m/z* (ESI-TOF) for $C_{12}H_{11}N_2O_2$ Calculated 215.0815 Found

215.08275.



4-carboxy-1,10-phenanthroline Ancillary ligand (**2**)

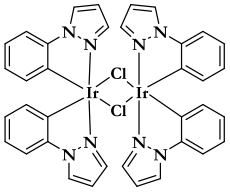
4- methyl-1,10-phenanthroline (1g, 5.15mmol, 1eq) and $KMnO_4$ (3.25g, 20.6mmol, 4eq) were stirred in 30mL of H_2O at reflux for 23h. The solution was filtered hot through celite and the resulting solution was evaporated *in vacuo*. The resulting solid was recrystallized from H_2O to yield white solid which was filtered and washed to give a white solid. The eluent was concentrated and recrystallized further to yield 331mg of white product (29%). $R_f = 0$ (6:1 DCM/MeOH). mp = 260.0 – 261.9 ^oC. IR (thin film) ~3400 (broad), 2934.16, 2839.67, 2356.59, 1558.2, 1540.85, 1521.56, 1507.1, 1456.96, 1075.12 cm^{-1}. ^1H NMR (350MHz, DMSO-d_6) δ 8.27 (t, 1H, J= 6.3Hz), 8.37 (s, 1H), 8.38 (d, 1H, J= 5.0 Hz), 8.91 (d, 1H, J= 9.3Hz). 9.17 (d, 1H, J= 7.5Hz), 9.30 (d, 1H, J= 4.8Hz), 9.38 (d, 1H, J= 4.5Hz). ^{13}C NMR (125MHz, DMSO-d_6) δ 125.83, 126.11, 126.18, 126.79, 129.41, 138.39, 141.00, 144.45, 146.64, 150.91, 167.11. HRMS *m/z* (ESI-TOF) for $C_{13}H_8N_2O_2$ Calculated 224.0586 Found 225.0645.



*Dichloro Iridium dimer (**3***

Dimer **3** was prepared using established literature procedure.[62,63] To a solution of Iridium trichloride monohydrate (1g, 3.35mmol, 1eq) in 2-methoxyethanol (30mL) and water

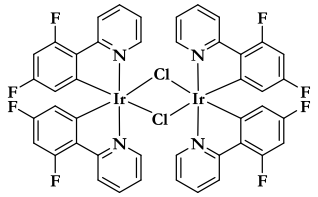
(10mL), 2-phenyl pyridine (1.2mL, 8.37mmol, 2.5eq) was added and the reaction was refluxed for 24h at 125-130 ^{o}C. The solution was cooled and the precipitate was filtered and washed with ethanol (60mL) and acetone (60mL). The solid was then dissolved in 250mL DCM and filtered. 55mL of toluene and 25mL of hexanes were added and evaporated to approximately 150mL. No precipitate was formed. The solvent was removed *in vacuo* and the compound purified by column chromatography (10:1 DCM/MeOH) to give 693mg of yellow product (39%). R_f = 0.81 (6:1 DCM/MeOH). mp > 250^{o}C. IR (thin film) 2919.7, 1680.66, 1599.66, 1572.66, 1555.31, 1475.28, 1426.1, 1401.03, 1291.11, 1266.04, 1245.79, 1206.26, 1159.01, 1137.8, 1102.12, 1067.41, 1040.41, 987.375, 845.633, 827.312, 781.993, 785.102 cm^{-1} ^{1}H NMR (500MHz, $CDCl_3$) δ 5.92 (d, 2H, J= 7.5Hz), 6.55 (t, 2H, J= 7.5Hz), 6.75 (m, 4H), 7.47 (d, 2H, J= 7.5Hz), 7.73 (t, 2H, J= 7.5Hz), 7.86 (d, 2H, J= 8Hz), 9.22 (d, 2H, J= 5.5Hz). ^{13}C NMR (125 MHz, $CDCl_3$) δ 118.63, 121.55, 122.34, 123.88, 129.32, 130.82, 136.39, 151.92. HRMS *m/z* (ESI-TOF) for $C_{22}H_{16}IrN_2^-$ Calculated 501.09427 Found 501.09502



*Synthesis of Blue dimer (**4**)*

1-phenyl pyrazole (1.11mL, 8.37mmol, 2.5eq) was added dropwise to a solution of Iridium trichloride monohydrate (1g, 3.35mmol, 1eq) in 2-methoxyethanol (36mL) and water (12mL) under argon. The solution was refluxed at 110 ^{o}C for 48h. No color change was noted. The solution was cooled and filtered. The solid was washed with ethanol and acetone but dissolved. The solvent was removed *in vacuo* to give 744mg of

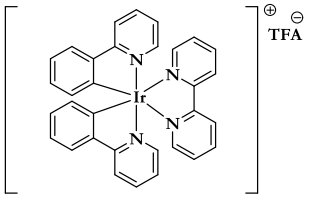
white solid (43%). R_f = 0.83 (6:1 DCM/MeOH). mp > 250 ^oC. (lit. 340 ^oC).[64] IR (thin film) 3129.9, 3054.69, 3007.44, 1705.73, 1586.16, 1507.1, 1480.1, 1445.39, 1426.1, 1414.53, 1337.39, 1275.68, 1243.86, 1107.9, 1069.33, 1052.94, 1030.77, 1022.09, 742.46, 713.533, 700.998 cm^{-1} ^1H NMR (500MHz, DMSO-d_6) δ 5.80-5.81 (dd, 2H, J= 0.5Hz, 7Hz), 6.18-6.19 (d, 2H, J= 7.5Hz), 6.64-6.71 (t, J= 8Hz, td, 1Hz, 7.5Hz, 4H total), 6.81-6.82 (t, 2H, J= 2.5Hz), 6.85-6.89 (td, 2H, J= 1Hz, 7.5Hz), 6.90-6.94 (td, 2H, J= 1Hz, 7Hz), 6.95-6.96 (t, 2H, J= 2.5Hz), 7.55-7.56 (d, 2H, J= 8Hz), 7.60-7.61 (d, 2H, J= 7.5Hz), 8.10-8.11 (d, 2H, J= 2Hz), 8.45-8.46 (d, 2H, J= 2Hz), 8.80-8.81 (d, 2H, J= 2.5Hz), 8.93-8.94 (d, 2H, J= 3Hz). ^{13}C NMR (125 MHz, DMSO-d_6) δ 107.35, 108.62, 111.12, 111.88, 122.65, 122.84, 125.17, 125.88, 127.50, 127.72, 128.97,131.81, 132.65, 135.48, 138.94, 139.87, 141.80, 142.51. HRMS *m/z* (ESI-TOF) for $C_{18}H_{14}IrN_4^-$ Calculated 479.0853 Found 479.0855.



*Synthesis of Green dimer (**5**)*

Dimer **5** was prepared using established literature procedure.[65] 2-(2,4-difluorophenyl)pyridine (1.28 mL, 8.37mmol, 2.5eq) was added dropwise to a solution of Iridium trichloride monohydrate (1g, 3.35mmol, 1eq) in 2-methoxyethanol (36mL) and water (12mL) under argon. The solution was refluxed at 110 ^oC for 48h. The color changed to bright yellow. The solution was cooled, the solvent evaporated, and the solid was purified by column chromatography (10:1 DCM/MeOH). The solvent was removed *in vacuo* to give 1.23g of yellow solid (60%). R_f = 0.81 (6:1 DCM/MeOH). mp > 270^oC.

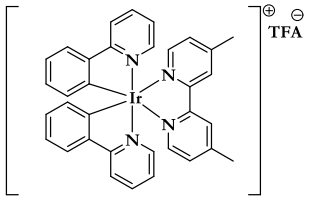
IR (thin film) 3044.09, 2029.71, 1603.52, 1579.41, 1561.09, 1476.24, 1448.28, 1436.71, 1414.53, 1266.04, 1223.61, 1158.04, 1060.66, 1028.84, 753.066, 732.817 cm^{-1} ^1H NMR (500MHz, $CDCl_3$) δ 5.31 (s, 1H), 6.35 (t, 1H, J= 10Hz), 6.84 (t, 1H, J= 6.5Hz), 7.84 (t, 1H, J= 9Hz), 8.31 (d, 1H, J= 8.5Hz), 9.13 (d, 1H, J= 5.5Hz). HRMS *m/z* (ESI-TOF) for $C_{22}H_{12}F_4IrN_2^-$ Calculated 573.0571 Found 573.0553.



*Synthesis of $[Ir(ppy)_2bpy]^+TFA^-$ (**6**)*

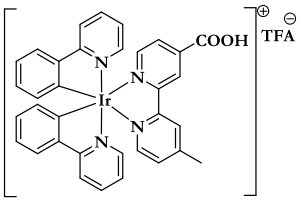
Compound **6** was prepared using established literature procedure.[62] Dichloro bridged Iridium dimer **3** (150mg, 0.140mmol, 1eq) and bipyridine (48.7mg, 0.280mmol, 2eq) were stirred in a 1:1 mixture of anhydrous DCM/MeOH (20mL) at reflux (50-60 ^oC) under argon for 4h. The solution was then cooled to RT and 1.0 mL of sat. NH_4PF_6 in MeOH was added while stirring. The solution was allowed to stir for 5min. The solvent was evaporated under vacuum and the resulting solid was purified with RP HPLC (60-75%B, 30min, 254nm, 20mL/min, t_R = 8.97min) to give 12.5mg of yellow solid (6%). R_f = 0.23 (10:1 DCM/MeOH). mp = 296.3 ^oC. IR (thin film) 3109.65, 3064.33, 1778.05, 1736.58, 1686.44, 1607.38, 1583.27, 1479.13, 1446.35, 1421.28, 1193.72, 1162.87, 1140.69, 759.816, 733.782, 705.819 cm^{-1}. ^1H NMR (DMSO-d_6, 500MHz) δ 6.15 (d, 2H, J= 7.5Hz), 6.87 (t, 2H, J= 7Hz), 6.98 (t, 2H, J= 7.5Hz), 7.12 (t, 2H, J= 6Hz), 7.58 (d, 2H, J= 6Hz), 7.66 (t, 2H, J= 6.5Hz), 7.83 (d, 2H, J= 5Hz), 7.90 (m, 4H, J= 8Hz, 8.5Hz), 8.24 (q, 4H, J= 5Hz), 8.85 (d, 2H, J= 8.5Hz). ^1H NMR (CD_2Cl_2, 500MHz) δ 6.31 (d, 2H, J= 7.5Hz), 6.94 (td, 2H, J= 1Hz, 7.5Hz), 6.98 (td, 2H, J= 1.5Hz, 7.5Hz), 7.08 (td, 2H, J=

1Hz, 8.5Hz), 7.45 (s, 1H), 7.48 (t, 3H, J= 5.5Hz), 7.74 (d, 2H, J= 7.5Hz), 7.79 (td, 2H, J= 1.5Hz, 8.5Hz), 7.96 (d, 2H, J= 8Hz), 8.09 (dd, 2H, J= 1.5Hz, 8Hz), 8.13 (td, 2H, J= 1Hz, 8Hz), 8.55 (d, 2H, J= 8Hz). HRMS *m/z* (ESI-TOF) for $C_{32}H_{24}IrN_4^+$ Calculated 657.16247 Found 657.16125.



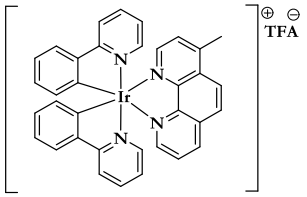
Synthesis of [Ir(ppy)$_2$bpyMe$_2$]$^+$TFA$^-$ (7)

Compound **7** was prepared using established literature procedure.[66] Dichloro bridged Iridium dimer **3** (150mg, 0.140mmol, 1eq) and 4,4'-dimethyl bipyridine ligand (60.0mg, 0.280mmol, 2eq) were stirred in a 1:1 mixture of anhydrous DCM/MeOH (20mL) at reflux (50-60 ^oC) under argon for 4h. The solution was then cooled to RT and 1.0 mL of sat. NH_4PF_6 in MeOH was added while stirring. The solution was allowed to stir for 5min. The solvent was evaporated under vacuum and the resulting solid was purified with RP HPLC (60-75%B, 25min, 254nm, 20mL/min, t_R = 10.4min) to give 80mg of yellow solid (36%). R_f = 0.33 (10:1 DCM/MeOH). mp >250^oC. IR (thin film) 3046.01, 1178.05, 1617.98, 1608.34, 1583.27, 1478.17, 1438.64, 1420.32, 1164.79, 1063.55, 1030.77, 842.74, 757.888, 737.639 cm^{-1}. ^{1}H NMR (acetone-d_6, 500MHz) δ 2.63 (s, 6H), 6.38 (d, 2H, J= 7.5Hz), 7.00 (t, 2H, J= 7.5Hz), 7.13 (m, 4H), 7.42 (d, 2H, J= 5.5Hz), 7.70 (d, 2H, J= 5.5Hz), 8.90 (m, 4H), 7.94 (t, 2H, J= 8Hz), 8.16 (d, 2H, J= 8Hz), 8.47 (s, 2H). HRMS *m/z* (ESI-TOF) for $C_{34}H_{28}IrN_4^+$ Calculated 685.19377 Found 685.19387.



*Synthesis of $[Ir(ppy)_2bpyCOOH]^+TFA^-$ (**8**)*

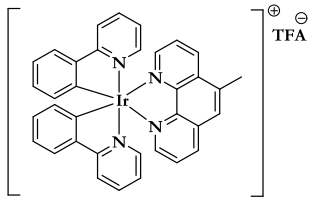
Compound **8** was prepared using established literature procedure.[57] Dichloro bridged Iridium dimer **3** (150mg, 0.140mmol, 1eq) and 4-carboxy-4'-methyl bipyridyl ligand **1** (60.0mg, 0.280mmol, 2eq) were stirred in a 1:1 mixture of anhydrous DCM/MeOH (20mL) at reflux (50-60 ^oC) under argon for 4h. The solution was then cooled to RT and 1.0 mL of sat. NH_4PF_6 in MeOH was added while stirring. The solution was allowed to stir for 5min. The solvent was evaporated under vacuum and the resulting solid was purified with RP HPLC (60-75%B, 30min, 254nm, 20mL/min, t_R = 8.85min) to give 174mg of orange solid (63%). R_f = 0.12 (10:1 DCM/MeOH). mp = 201.8-207.7 ^oC. (lit. 201 ^oC)[57] IR (thin film) 3046.01. 2925.48. 1727.81., 1608.34, 1583.27, 1479.13, 1438.64, 1422.24, 1267.97, 1228.43, 1196.61, 1165.76, 841.776, 757.888, 736.674 cm^{-1}. ^1H NMR (DMSO-d_6, 500MHz) δ 2.50 (s, 3H), 6.87 (tt, 2H, J= 3Hz, 4.5Hz), 6.98 (tt, 2H, J= 3.5Hz), 7.10 (tt, 2H, J= 7Hz, 22Hz), 7.51 (d, 1H, J= 6Hz), 7.57 (d, 1H, J= 6Hz), 7.64 (q, 2H, J= 6Hz), 7.89 (m, 4H), 7.99 (d, 1H, J= 5.5Hz), 8.03 (dd, 1H, J= 1.2Hz, 7Hz), 8.23 (t, 2H, J= 8.5Hz), 8.99 (s, 1H), 9.11 (s, 1H). ^1H NMR (acetone-d_6, 500MHz) δ 2.63 (s, 3H), 6.37 (dd, 2H, J= 8Hz, 15Hz), 7.02 (m, 2H), 7.12 (m, 3H), 7.46 (d, 1H, J= 5.5Hz), 7.68 (d, 1H, J= 5.5Hz), 7.70 (d, 1H, J= 6Hz), 7.91 (t, 2H, J= 6.5Hz), 7.96 (m, 2H), 8.17 (m, 2H), 8.22 (d, 1H, J= 5.5Hz), 8.65 (s, 2H), 9.06 (s, 1H), 14.33 (b, 1H). HRMS *m/z* (ESI-TOF) for $C_{34}H_{26}IrN_4O_2^+$ Calculated 715.16795 Found 715.16812.



*Synthesis of [Ir(ppy)$_2$^{4}Mephen]$^+$TFA$^-$ (**9**)*

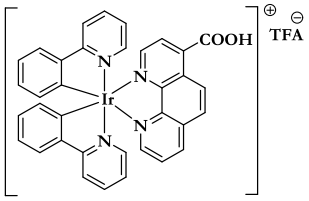
Compound **9** was prepared using established literature procedure.[43] Dichloro bridged Iridium dimer **3** (150 mg, 0.140 mmol, 1eq) and 4-methyl-1,10-phenanthroline (54.4 mg, 0.280 mmol, 2 eq) were stirred in a 1:1 mixture of anhydrous DCM/MeOH (20mL) at reflux (50-60 ^{o}C) under argon for 4h. The solution was then cooled to RT and 1.0 mL of sat. NH_4PF_6 in MeOH were added while stirring. The solution was allowed to stir for 5min. The solvent was evaporated under vacuum and the resulting solid was purified with RP HPLC (60-75%B, 25min, 254nm, 20mL/min, t_R = 10.2min) to give 131.3 mg solid (56%). R_f = 0.23 (10:1 DCM/MeOH). mp = 194.5-197.8 ^{o}C. IR (thin film) 3062.41, 2956.34, 2925.48, 2854.13, 1779.01, 1734.66, 1687.41, 1607.38, 1583.27, 1479.13, 1438.64, 1427.07, 1268.93, 1191.79, 1164.79, 1140.69, 1063.55, 1031.73, 842.74, 795.493, 760.78, 729.925, 704.855 cm^{-1}. ^{1}H NMR (DMSO-d_6, 500MHz) δ 2.87 (s, 3H), 6.24 (t, 2H, J= 7.5Hz), 6.90 (t, 2H, J= 7Hz), 6.93 (q, 2H, J= 6Hz), 7.01 (t, 2H, J= 7.5Hz), 7.39 (d, 1H, J= 6Hz), 7.42 (d, 1H, J= 5.5Hz), 7.82 (mt, 3H, J= 5Hz), 7.89 (d, 2H, J= 8Hz),7.97 (p, 1H, J= 3Hz), 7.99 (d, 1H, J= 5Hz), 8.34 (d, 1H, J= 9Hz), 8.42 (d, 1H, J= 9Hz), 8.83 (d, 1H, J= 8.5Hz). ^{1}H NMR (acetone- d_6, 500MHz) δ 3.07 (s, 3H), 6.49 (t, 2H, J= 11Hz), 6.96 (td, 2H, J= 1.5Hz, 6Hz), 7.07 (td, 2H, J= 1.5Hz, 7.5Hz), 7.19 (t, 2H, J= 7.5Hz), 7.52 (t, 2H, J= 5.5Hz), 7.79 (d, 1H, J= 5Hz), 7.88 (td, 2H, J= 1.5Hz, 8Hz), 7.94 (m, 3H), 8.16 (d, 2H, J= 8Hz), 8.25 (d, 1H, J= 8Hz), 8.35 (d, 1H, J= 9.5Hz), 8.41 (dd, 1H, J= 1.5Hz, 5Hz), 8.47 (d, 1H, J= 9Hz), 8.78 (dd, 1H, J= 1Hz, 8.5Hz). HRMS *m/z* (ESI-

TOF) for $C_{35}H_{26}IrN_4^+$ Calculated 695.17812 Found 695.17733.



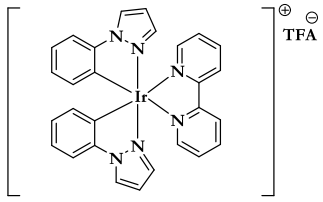
*Synthesis of [Ir(ppy)$_2$^{5}Mephen]$^+$TFA$^-$ (**10**)*

Compound **10** was prepared using established literature procedure.[67] Dichloro bridged Iridium dimer **3** (150 mg, 0.140 mmol, 1eq) and 5-methyl-1,10-phenanthroline (54.4 mg, 0.280 mmol, 2 eq) were stirred in a 1:1 mixture of anhydrous DCM/MeOH (20mL) at reflux (50-60 ^{o}C) under argon for 4h. The solution was then cooled to RT and 1.0 mL of sat. NH_4PF_6 in MeOH was added while stirring. The solution was allowed to stir for 5min. The solvent was evaporated under vacuum and the resulting solid was purified with RP HPLC (60-75%B, 25min, 254nm, 20mL/min, t_R = 11 min) to give 19.4 mg of yellow solid (8%). R_f = 0.28 (10:1 DCM/MeOH). mp = 191.3 ^{o}C. IR (thin film) 3064.33, 2923.56, 1778.05, 1730.8, 1680.66, 1627.63, 1607.38, 1583.27, 1479.13, 1438.64, 1424.17, 1191.79, 1137.8, 1063.55, 1031.73, 798.385, 759.816, 728.961, 705.819 cm^{-1}. ^{1}H NMR (acetone- d_6, 500MHz) δ 3.03 (s, 3H), 6.47 (d, 1H, J= 3.5Hz), 6.49 (d, 1H, J= 3Hz), 6.96 (t, 2H, J= 7Hz), 7.08 (td, 2H, J= 1Hz, 8.5Hz), 7.19 (td, 2H, J= 1.5Hz, 8H), 7.90 (m, 3H), 7.97 (m, 3H), 8.15 (s, 2H), 8.17 (s, 1H), 8.33 (dd, 1H, J= 1.5Hz, 5Hz), 8.41 (dd, 1H, J= 1.5Hz, 5Hz), 8.67 (d, 1H, J= 8Hz), 8.88 (dd, 1H, J= 1.5Hz, 8.5Hz). HRMS *m/z* (ESI-TOF) for $C_{35}H_{26}IrN_4^+$ Calculated 695.17812 Found 695.17757.



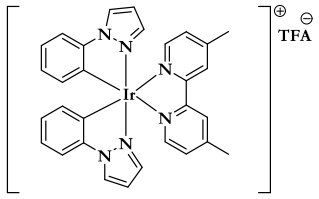
*Synthesis of [Ir(ppy)$_2$phenCOOH]$^+$TFA$^-$ (**11**)*

Iridium dimer **3** (100mg, 0.0932mmol, 1eq) and phenanthroline ligand **2** (41.8mg, 0.187mmol, 2eq) were stirred in a solution of 1:1 DCM/MeOH (14mL) under argon at reflux (60 ^{o}C) for 24h. The solution was cooled to RT and 1mL of concentrated NH_4PF_6 was added and stirred for 20min. The solution was rotovapped and purified by RP HPLC (50-85%B, 40min, 20mL/min, 254nm, t_R =11.1m) to yield 31.5 mg of yellow solid (40%). mp = 201.8 ^{o}C. Rf = 0.49 (6:1 DCM/MeOH). IR (thin film) 3413.39, 3062.41, 2922.59, 1709.59, 1688.37, 1607.38, 1583.27, 1479.13, 1438.64, 1420.32, 1268.93, 1226.5, 1184.08, 1132.01, 1063.55, 1030.77, 1008.59, 759.816, 730.889, 715.461 cm^{-1}. ^{1}H NMR (500MHz, DMSO- d_6) δ 6.238 (t, 2H, J= 8Hz), 6.95 (s, 4H, J= 7.5Hz), 7.02 (t, 2H, J= 7.5Hz), 7.41 (d, 1H, J= 5.5Hz), 7.51 (d, 1H, J = 6Hz), 7.84 (t, 2H, J= 3Hz), 7.92 (d, 2H, J= 8Hz), 8.05 (q, 1H, J= 5Hz), 8.22 (q, 3H, J = 8.5Hz), 8.32 (d, 1H, J= 5Hz), 8.37 (d, 1H, J= 5.5Hz), 8.44 (d, 1H, J= 9Hz), 8.90 (d, 1H, J= 6.5Hz), 8.96 (d, 1H, J= 12Hz). ^{13}C NMR (125MHz, DMSO- d_6) δ 120.42, 122.92, 124.33, 125.53, 12621, 127.96, 128.09, 129.14, 129.91, 130.70, 131.33, 131.60, 131.68, 138.68, 139.20, 144.39, 144.49, 146.48, 147.60, 149.67, 149.93, 150.17, 150.32, 151.40, 151.47, 158.31, 158.57, 166.64, 167.12, 167.24. HRMS *m/z* (ESI-TOF) for $C_{35}H_{24}IrN_4O_2$ Calculated 725.1523 Found 725.1529.



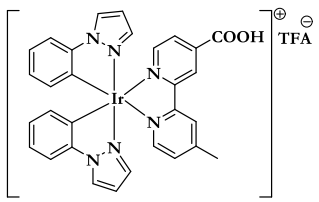
*Synthesis of $[Ir(ppyz)_2bpy]^+TFA^-$ (**12**)*

Compound **10** was prepared using established literature procedure.[37] Dichloro bridged Iridium dimer **4** (105.5 mg, 0.103 mmol, 1eq) and bipyridine (49.0 mg, 0.314 mmol, 3 eq) were stirred in a 1:1 mixture of anhydrous DCM/MeOH (20mL) at reflux (50-60 ^oC) under argon for 4h. The solution was then cooled to RT and 1.2 mL of sat. NH_4PF_6 in MeOH was added while stirring. The solution was allowed to stir for 5min. The solvent was evaporated under vacuum and the resulting solid was purified with RP HPLC (50-70%B, 35min, 254nm, 20mL/min, t_R = 12.7min) to give 44.7mg of brownish yellow solid (29%). R_f = 0.15 (10:1 DCM/MeOH). mp = 165.7-168.3 ^oC. IR (thin film) 3372.89, 3118.33, 2922.59, 2853.17, 1735.62, 1681.62, 1602.56, 1481.06, 1470.46, 1446.35, 1412.6, 1194.69, 1141.65, 1075.12, 1058.73, 1034.62, 754.995, 732.817, 719.318, 703.89 cm^{-1}. ^1H NMR (DMSO- d_6, 300MHz) δ 6.14 (d, 2H, J= 7.2Hz), 6.65 (s, 2H), 6.81 (t, 2H, J= 7.2Hz), 7.01 (t, 2H, J= 7.5Hz), 7.15 (d, 2H, J= 1.8Hz), 7.65 (d, 4H, J= 7.2Hz), 7.98 (d, 2H, J= 5.1Hz), 8.24 (t, 2H, J= 7.8Hz), 8.83 (d, 4H, J= 7.2Hz). ^1H NMR (CD_2Cl_2, 500MHz) δ 6.31 (d, 2H, J= 7Hz), 6.55 (d, 2H, J= 2Hz), 6.85 (d, 2H, J= 2Hz), 6.90 (t, 2H, J= 7.5Hz), 7.10 (t, 2H, J= 7.5Hz), 7.34 (d, 2H, J= 8Hz), 7.48 (t, 2H, J= 5.5Hz), 8.17 (m, 6H), 8.51 (d, 2H, J= 8Hz). HRMS *m/z* (ESI-TOF) for $C_{28}H_{22}IrN_6^+$ Calculated 635.15297 Found 635.15635.



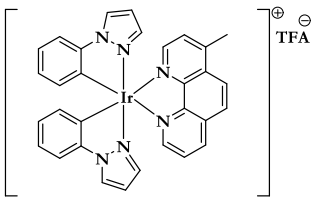
*Synthesis of $[Ir(ppyz)_2bpyMe_2]^+TFA^-$ (**13**)*

Dichloro bridged Iridium dimer **4** (100 mg, 0.097 mmol, 1eq) and 4,4'-dimethyl bipyridine ligand (42.5 mg, 0.231 mmol, 2.4 eq) were stirred in a 1:1 mixture of anhydrous DCM/MeOH (20mL) at reflux (50-60 ^oC) under argon for 4h. The solution was then cooled to RT and 1.2 mL of sat. NH_4PF_6 in MeOH was added while stirring. The solution was allowed to stir for 5min. The solvent was evaporated under vacuum and the resulting solid was purified with RP HPLC (30-70%B, 30min, 254nm, 20mL/min, t_R = 17.7min) to give 25.3 mg of yellow solid (17%). R_f = 0.20 (10:1 DCM/MeOH). mp = 187.0 ^oC. IR (thin film) 3348.78, 2922.59, 2850.27, 1721.16, 1680.66, 1618.95, 1479.13, 1438.64, 1413.57, 1198.54, 1136.83, 1076.08, 1034.62, 756.923 cm^{-1}. ^1H NMR (DMSO- d_6, 500MHz) δ 2.53 (s, 6H), 6.18 (d, 2H, J= 7Hz), 6.68 (t, 2H, J= 2.5Hz), 6.83 (t, 2H, J= 7Hz), 7.03 (t, 2H, J= 7.5Hz), 7.16 (d, 2H, J= 2Hz), 7.50 (d, 2H, J= 5.5Hz), 7.67 (d, 2H, J= 8Hz), 7.82 (d, 2H, J= 6Hz), 8.73 (s, 2H), 8.87 (d, 2H, J= 3Hz). ^{13}C NMR (DMSO- d_6, 125MHz) δ 21.35, 108.92, 112.49, 123.29, 125.66, 126.77, 129.01, 129.16, 133.03, 133.09, 139.04, 143.45, 149.88, 151.90, 156.12. HRMS *m/z* (ESI-TOF) for $C_{30}H_{26}IrN_6^+$ Calculated 663.18427 Found 663.18733.



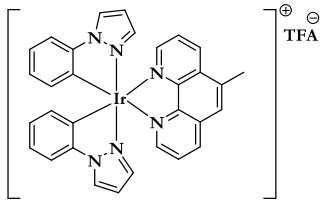
*Synthesis of [Ir(ppyz)$_2$bpyCOOH]$^+$TFA$^-$ (**14**)*

Dichloro bridged Iridium dimer **4** (155 mg, 0.151 mmol, 1eq) and 4-carboxy-4'-methyl bipyridyl ligand **1** (65.6 mg, 0.306 mmol, 2 eq) were stirred in a 1:1 mixture of anhydrous DCM/MeOH (20mL) at reflux (50 ^{o}C) under argon for 4.5h. The solution was then cooled to RT and 1.0-1.2 mL of sat. NH_4PF_6 in MeOH was added while stirring. The solution was allowed to stir for 5min. The solvent was evaporated under vacuum and the resulting solid was purified with RP HPLC (30-80%B, 35min, 254nm, 20mL/min, t_R = 11.1min) to give 127 mg orange solid (52%). R_f = 0.10 (10:1 DCM/MeOH). mp = 229.4-233.7 ^{o}C. IR (thin film) 3130.87, 3051.8, 2923.56, 2853.17, 1716.34, 1620.88, 1480.1, 1411.64, 1275.68, 1237.11, 1185.04, 1142.62, 1056.8, 1024.98, 840.812, 755.959 cm^{-1}. ^{1}H NMR (DMSO- d_6, 500MHz) δ 2.49 (s, 3H), 6.16 (1H, J= 7Hz), 6.18 (d, 1H, J= 7.5Hz), 6.68 (p, 2H, J= 3Hz), 6.85 (m, 2H), 7.03 (m, 2H), 7.19 (d, 1H, J= 2Hz), 7.30 (d, 1H, J= 2.5Hz), 7.54 (d, 1H, J= 5.5Hz), 7.68 (t, 2H, J= 7Hz), 7.83 (d, 1H, J= 6Hz), 8.06 (dd, 1H, J= 1Hz, 5.5Hz), 8.17 (d, 1H, J= 5.5Hz), 8.88 (dd, 2H, J= 3Hz, 8Hz), 9.00 (s, 1H) 9.12 (s, 1H), 14.32 (b, 1H). ^{13}C NMR (DMSO- d_6, 125 MHz) δ 20.57, 108.35, 108.42, 111.99, 122.90, 123.45, 125.91, 126.24, 126.30, 127.28, 128.50, 128.57, 128.99, 132.12, 132.29, 132.49, 138.73, 138.90, 140.82, 142.72, 142.86, 149.32, 151.26, 151.76, 154.86, 157.16, 164.79, 176.61, 181.37. HRMS *m/z* (ESI-TOF) for $C_{30}H_{24}IrN_6O_2^+$ Calculated 693.15845 Found 693.16035.



*Synthesis of [Ir(ppyz)$_2$^{4}Mephen]$^+$TFA$^-$ (**15**)*

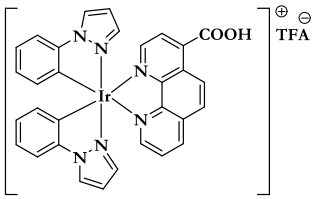
Dichloro bridged Iridium dimer **4** (100 mg, 0.097 mmol, 1eq) and 4-methyl-1,10-phenanthroline (38.4 mg, 0.198 mmol, 2 eq) were stirred in a 1:1 mixture of anhydrous DCM/MeOH (20mL) at reflux (50 ^{o}C) under argon for 4.5h. The solution was then cooled to RT and 1.0-1.2 mL of sat. NH_4PF_6 in MeOH was added while stirring. The solution was allowed to stir for 5min. The solvent was evaporated under vacuum and the resulting solid was purified with RP HPLC (30-80%B, 35min, 254nm, 20mL/min, t_R = 13.6min) to give 51.0 mg of yellow solid (33%). R_f = 0.20 (10:1 DCM/MeOH). mp = 154.7-158.4 ^{o}C. IR (thin film) 3122.19, 3059.51, 2922.59, 2853.17, 1779.97, 1735.62, 1686.44, 1481.06, 1431.89, 1412.6, 1193.72, 1141.65, 1058.73, 1034.62, 754.995, 704.855 cm^{-1}. ^{1}H NMR (DMSO- *d_6*, 500MHz) δ 2.94 (s, 3H), 6.29 (t, 2H, J= 7.5Hz), 6.58 (q, 2H, J= 2.5Hz), 6.88 (t, 2H, J= 7.5H), 7.07 (pd, 4H, J= 2Hz, 2Hz), 7.71 (d, 2H, J= 8H), 7.88 (d, 1H, J= 5.5Hz), 8.02 (q, 1H, J= 5Hz), 8.17 (d, 1H, J= 5Hz), 8.33 (dd, 1H, J= 1Hz, 5Hz), 8.39 (d, 1H, J= 9Hz), 8.47 (d, 1H, J= 9Hz), 8.86 (t, 2H, J= 2.5Hz), 8.89 (dd, 1H, J= 1Hz, 8Hz). ^{13}C NMR (DMSO- *d_6*, 125MHz) δ 18.56, 108.24, 111.96, 122.88, 124.84, 126.20, 127.05, 127.66, 128.44, 130.60, 131.93, 132.57, 138.20, 138.55, 138.80, 143.08, 146.32, 146.75, 148.73, 150.03, 150.91. HRMS *m/z* (ESI-TOF) for $C_{13}H_{24}IrN_6^+$ Calculated 673.16862 Found 673.16731.



*Synthesis of [Ir(ppyz)$_2$^{5}Mephen]$^+$TFA$^-$ (**16**)*

Dichloro bridged Iridium dimer **4** (99.7 mg, 0.097 mmol, 1eq) and 5-methyl-1,10-phenanthroline (37.8 mg, 0.195 mmol, 2 eq) were stirred in a 1:1 mixture of anhydrous

DCM/MeOH (20mL) at reflux (50-60 ^{o}C) under argon for 4h. The solution was then cooled to RT and 1.2 mL of sat. NH_4PF_6 in MeOH was added while stirring. The solution was allowed to stir for 5min. The solvent was evaporated under vacuum and the resulting solid was purified with RP HPLC (30-80%B, 35min, 254nm, 20mL/min, t_R = 18.5min) to give 16.5 mg of yellow solid (11%). R_f = 0.20 (10:1 DCM/MeOH). mp = 110.3-112.4 ^{o}C. IR (thin film) 3121.22, 2965.02, 2918.73, 2850.27, 1730.8, 1686.44, 1481.06, 1428.03, 1412.6, 1191.79, 1138.76, 754.995, 727.032 cm^{-1}. ^{1}H NMR (DMSO-*d*$_6$, 500MHz) δ 2.88 (s, 3H), 6.29 (d, 2H, J= 7.5Hz), 6.59 (d, 2H, J= 2Hz), 6.89 (tt, 2H, J= 1Hz, 7.5Hz), 7.72 (d, 2H, J= 8H), 7.98 (td, 1H, J= 2H, 5Hz), 8.06 (td, 1H, J= 1.5Hz, 5Hz), 8.20 (s, 1H), 8.26 (d, 1H, J= 5Hz), 8.34 (d, 1H, J= 5Hz), 8.77 (d, 1H, J= 8Hz), 8.87 (s, 2H), 8.93 (d, 1H, J= 8.5Hz). ^{13}C NMR (DMSO- *d*$_6$, 500MHz) δ 18.29, 108.26, 111.98, 122.92, 126.20, 126.45, 126.55, 126.67, 128.48, 130.48, 130.91, 131.51, 141.67, 131.97, 132.57, 135.77, 135.91, 137.77, 138.82, 143.02, 145.98, 146.81, 149.93, 150.49. HRMS *m/z* (ESI-TOF) for $C_{31}H_{24}IrN_6^+$ Calculated 673.16862 Found 673.16990.

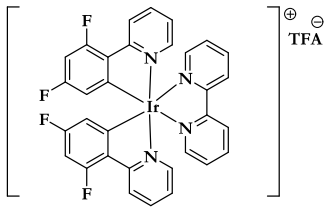


*Synthesis of [Ir(ppyz)$_2$phenCOOH]$^+$TFA$^-$ (**17**)*

Iridium dimer **4** (203mg, 0.195mmol, 1eq) and phenanthroline ligand **2** (87.2mg, 0.389mmol, 2eq) were stirred in a solution of 1:1DCM/MeOH (20mL) under argon at reflux (60 ^{o}C) for 4h. The solution was cooled to RT and 1 mL of concentrated NH4PF6 was added and stirred for 10min. The solution was rotovapped and the resulting orange solid was purified by RP HPLC (60-90%B, 40min, 20mL/min, 254nm) to yield 61.8 mg

of orange solid (38%). Rf = 0.50 (6:1DCM/MeOH). mp = 166.5-168.9 ^{o}C. IR (thin film) 3417.24, 3122.19, 3057.58, 2921.63, 1711.51, 1687.41, 1482.03, 1445.39, 1428.99, 1412.6, 1338.36, 1276.65, 1187.94, 1133.94, 1111.76, 1075.12, 1058.73, 1034.62, 754.995, 730.889, 717.39 cm^{-1}. ^{1}H NMR (500MHz, DMSO- d_6) δ 6.249 (t, 2H, J= 7.5Hz), 6.549 (s, 2H), 6.848 (t, 2H, J= 7.5Hz), 7.050 (p,d, 3H, J= 3.5Hz, 2.5Hz), 7.196 (d, 1H, J= 2Hz), 7.681 (d, 2H, J= 8Hz), 8.013 (q, 1H, J= 5.5Hz), 8.334 (t, 2H, J= 5Hz), 8.412 (d, 1H, J= 9Hz), 8.454 (d, 1H, J= 5Hz), 8.826 (t, 2H, J= 3Hz), 8.869 (d, 1H, J= 8Hz), 8.949 (d, 1H, J= 9Hz), 14.40 (b, 1H). ^{13}C NMR (125MHz, DMSO- d_6) δ 108.87, 109.90, 112.58, 113.31, 123.65, 125.59, 125.97, 126.84, 127.11, 127.52, 127.67, 128.92, 129.06, 129.69, 130.00, 131.12, 132.08, 132.22, 132.38, 133.06, 133.14, 138.78, 139.16, 139.55, 139.76, 141.43, 141.65, 143.47, 143.56, 147.16, 148.27, 151.69, 151.76, 158.57, 158.84, 159.18, 166.64.

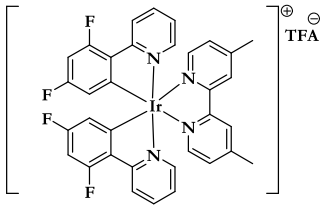
HRMS *m/z* (ESI-TOF) for $C_{31}H_{22}IrN_6O_2Na$ Calculated 725.12529 Found 725.1305.



*Synthesis of [Ir(F$_2$ppy)$_2$bpy]$^{+}$TFA^{-} (**18**)*

Compound **18** was made using established literature procedures.[68] Dichloro bridged Iridium dimer **5** (109 mg, 0.0896 mmol, 1eq) and bipyridine (28.6 mg, 0.183 mmol, 2 eq) were stirred in a 1:1 mixture of anhydrous DCM/MeOH (20mL) at reflux (50-60 ^{o}C) under argon for 4h. The solution was then cooled to RT and 1.0 mL of sat. NH_4PF_6 in MeOH was added while stirring. The solution was allowed to stir for 5min. The solvent was evaporated under vacuum and the resulting solid was purified with RP HPLC (60-

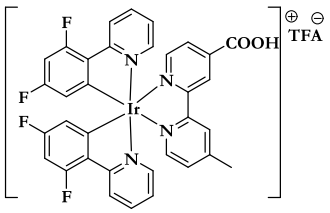
75%B, 30min, 254nm, 20mL/min, t_R = 9.7min) to give 55.3mg of yellow solid (37%). R_f = 0.18 (10:1 DCM/MeOH). mp = 195.8-200.2 ^oC. IR (thin film) 3083.62, 2926.45, 1779.01, 1737.55, 1604.48, 1575.56, 1560.13, 1479.13, 1448.28, 1429.96, 1406.82, 1313.29, 1294.97, 1268.93, 1248.68, 1191.79, 1165.76, 1143.58, 117.55, 1105.98, 989.304, 843.704, 787.779, 760.78, 734.746, 720.282, 705.819 cm^{-1}. ^1H NMR (DMSO-d_6, 500MHz) δ 5.57 (dd, 2H, J= 2.4Hz, 8.4Hz), 6.93 (td, 2H, J= 2.1Hz, 9.9Hz), 7.21 (t, 2H, J= 6.9Hz), 7.67 (m, 2H, J= 8.4Hz, 5.7Hz), 7.88 (d, 2H, J= 5.1Hz), 8.00 (t, 2H, J= 7.8Hz), 8.28 (t, 4H, J= 8.7Hz), 8.87 (d, 2H, J= 8.1Hz). ^1H NMR (CD_2Cl_2, 500MHz) δ 5.74 (dd, 2H, J= 2Hz, 8.5Hz), 6.61 (td, 2H, J= 2Hz, 10Hz), 7.04 (t, 2H, J= 6.5Hz), 7.47 (d, 2H, J= 5.5Hz), 7.54 (t, 2H, J= 6Hz), 7.85 (t, 2H, J= 8Hz), 8.02 (d, 2H, J= 5.5Hz), 8.20 (t, 2H, J= 7.5Hz), 8.33 (d, 2H, J= 8.5Hz), 8.62 (d, 2H, J= 7.5Hz). HRMS *m/z* (ESI-TOF) for $C_{32}H_{20}F_4IrN_4^+$ Calculated 729.12478 Found 729.12179.



*Synthesis of [Ir(F$_2$ppy)$_2$Me$_2$bpy]$^+$TFA$^-$ (**19**)*

Dichloro bridged Iridium dimer **5** (102.5 mg, 0.084 mmol, 1eq) and 4,4'-dimethyl bipyridine ligand (36.1 mg, 0.196 mmol, 2.3 eq) were stirred in a 1:1 mixture of anhydrous DCM/MeOH (20mL) at reflux (50-60 ^oC) under argon for 4h. The solution was then cooled to RT and 1.2 mL of sat. NH_4PF_6 in MeOH was added while stirring. The solution was allowed to stir for 5min. The solvent was evaporated under vacuum and the resulting solid was purified with RP HPLC (60-75%B, 30min, 254nm, 20mL/min, t_R = 12min) to give 29.8mg of yellow solid (20%). R_f= 0.30 (10:1 DCM/MeOH). mp =

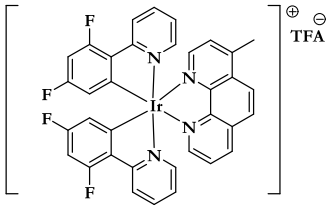
172.8-180.8 °C. IR (thin film) 3072.05, 2927.41, 2855.1, 1735.62, 1687.41, 1603.52, 1574.59, 1559.17, 1478.17, 1428.99, 1405.85, 1294.97, 1247.72, 1194.69, 1164.79, 1140.69, 1118.51, 1105.01, 1069.33, 989.304, 830.205, 788.743, 757.888, 705.819 cm^{-1}. ^{1}H NMR (DMSO- d_6, 500MHz) δ 2.50 (s, 6H), 5.57 (dd, 2H, J= 2Hz, 8Hz) 6.94 (td, 2H, J= 2.5Hz, 9.5Hz), 7.21 (t, 2H, J= 7.5Hz), 7.49 (d, 2H, J= 5.5Hz), 7.65 (d, 2H, J= 5.5Hz), 7.70 (d, 2H, J= 6Hz), 7.80 (t, 2H, J= 8Hz), 8.25 (d, 2H, J= 8.5Hz), 8.74 (s, 2H). ^{13}C NMR (DMSO- d_6, 125 MHz) δ 20.92, 98.70, 98.91, 99.12, 113.14, 113.28, 123.24, 123.39, 124.48, 125.76, 127.56, 129.55, 139.93, 149.40, 149.45, 152.08, 154.77, 154.85, 159.70, 161.82, 162.74. HRMS *m/z* (ESI-TOF) for $C_{34}H_{24}F_4IrN_4^+$ Calculated 757.15609 Found 757.15480.



*Synthesis of [Ir(F_2ppy)$_2$bpyCOOH]$^+$TFA$^-$ (**20**)*

Dichloro bridged Iridium dimer **5** (114 mg, 0.094 mmol, 1eq) and 4-carboxy-4'-methyl bipyridyl ligand **1** (43.0 mg, 0.200 mmol, 2.1 eq) were stirred in a 1:1 mixture of anhydrous DCM/MeOH (20mL) at reflux (50-60 °C) under argon for 4h. The solution was then cooled to RT and 1.0 mL of sat. NH_4PF_6 in MeOH was added while stirring. The solution was allowed to stir for 5min. The solvent was evaporated under vacuum and the resulting solid was purified with RP HPLC (50-80%B, 35min, 254nm, 20mL/min, t_R = 12.8min) to give 67.7mg of yellow solid (40%). R_f= 0.075 (10:1 DCM/MeOH). mp = 161.1-164.0 °C. IR (thin film) 3367.1, 3080.73, 2924.52, 1725.01, 1673.91, 1604.48, 1575.56, 1559.17, 1479.13, 1429.96, 1406.82, 1294.97, 1268.93, 1248.68, 1236.15,

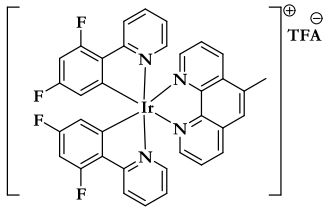
1192.76, 1165.76, 1142.62, 1118.51, 1105.98, 1043.3, 989.304, 843.704 cm^{-1} ^{1}H NMR (DMSO- d_6, 500MHz) δ 2.52 (s, 3H), 5.56 (qd, 2H, J= 2Hz, 8.5Hz), 6.95 (m, 2H), 7.19 (dt, 2H, J= 2.2Hz, 7H), 7.53 (d, 1H, J= 5.5Hz), 7.66 (d, 1H, J= 6Hz), 7.72 (d, 2H, J= 5.5Hz), 8.01 (p, 2H, J= 7.5Hz), 8.03 (s, 2H), 8.25 (t, 2H, J= 6.5Hz), 9.03 (s, 1H), 9.12 (s, 1H). ^{13}C NMR (DMSO- d_6, 125 MHz) δ 21.19, 99.60, 113.66, 123.67, 123.76, 123.93, 124.59, 125.01, 127.07, 127.96, 128.08, 128.59, 129.10, 130.41, 140.52, 141.82, 149.91, 150.15, 150.39, 151.88, 152.96, 154.60, 154.77, 154.93, 156.96, 158.20, 158.46, 162.33, 162.96, 163.12, 163.22. HRMS *m/z* (ESI-TOF) for $C_{34}H_{22}F_4IrN_4O_2^+$ Calculated 787.13026 Found 787.13469.



Synthesis of [Ir(F_2ppy)$_2$^{4}Mephen]$^+$TFA$^-$ ***(21)***

Dichloro bridged Iridium dimer **5** (100 mg, 0.082 mmol, 1eq) and 4-methyl-1,10-phenanthroline (34.9 mg, 0.164 mmol, 2 eq) were stirred in a 1:1 mixture of anhydrous DCM/MeOH (20mL) at reflux (50-60 ^{o}C) under argon for 4h. The solution was then cooled to RT and 1.2 mL of sat. NH_4PF_6 in MeOH was added while stirring. The solution was allowed to stir for 5min. The solvent was evaporated under vacuum and the resulting solid was purified with RP HPLC (50-80%B, 35min, 254nm, 20mL/min, t_R = 16.2min) to give 37.5mg of yellow/orange solid (26%). R_f = 0.23 (10:1 DCM/MeOH). mp = 188.3-192.5 ^{o}C. IR (thin film) 3076.87, 2926.45, 1779.01, 1736.58, 1603.52, 1574.59, 1560.13, 1479.13, 1428.99, 1405.85, 1294.97, 1248.68, 1190.83, 1165.76, 1142.62, 1118.51, 1105.01, 989.304, 844.669, 831.169, 788.743, 705.819 cm^{-1}. ^{1}H NMR

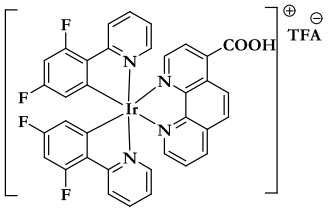
(DMSO- d_6, 500MHz) δ 2.95 (s, 3H), 5.71 (td, 2H, J= 2.5Hz, 8.5Hz) 7.01 (t, 2H, J= 11Hz), 7.07 (q, 2H, J= 16Hz), 7.51 (dd, 2H, J= 5.5Hz, 14.5Hz), 7.90 (d, 1H, J= 7Hz), 7.96 (ts, 2H, J= 2Hz, 3Hz), 8.05 (dd, 1H, J= 5Hz, 8Hz), 8.14 (d, 1H, J= 5.5Hz), 8.30 (d, 2H, J= 8.5Hz), 8.33 (s, 1H), 8.43 (d, 1H, J= 9.5Hz), 8.50 (d, 1H, J= 9Hz), 8.95 (d, 1H, J= 8Hz). ^{13}C NMR (DMSO- d_6, 500MHz) δ 18.54, 98.66, 98.87, 99.09, 113.19, 123.01, 123.15, 124.23, 125.08, 127.16, 127.66, 127.89, 130.66, 130.84, 139.03, 139.70, 145.19, 145.65, 149.36, 149.51, 150.19, 151.12, 154.06, 157.65, 157.92, 159.43, 159.53, 161.54, 162.62, 163.57, 163.67. HRMS *m/z* (ESI-TOF) for $C_{35}H_{22}F_4IrN_4^+$ Calculated 767.14043 Found 767.14087.



Synthesis of [Ir(F$_2$ppy)$_2$^{5}Mephen]$^+$TFA$^-$ ***(22)***

Dichloro bridged Iridium dimer **5** (103.6 mg, 0.085 mmol, 1eq) and 5-methyl-1,10-phenanthroline (32.6 mg, 0.168 mmol, 2 eq) were stirred in a 1:1 mixture of anhydrous DCM/MeOH (20mL) at reflux (50-60 ^{o}C) under argon for 4h. The solution was then cooled to RT and 1.0 mL of sat. NH_4PF_6 in MeOH was added while stirring. The solution was allowed to stir for 5min. The solvent was evaporated under vacuum and the resulting solid was purified with RP HPLC (60-75%B, 30min, 254nm, 20mL/min, t_R = 11.0min) to give 38.3 mg of yellow solid (26%). R_f = 0.23 (10:1 DCM/MeOH). mp = 143.5-146.0 ^{o}C. IR (thin film) 3079.76, 1778.05, 1736.58, 1604.48, 1574.59, 1559.17, 1479.13, 1428.99, 1405.85, 1294.97, 1248.68, 1189.86, 1165.76, 1143.58, 1118.51, 1105.01, 989.304, 843.704, 831.169, 789.707, 757.888, 727.996, 704.855 cm^{-1}. ^{1}H

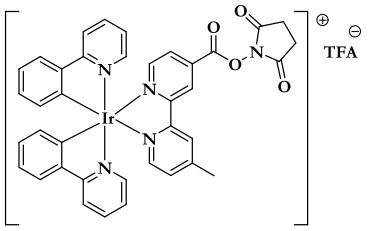
NMR (DMSO- d_6, 500MHz) δ 2.50 (s, 3H), 6.13 (q, 2H, J= 7.5Hz), 6.87 (t, 2H, J= 7Hz), 6.97 (m, 2H), 7.10 (dt, 2H, J= 7Hz, 22Hz), 7.51 (d, 1H, J= 5.5Hz), 7.58 (d, 1H, J= 6Hz), 7.65 (t, 2H, J= 7.5Hz), 7.89 (p, 4H, J= 8Hz), 7.98 (dd, 1H, J= 1.5Hz, 4Hz), 8.03 (d, 1H, J= 5Hz), 8.23 (t, 2H, J= 8.5Hz), 8.99 (s, 1H), 9.11 (s, 1H). ^{13}C NMR (DMSO- d_6, 500MHz) δ 18.36, 98.87, 99.08, 99.29, 113.32, 113.46, 123.18, 123.33, 124.42, 126.98, 127.21, 127.46, 127.77, 130.89, 131.29, 136.22, 136.54m, 138.41, 139.89, 145.00, 145.94, 149.69, 149.75, 150.29, 150.83, 159.69, 161.72, 162.72, 163.72. HRMS *m/z* (ESI-TOF) for $C_{35}H_{22}F_4IrN_4^+$ Calculated 767.14043 Found 767.13730.



*Synthesis of [Ir(F$_2$ppy)$_2$phenCOOH]$^+$TFA$^-$ (**23**)*

Dichloro bridged Iridium dimer **5** (108.3 mg, 0.089 mmol, 1eq) and 4-carboxy-1,10-phenanthroline ligand **2** (48.0 mg, 0.214 mmol, 2.4 eq) were stirred in a 1:1 mixture of anhydrous DCM/MeOH (20mL) at reflux (50-60 ^{o}C) under argon for 4h. The solution was then cooled to RT and 1.0 mL of sat. NH_4PF_6 in MeOH was added while stirring. The solution was allowed to stir for 5min. The solvent was evaporated under vacuum and the resulting solid was purified with RP HPLC (50-80%B, 35min, 254nm, 20mL/min, t_R = 16.7min) to give 21.1mg of yellow solid (13%). R_f = 0.075 (10:1 DCM/MeOH). mp = 171.5-175.6 ^{o}C. IR (thin film) 3426.89, 3084.58, 2922.59, 1717.3, 1676.8, 1603.52, 1574.59, 1560.13, 1479.13, 1429.96, 1405.85, 1294.97, 1248.68, 1190.83, 1165.76, 1118.51, 1105.98, 989.304, 843.704, 931.169 cm^{-1}. ^{1}H NMR (^{d}DMSO, 500MHz) δ 5.64 (td, 2H, J= 2Hz, 8.5Hz), 7.02 (m, 4H), 7.47 (d, 1H, J= 5.5Hz), 7.58 (d, 1H, J= 6Hz), 7.95

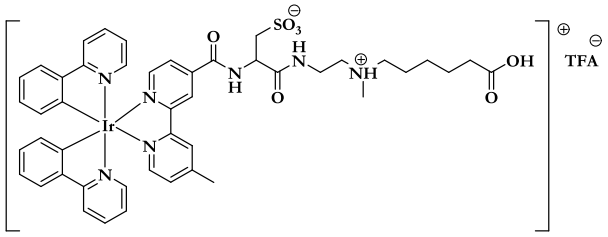
(t, 2H, J= 7.5Hz), 7.58 (d, 1H, J= 6Hz), 7.95 (t, 2H, J= 7.5Hz), 8.05 (m, 1H), 8.25 (d, 2H, J= 9Hz), 8.30 (d, 1H, J= 5Hz), 8.34 (d, 1H, J= 5Hz), 8.40 (d, 1H, J= 5Hz), 8.46 (d, 1H, J= 9Hz), 8.94 (d, 1H, J= 8.5Hz), 8.98 (d, 1H, J= 9.5Hz). ^{13}C NMR (DMSO- d_6, 125MHz) δ 99.00, 99.22, 99.40, 113.38, 123.20, 123.34, 124.44, 125.79, 127.78, 127.86, 128.77, 129.50, 130.94, 138.47, 139.20, 139.95, 145.62, 146.79, 149.91, 150.14, 151.57, 153.63, 153.93, 157.95, 159.56, 159.67, 161.67, 162.64, 163.69, 166.02. HRMS *m/z* (ESI-TOF) for $C_{35}H_{20}F_4IrN_4O^+$ Calculated 797.11461 Found 797.11879.



*Succinimide Ester of [Ir(ppy)$_2$bpyCOOH] (**31**)*

Iridium complex **8** (25.5mg, 0.036mmol, 1eq), N-hydroxysuccinimide (34.6mg, 0.301 mmol, 8.4eq), and 1,3-dicyclohexylcarbodiimide (53.0mg, 0.257mmol, 7eq) were stirred in a solution of anhydrous DCM (8mL) under argon overnight. The solvent was removed under reduced pressure and the resulting orange solid purified by RP HPLC (40-75%B, 40min, 20mL/min, 254nm, t_R= 26min) to yield 13.5mg of orange solid **31** (47%). R_f = 0.84 (6:1 DCM/MeOH). ^{1}H NMR (500MHz, $CDCl_3$) δ 2.61 (s, 3H), 3.06 (s, 4H), 6.29 (t, 2H, J= 7.5Hz), 6.96 (t, 3H, 7.5Hz), 7.06 (p, 4H, J= 7.5Hz), 7.29 (d, 1H, J= 5.5Hz), 7.50 (d, 1H, J= 5.5Hz), 7.54 (d, 1H, J= 5.5Hz), 7.70 (d, 2H, J= 6.5 Hz), 7.77 (t, 2H, J= 7Hz), 7.93 (t, 3H, 5.5Hz), 7.96 (d, 1H, J= 5.5Hz), 8.18 (d, 1H, 5.5Hz), 8.85 (s, 1H), 9.35 (s, 1H). ^{13}C NMR (125MHz, $CDCl_3$) δ 21.4, 25.401, 119.54, 122.74, 123.45, 124.70, 126.47, 127.72, 129.14, 131.80, 138.02, 143.35, 148.32, 150.10, 150.81, 152.41, 155.25, 156.49, 167.86, 173.01. HRMS *m/z* (ESI-TOF) for $C_{38}H_{29}IrN_5O_4^+$ Calculated 812.18433 Found

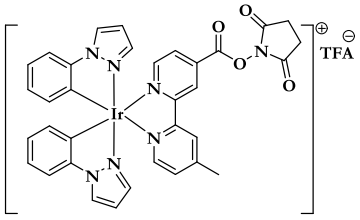
812.18590.



*[Ir(ppy)$_2$bpyCOOH] with zwitterionic side chain (**30**)*

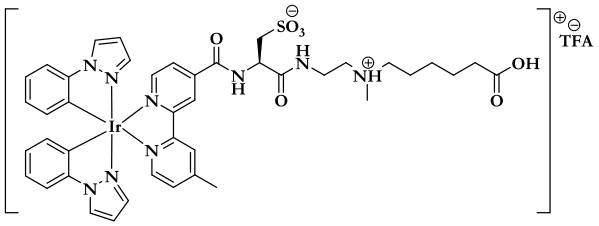
Activated complex **31** (13.5mg, 0.014mmol, 1eq), N-methylmorpholine (0.03mL, 0.282mmol, 20eq), and peptide side chain **4** (41.3mg, 0.085, 6eq) were stirred in DMF (3mL) under argon at RT overnight. The solvent was then removed under reduced pressure and the solid purified by RP HPLC (30-60%B, 4mL/min, 254nm, 30m) to yield 2.2mg of yellow solid (15%). R_f = 0.69 (6:1 DCM/MeOH). mp= 207.6-212.6 ^oC. IR (thin film) 3292.86, 3053.73, 2851.24, 1721.16, 1619.91, 1583.27, 1438.64, 1419.35, 1306.54, 1267.97, 1063.55, 798.385, 733.782, 720.282, 703.89 cm^{-1}. ^1H NMR (500MHz, $CDCl_3$) δ 1.43 (m, 2H), 1.74 (m, 2H), 1.93 (m, 2H), 2.36 (m, 2H), 2.43 (m, 2H), 2.62 (s, 3H), 2.91 (s, 3H), 3.28 (m, 2H), 3.35 (m, 2H), 3.61 (m, 1H), 3.89 (m, 2H), 5.16 (m, 1H), 6.29 (s, 2H), 6.94 (m, 3H), 7.05 (d, 3H, J= 4.0Hz), 7.45 (m, 1H), 7.58 (s, 1H), 7.69 d, 2H, J= 7.5Hz), 7.77 (t, 3H, J= 6Hz), 7.91 (q, 3H, J= 8Hz), 8.03 (s, 1H), 8.87 (m, 1H), 9.35 (m, 1H), 9.77 (m, 1H). ^{13}C NMR (125MHz, $CDCl_3$) δ 21.76, 23.12, 23.92, 24.98, 25.60, 26.60, 27.93, 29.32, 29.91, 33.64, 34.08, 34.82, 41.37, 41.99, 45.20, 50.00, 50.56, 51.23, 51.74, 53.48, 54.39, 56.06, 56.55, 57.73, 114.28, 114.83, 119.63, 119.93, 122.79, 123.04, 123.36, 123.78, 124.87, 125.07, 126.54, 126.88, 129.28, 130.91, 131.12, 131.94, 138.27, 143.70, 144.71, 148.47, 149.82, 150.56, 151.25, 152.30, 155.36, 156.68, 160.80, 163.51, 167.69, 168.11. HRMS *m/z* (ESI-TOF) for $C_{46}H_{49}O_7N_7IrS^+$ Calculated 1036.30

Found 1036.3013.



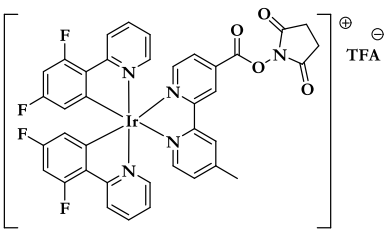
*Succinimide Ester of [Ir(pyz)$_2$bpyCOOH] (**34**)*

A mixture of Iridium complex **14** (50.0mg, 0.0621mmol, 1eq), NHS (57.1mg, 0.496mmol, 6eq), and DCC (76.8mg, 0.372mmol, 6eq) was stirred in anhydrous DCM (4mL) under argon at RT overnight. The solvent was removed under reduced pressure to yield an orange solid, which was purified by RP HPLC (40-75%, 20mL/min, 254nm, 40min, t_R =49m) to yield 27.7 mg of orange solid **34** (49%). R_f = 0.84 (6:1 DCM/MeOH). IR (thin film) 3386.39, 2849.31, 1710.55, 1456.96, 1375.96, 1202.4, 1144.55, 1074.16, 751.138, 719.318 cm^{-1}. ^{1}H NMR (500MHz, $CDCl_3$) δ 2.62 (s, 3H), 2.91 (s, 4H), 6.28 (q, 2H, J= 7.5Hz), 6.56 (s, 2H), 6.91 (td, 4H, J= 2Hz, 6.5Hz), 7.06 (td, 2H, J= 1.5Hz, 7.5Hz), 7.31 (d, 3H, J= 7Hz), 7.97 (t, 2H, J=5.5Hz), 8.13 (q, 2H, J= 5.5Hz), 8.36 (d, 1H, J= 5.5 Hz), 8.70 (s, 1H), 9.23 (s, 1H). ^{13}C NMR (125MHz, $CDCl_3$) δ 21.34, 25.63, 108.39, 108.49, 108.61, 111.68, 123.65, 123.75, 124.30, 126.56, 126.90, 126.98, 127.03, 127.08, 127.14, 129.37, 131.13, 131.19, 133.07, 13324, 135.24, 137.89, 138.04, 138.30, 142.41, 142.65, 150.29, 151.85, 152.89, 154.55, 158.56, 159.23. HRMS *m/z* (ESI-TOF) for $C_{34}H_{27}IrN_7O_4^+$ Calculated 790.17538 Found 790.17891.



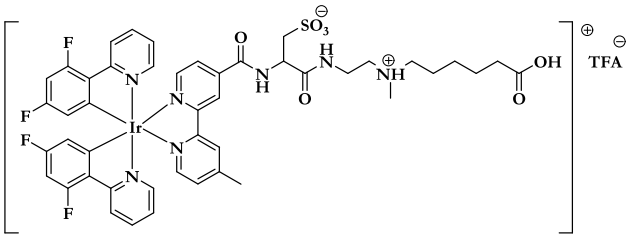
*[Ir(pyz)$_2$bpyCOOH] with zwitterionic side chain (**35**)*

Activated complex **34** (27.7mg, 0.0307mmol, 1eq), N-methylmorpholine (0.07mL, 0.614mmol, 20eq), and peptide side chain **4** (84.9mg, 0.187mmol, 6eq) were stirred in DMF (3mL) under argon at RT overnight. The solvent was then removed under reduced pressure and the solid purified by RP HPLC (30-70%B, 35min, 20mL/min, 254nm, t_R = 26m) to yield 1.0mg of yellow solid **35** (3%). R_f = 0 (6:1 DCM/MeOH) . IR (thin film) 3279.36, 3057.58, 2919.7, 2850.27, 1541.81, 1480.1, 1412.6, 1338.36, 1276.65, 1136.83, 1075.12, 1037.52, 833.098, 798.385, 753.066, 720.282 cm^{-1}. ^{1}H NMR (500MHz, $CDCl_3$) δ 1.43 (p, 2H, J= 5Hz), 1.65 (p, 2H, J= 6.5Hz), 1.89 (m, 2H), 2.30 (m, 4H), 2.61 (s, 3H), 3.56 (d, 3H, J= 5.5Hz), 3.79 (m, 2H), 4.02 (s, 2H), 4.08 (m, 2H), 5.30 (s, 1H), 6.29 (d, 2H, J= 7.5Hz), 6.53 (dt, 2H, J= 3Hz, 9Hz), 6.80 (t, 1H, J= 2Hz), 6.88 (d, 2H, J= 7.5Hz), 6.91 (d, 1H, J= 2Hz), 7.06 (q, 2H, J= 5.5Hz), 7.27 (m, 2H), 7.91 (d, 1H, J= 5.5Hz), 7.99 (d, 1H, J= 6Hz), 8.09 (dd, 2H, J= 3Hz, 7Hz), 8.19 (d, 1H, J= 6Hz), 8.70 (s, 1H), 9.31 (s, 1H), 10.16 (s, 1H). HRMS *m/z* (ESI-TOF) for $C_{42}H_{47}IrN_9O_7S^+$ Calculated 1014.29484 Found 1014.29368.



*Succinimide Ester of [Ir(F$_2$pyp)$_2$bpyCOOH] (**36**)*

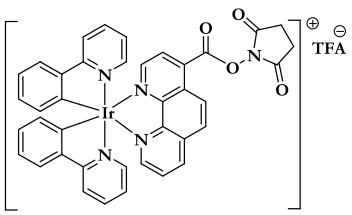
Iridium complex **20** (34.0mg, 0.038mmol, 1eq), DCC (53.7mg, 0.226mmol, 6eq), and NHS (40.1mg, 0.302mmol, 8eq) were stirred in anhydrous DCM (8mL) under argon at RT overnight. The solvent was removed under reduced pressure and the resulting orange solid was purified by RP HPLC (40-75%B, 20mL/min, 254nm, 40min, t_R=31m) to give 14.5 mg of yellow/orange solid **36** (33%). R_f = 0.81 (6:1DCM/MeOH). ^{1}H NMR (500MHz, $CDCl_3$) δ 2.61 (s, 3H), 2.92 (s, 4H), 5.67 (qd, 2H, J= 2Hz, 8Hz), 6.58 (t, 2H, J= 9.5 Hz), 7.07 (p, 2H, J=7.5Hz), 7.32 (d, 1H, J= 5Hz), 7.53 (t, 2H, J= 6Hz), 7.78 (d, 1H, J=4.5Hz), 7.80 (t, 2H, J= 8Hz), 8.03 (d, 1H, J= 5Hz), 8.18 (d, 1H, J= 5.5Hz), 8.31 (d, 2H, J= 7Hz), 9.09 (s, 1H), 9.37 (s, 1H). ^{13}C NMR (125MHz, $CDCl_3$) δ 21.35, 25.63, 99.58, 113.98, 123.62, 123.75, 123.91, 124.81, 125.42, 126.60, 127.74, 129.49, 130.07, 135.77, 139.16, 139.30, 139.41, 148.53, 148.68, 148.91, 149.45, 149.55, 150.82, 151.09, 153.20, 153.39, 153.74, 154.76, 156.45, 157.93, 159.07, 160.43, 162.81, 164.23,, 164.77, 168.48, 172.63. HRMS *m/z* (ESI-TOF) for $C_{38}H_{25}F_4IrN_5O_4^+$ Calculated 884.14719 Found 884.14599.



*[Ir(F$_2$ppy)$_2$bpyCOOH] with zwitterionic side chain (**37**)*

To a stirred solution of Compound **36** (7.4mg, 0.007mmol, 1eq) and peptide **4** (24.2mg, 0.044mmol, 7.6eq) in DMF (3mL) under argon was added NMM (0.02mL, 0.15mmol, 20eq) dropwise while stirring. The solution was allowed to stir overnight and the solvent was removed *in vacuo*. The resulting yellow solid was purified by RP HPLC (30-60%B, 30min, 254nm, 4mL/min) to give 1.9mg of yellow solid **37** (23%). mp = 150.0-154.7 ^{o}C.

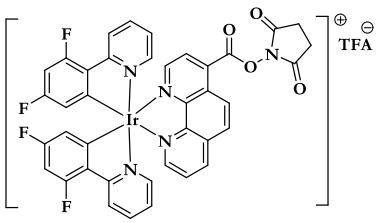
IR (thin film) 3287.07, 2918.73, 2850.27, 2345.02, 1670.05, 1603.52, 1574.59, 1559.17, 1477.21, 1428.99, 1405.85, 1294, 1167.69, 1131.05, 1040.41, 989.304, 830.205, 796.457, 717.39 cm^{-1}. ^1H NMR (500MHz, $CDCl_3$) δ 1.58 (m, 2H), 1.73 (m, 2H), 1.98 (m, 2H), 2.40 (m, 4H) 2.63 (s, 3H), 3.01 (s, 3H), 3.41 (m, 2H), 3.84 (m, 2H), 4.32 (m, 2H), 4.44 (m, 1H), 5.67 (t, 2H, J= 5Hz), 6.59 (q, 2H, J= 3Hz), 7.01 (t, 1H, J= 6Hz), 7.07 (m, 1H), 7.31 (t, 1H, J= 6Hz), 7.45 (m, 1H), 7.55 (m, 1H), 7.73 (d, 1H, J = 9Hz), 7.81 (q, 2H, J= 7Hz), 7.95 (dd, 1H, J= 6Hz, 10Hz), 8.32 (q, 2H, J= 6.5Hz), 9.16 (m, 1H), 9.81 (m, 1H). HRMS *m/z* (ESI-TOF) for $C_{46}H_{45}F_4IrN_7O_7S^+$ Calculated 1108.2665 Found 1108.26240.



*Succinimide Ester of [Ir(ppy)$_2$phenCOOH] (**32**)*

Starting material [Ir(ppy)$_2$phenCOOH], compound **11** (25.2mg, 0.03mmol, 1eq), N-hydroxysuccinimide (7.6mg, 0.066mmol, 2.2eq), 1-ethyl-3-(3-dimethylaminopropyl) carbodiimide (EDC) (6.33mg, 0.033mmol, 1.1eq), and 1-hydroxy-benzotriazole (HOBt) (1.5mg, 0.011mmol, 0.37eq) were stirred at room temperature in dichloromethane (4-5mL) overnight. The resulting solid was purified by RP HPLC (40-75%B, 40m, 20mL/m, 254nm, t_R = 25m) to give 8.8mg of yellow solid **32** (25%). Rf = 0.84 (6:1 DCM/MeOH). IR (thin film) 3063.37, 2918.73, 2849.31, 2846.42, 1715.37, 1607.38, 1583.27, 1561.09, 1479.13, 1420.32, 1267.97, 1191.79, 1133.94, 1065.48, 1031.73, 759.816, 730.889, 714.497 cm^{-1}. ^1H NMR (500MHz, $CDCl_3$) δ 2.97 (s, 4H), 6.36 (dd, 1H, J= 1.5Hz, 7.5Hz), 6.41 (dd, 1H, J= 1.5Hz, 7.5Hz), 6.83 (m, 1H), 6.89 (t, 1H, J= 5.5Hz), 6.98 (p, 2H, J= 3.5Hz), 7.08 (p, 2H, J= 3.5Hz), 7.35 (d, 1H, J= 4Hz), 7.71 (t, 4H,

J= 8Hz), 7.80 (t, 1H, J= 3Hz), 8.15 (d, 1H, J=3Hz), 8.29 (d, 1H, J= 8Hz), 8.59 (d, 1H, J= 8Hz), 8.96 (d, 1H, J= 9Hz). ^{13}C NMR (125 MHz, $CDCl_3$) δ 25.57, 29.90, 119.71. 119.95. 123.03. 123.20. 123.27. 123.62. 124.98. 125.14. 126.05. 126.57, 128.13, 128.47, 129.31, 131.01, 131.25, 131.37, 132.05, 138.28, 138.35, 138.49, 143.61, 143.87, 146.95, 147.25, 148.37, 149.18, 149.63, 149.83, 150.77, 151.11, 168.18, 172.16. HRMS *m/z* (ESI-TOF) for $C_{39}H_{27}IrN_5O_4^+$ Calculated 822.16889 Found 822.17075.



*Succinimide Ester of [Ir(F_2ppy)$_2$phenCOOH] (**38**)*

Starting material [Ir(F_2ppy)$_2$phenCOOH], compound **17** (20.1mg, 0.022mmol, 1eq), N-hydroxysuccinimide (5.4mg, 0.0469 mmol, 2.1eq), 1-ethyl-3-(3-dimethylaminopropyl) carbodiimide (EDC) (4.64mg, 0.0242mmol, 1.1eq), and 1-hydroxy-benzotriazole (HOBt) (0.9mg, 0.0067mmol, 0.30eq) were stirred at room temperature in dichloromethane (4-5mL) overnight. The resulting solid was purified by RP HPLC (40-75%B, 40m, 20mL/min, 254nm, t_R = 33m) to give 3.9mg of yellow solid **38** (20%). Rf = 0.84 (6:1 DCM/MeOH). IR (thin film) 2955.38, 2918.73, 2849.31, 1715.37, 1603.52, 1574.59, 1560.13, 1479.13, 1429.96, 1405.85, 1294.97, 1248.68, 1189.86, 1165.76, 1134.9, 1117.55, 1105.01, 989.304 cm^{-1}. ^{1}H NMR (500MHz, $CDCl_3$) δ 3.00 (s, 4H), 5.76 (d, 1H, J= 12Hz), 5.79 (dd, 1H, J= 2Hz, 8.5Hz), 6.64 (t, 2H, J= 10Hz), 6.86 (t, 1H, J= 7.5Hz), 6.96 (q, 1H, J= 5.5Hz), 7.32 (d, 1H, J= 5Hz)), 7.32 (d, 1H, J= 6Hz), 7.41 (s, 1H), 7.79 (d, 2H, J= 7Hz), 7.89 (q, 2H, J= 3.5Hz), 8.05 (t, 1H, J= 5Hz), 8.18 (m, 1H), 8.34 (t, 2H, J= 5Hz), 8.41 (d, 1H, J= 4.5Hz), 8.47 (d, 1H, J= 11Hz), 8.49 (d, 1H, J= 5Hz), 8.54 (d, 1H, J=

5Hz), 8.64 (d, 1H, J= 8Hz), 8.88 (d, 1H, J= 8.5Hz), 8.96 (d, 1H, J= 9.5Hz). ^{13}C NMR (125MHz, $CDCl_3$) δ 25.54, 29.88, 91.03, 93.33, 99.68, 99.89, 106.68, 113.42, 114.31, 114.44, 120.00, 123.55, 123.80, 124.08, 124.24, 125.87, 126.69, 128.38, 128.57, 129.51, 129.70, 131.60, 139.08, 139.35, 139.40, 146.72, 148.28, 149.52, 150.55, 151.03, 153.26, 162.70, 164.24, 166.05, 167.93. HRMS *m/z* (ESI-TOF) for $C_{39}H_{23}F_4IrN_5O_4^+$ Calculated 894.13121 Found 894.13134.

REFERENCES CITED

[1] Dove, A. Proteomics: translating genomics into products? *Nature Biotech.*, 1999, *17*, 233-236.

[2] Voet, Voet Biochemistry 3rd Edition, *Wiley*, Vol. 1, 2004, pp.144-150.

[3] Patton, W.F. Rainbow's End: The Quest for Multiplexed Fluorescence Quantitative Analysis in Proteomics, *Curr. Opin. Chem. Bio.*, 2002, 6, 63-69.

[4] Corthals, G.L. *et al.* The dynamic range of protein expression: A challenge for proteomic research. *Electrophoresis*, 2000, *21*, 1104-1115.

[5] Voet, Voet Biochemistry 3rd Edition, *Wiley*, Vol. 1, 2004, pp.70.

[6] Rabilloud, T. Detecting Proteins Separated by 2-D Gel Electrophoresis, *Anal. Chem.*, 2000, 72, 48A-55A.

[7] Matejovicova, M., Flameng, W. Effect of Vanadate on Protein Determination by the Coomassie Brilliant Blue Microassay Procedure, *Anal. Biochem.*1997, *245*, 252-254.

[7] Patton, W.F. A Thousand Points of Light: The Application of Florescence Detection Technologies to Two Dimensional Gel Electrophoresis and Proteomics, *Electrophoresis*, 2000, *21*, 1123-1144.

[8] Patton, W.F. A Thousand Points of Light: The Application of Florescence Detection Technologies to Two Dimensional Gel Electrophoresis and Proteomics, *Electrophoresis*, 2000, *21*, 1123-1144.

[9] Haebel, S. *et al.* Electrophoresis-related protein modification: Alkylation of carboxy residues revealed by mass spectrometry, *Electrophoresis*, 1998, *19*, 679 686.

[10] Berggren, K. Background-free, High Sensitivity Staining of Proteins in One and Two Dimensional Sodium Dodecyl Sulfate-polyacrylamide Gels Using a Luminescent Ruthenium Complex, *Electrophoresis*, 2000, *21*, 2509-2521.

[11] Candiano, G. Blue silver: A Very sensitive colloidal Coomassie G-250 staining for proteome analysis, *Electrophoresis*, 2004, *25*, 1327-1333.

[12] Invitrogen website, www.products.invitrogen.com, Cat. No. S-12001

[13] Unlu, M., Morgan, M.E., Minden, J.S. Difference gel electrophoresis: A single gel method for detecting changes in protein extracts, *Electrophoresis*, 1997, *18*, 2071-2077.

[14] Wang, F. Biomarker methods in drug discovery and development, Springer, March 10,

2008.

[15] GE Healthcare, 2009. CyDye™ DIGE Fluors 10 December 2009. www.gelifesciences.com.

[16] McNamara, P. Fluorescent gel imaging with Typhoon 8600, *Life Science News*, 2000, 5.

[17] Fan, J., Chen, X., Peng, X., Zhang, L., Development of Rhodamine Dyes for Biochemical Application, *3rd. Internat. Conf. On Functional Mol.*

[18] Peterson, B.R., Kovel, R.E., et al., The Pennsylvania Green Fluorophore: A Hybrid of Oregon Green and Tokyo Green for the Construction of Hydrophobic and pH-Insensitive Molecular Probes, *Org. Lett.*, 2006, *8,* 4, 581-584.

[19] Shi, Z., Jian, L.L., Gao, Y. Synthesis and application of rhodamine-based fluorescent probe dyes with spacer linker arm. *Chin. Chem. Lett.*, 2007, *18*, 667-669.

[20] Haugland, R.P. et al, Alexa Dyes, a series of new fluorescent dyes that yield exceptionally bright, photostable conjugates, *J. Histochem. Cytochem.*, 1999, *47*, 1179-1188.

[21] Invitrogen website. Molecular Probes The Handbook. www.invitrogen.com

[22] David, E. Synthesis of fluorescent rhodamine dyes using an extension of the Heck reaction. *Tet. Lett.*, 2008, *49*, 1860-1864.

[23] Haugland, R., Titus, J. et al. Texas Red, a hydrophilic, red-emitting fluorophores for use with fluorescein in dual parameter flow microfluorometric and fluorescence microscopic studies. *J. Immun. Meth.*, 1982, *50*, 193-204.

[24] Burgess, K. Wu, L. Synthesis and Spectroscopic Properties of Rosamines with Cyclic Amine Substituents. *J. Org. Chem.*, 2008, *73,* 22, 8711-8718.

[25] Detty, M.R., Autschbach, J. Tellurium Analogues of Rosamine and Rhodamine Dyes: Synthesis, Structure, ^{125}Te NMR, and Heteroatom Contributions to Excitation Energies. *Organometallics,* 2007, *26*, 6248-6257.

[26] Dratz, E.A., Grieco, P.A. Novel Optical Labeling Molecules in Proteomics and Other Biological Analyses. International Patent No. PCT/US2008/059963, 8 January 2009.

[27] Detty, M.R., Gannon, M.K. Generation of 3- and 5- Lithiothiophene-2-carboxylates via Metal-Halogen Exchange and Their Addition Reactions to Chalcogenoxanthones. *J. Org. Chem.*, 2007, *72*, 7, 2647-2650.

[28] a) Wang, X.-j., Zhang, L., Sun, X., Xu, Y., Krishnamurthy, D., Senanayake, C.H.,

Addition of Grignard Reagents to Aryl Acid Chlorides: An Efficient Synthesis of Aryl Ketones. *Org. Lett*, 2005, *7*, 5593-5595. b) Wang, X.-j., Zhang, L., Sun, X., Xu, Y., Krishnamurthy, D., Noncryogenic I/Br-Mg Exchange of Aromatic Halides Bearing Sensitive Functional Groups Using i-PrMgCl-Bis[2-(N,N-dimethylamino)ethyl] Ether Complexes, *Org. Lett*, 2006, *8*, 305-307.

[29] Ehrlich, P, Brenda, L. Action of potassium cyanide on pyronine and Acridinium dyes, *Ber. Dtsch. Chem. Ges*. 1913, *48*, 1931-1943.

[30] Uddin, M. J., Marnett, L.J. Synthesis of 5- and 6-Carboxy-X-rhodamines. *Org. Lett.*, 2008, *10*, 21, 4799-4801.

[31] Schubert, U.S. *et al.* New Trends in the Use of Transition Metal-Ligand Complexes for Applications in Electroluminescent Devices, *Adv. Mater*., 2005, *17*, 1109-1121.

[32] Miessler, G.L, Tarr, D.A. Inorganic Chemistry 3rd Edition, 2004, Pearson Education Prentice Hall, NJ, 07458.

[33] Yersin, H. Highly efficient OLEDs with phosphorescent materials. 2007, Weinheim: Wiley-VCH

[34] Engel, T. Quantum Chemistry and Spectroscopy 1st Ed. 2006, Pearson Education Benjamin Cummings, CA, 94111. Ch 15.

[35] Evans, R.C. *et al.*, Coordination complexes exhibiting room-temperature phosphorescence: Evaluation of their suitability as triplet emitters in organic light emitting diodes. *Coord. Chem. Rev.*, 2005, *250*, 2093-2126.

[36] Zhi, Q. *et al.* Series of New Cationic Iridium(III) Complexes with Tunable Emission Wavelength and Excited State Properties: Structures, Theoretical Calculations, and Photophysical and Electrochemical Properties. *Inorg. Chem.*, 2006, *45*, 6152-6160.

[37] Tamayo, A.B. *et al.* Cationic Bis-cyclometalated Iridium(III) Diimine Complexes and Their Use in Efficient Blue, Green, and Red Electroluminescent Devices, *Inorg. Chem.*, 2005, *44*, 24, 8723-8732.

[38] Park, S.Y., You, Y. Phosphorescent Iridium(III) complexes: toward high phosphorescence quantum efficiency through ligand control. *Dalton Trans.*, 2009, *8*, 1253-1472.

[39] Thompson, M.E. Highly Phosphorescent Bis-Cyclometalated Iridium Complexes: Synthesis, Photophysical Characterization, and Use in Organic Light Emitting Diodes. *J. Am. Chem. Soc.*, 2001, *123.*

[40] Meyer, T.J. *et al.* Influence of Electronic Delocalization in Metal to Ligand Charge Transfer Excited States, *Inorg. Chem*, 1995, *34*, 473-487.

[41] De Angelis, F., *et al.*, Controlling Phosphorescence Color and Quantum Yields in Cationic Iridium Complexes: A Combined Experimental and Theoretical Study. *Inorg. Chem*., 2007, *46*, 5989-6001.

[42] Williams, J.A.G., *et al.*, Light-emitting iridium complexes with tridentate ligands, *Dalton Trans.*, 2008, 2081-2099.

[43] Bernhard, S., Lowry, M.S. *et al.* Accelerated Luminophore Discovery through Combinatorial Synthesis, *J. Am. Chem. Soc.*, 2004, *126*, 14129-14135.

[44] Bernhard, S., Lowry, M.S. Synthetically Tailored Excited States: Phosphorescent, Cyclometalated Iridium(III) Complexes and Their Applications. *Chem. Eur. J.*, 2006, *12*, 7970-7977.

[45] Berhnhard, S., *et al.* Discovery and High-Throughput Screening of Heteroleptic Iridium Complexes for Photoinduced Hydrogen Production. *J. Am. Chem. Soc.*, 2005, *127*, 20, 7502-7510.

[46] Sauvage, J.P., *et al.* From ruthenium(II) to Iridium(III): 15 years of triads based on bis-terpyridine complexes. *Chem. Soc. Rev.*, 2004, *119*, 17, 12114-12124.

[47] Lo, K. *et al.* First Examples of Luminescent Cyclometalated Iridium(III) Complexes as Labeling Reagents for Biological Substrates. *Organomet.*, 2001, *20*, 4999-5001.

[48] Lo, K. *et al.* Syntheses, characterization and photophysical studies of novel biological labeling reagents derived from luminescent Iridium(III) terpyridine complexes. *New J. Chem.*, 2002, *26*, 81-88.

[49] Lo, K. *et al.* New Luminescent Cyclometalated Iridium(III) Diimine Complexes as Biological Labeling Reagents. *Inorg. Chem*., 2003, *42*, 6886-6897.

[50] Lo, K. *et al.* Synthesis, photophysical and electrochemical properties, and biological labeling studies of luminescent cyclometalated Iridium(III) bipyridine-aldehyde complexes. *Inorg. Chim. Acta*, 2004, *354*, 3109-3188.

[51] a) Lo, K. *et al.* Novel Luminescent Cylometalated Iridium(III) Diimine Complexes that Contain a Biotin Moiety. *Organomet.,* 2004, *23*, 3108-3116. b) Lo, K. *et al.* Luminescent Cylometalated Iridium(III) Arylbenzothiazole Biotin Complexes. *Organomet.,* 2005, *24*, 4594-4601. c) Lo, K. *et al.* Luminescent transition metal complex biotin conjugates. *Coord. Chem. Rev.*, 2006, *250*, 1724-1736. d) Lo, K. *et al.* Cyclometalated Iridium(III) Diimine Bis(biotin) Complexes as the First Luminescent Biotin-Based Cross-Linkers for Avidin. *Inorg. Chem*., 2007, *46*, 700-709. e) Lo, K. *et al.*, Exploitation of the Dual-emissive Properties of Cylometalated Iridium(III)-Polypyridine Complexes in the Development of Luminescent Biological Probes. *Angew. Chem. Int. Ed.*, 2008, *47*, 2213-2216.

[52] a) Lo, K. *et al.*, Synthesis, Photophysical and Electrochemical Properties, and Protein Binding Studies of Luminescent Cyclometalated Iridium(III) Bipyridine Estradiol Conjugates. *Chem. Eur. J.*, 2007, *13*, 7110-7120. b) Lo, K. *et al.*, Luminescent Cyclometalated Iridium(III) Polypyridine Complexes Containing a Thiourea Moiety: Synthesis, Characterization, Photophysics, Electrochemistry and Anion-Binding Properties, *Eur. J. Inorg. Chem.*, 2006, 4054-4062. c) Lo, K. *et al.* Synthesis, Characterization, and Properties of Luminescent Organoirdium(III) Polypyridine Complexes Appended with an Alkyl Chain and Their Interactions with Lipid Bilaryers, Surfactants, and Living Cells. *Organomet.,* 2008, *27*, 2998-3006.

[53] Huang, C. *et al.*, Cationic Iridium(III) complexes for phosphorescence staining in the cytoplasm of living cells. *Chem. Commun.*, 2008, 2115-2117.

[54] Nonoyama, M. Benzo[h]quinolin-10-yl-N Iridium(III) Comlexes. *Bull. Chem. Soc. Jap.*, 1974, *47*, 3, 767-768.

[55] McCafferty, D.G., *et al.*, Synthesis of Redox Derivatives of Lysine and Their Use in Solid-Phase Synthesis of a Light-Harvesting Peptide, *Tetrahedron*, 1995, *51*, 4, 1093-1106.

[56] Bolink, H.J. *et al.*, Stable Single-Layer Light-Emitting Electrochemical Cell Using 4,7-Diphenyl-1,10-phenanthroline-bis(2-phenylpyridine)iridium(III) Hexafluorophosphate. *J. Am. Chem. Soc.*, 2006, *128*, 14786-14787.

[57] Waern, J. B., *et al.*, Luminescent Cyclometalated RhIII, IrIII, and (DIP)2RuII Comlexes with Carboxylated Bipyridyl Ligands: Synthesis, X-ray Molecular Structure, and Photophysical Properties. *Inorg. Chem.*, 2008, *47*, 3340-3348.

[58] Huang, C. *et al.*, Cationic Iridium(III) complexes for phosphorescence staining in the cytoplasm of living cells. *Chem. Commun.*, 2008, 2115-2117.

[59] Crosby, G. A, Demas, J.N. The Measurement of Photoluminescence Quantum Yields. A Review. *J. Phys. Chem.*, 1971, *75*, 8, 991-1024.

[60] A Guide to Recording Fluorescence Quantum Yields, Jobin Yvon, Horiba, jyhoriba.uk.com

[61] Spicka, K.J. 2008, Design and Synthesis of Fluorescent Dyes for Use in Proteomic Research. PhD. Thesis, Montana State University, Bozeman MT.

[62] Sprouse, S., King, K.A., Spellane, P.J., Watts, R.J. Photophysical Effects of Metal-Carbon Bonds in Ortho-Metalated Complexes of Ir(III) and Rh(III). *J. Am. Chem. Soc.,* 1984, *106*, 6647-6653.

[63] Tian, N. *et al.* Efficient Synthesis of Carbazolyl- and Thienyl-Substituted B-

Diketonates and Properties of Their Red- and Green-Light-Emitting Ir(III) Complexes, *J. Org. Chem.*, 2009, *74*, 2718-2725.

[64] Nonoyama, M. Chelating C-Metallation of N-Phenylpyrazole with Rhodaium(III) and Iridium(III), *J. Organomet. Chem.*, 1975, 86, 263-267.

[65] Coppo, P., Plummer, E.A., Cola, L.D. Tuning iridium(III) phenylpyridine complexes in the almost blue region. *Chem. Commun.* 2004, *15*, 1774-1775.

[66] Lepeltier, M. *et al.* Synthesis, Structure, and Photophysical and Electrochemical Properties of Cyclometallated Iridium(III) Complexes with Phenylated Bipyridine Ligands, 2005, 110-117.

[67] Dragonetti, C. *et al.* The Role of Substituents on Functionalized 1,10-Phenanthroline in Controlling the Emission Properties of Cationic Iridium(III) Complexes of Interest for Electroluminescent Devices, *Inorg. Chem.* 2007, *46*, 8533-8547.

[68] Lafolet, F. *et al.* Iridium complexes containing p-phenylene units. The influence of the conjugation on the excited state properties, *J. Mat. Chem.* 2005, *15*, 2820-2828.